uOttawa

L'Université canadienne
Canada's university

FACULTÉ DES ÉTUDES SUPÉRIEURES ET POSTOCTORALES

u Ottawa

L'Université canadienne
Canada's university

FACULTY OF GRADUATE AND POSDOCTORAL STUDIES

Neil McKenna
AUTEUR DE LA THÈSE / AUTHOR OF THESIS

Ph.D. (Microbiology and Immunology)
GRADE / DEGREE

Department of Microbiology and Immunology
FACULTÉ, ÉCOLE, DÉPARTEMENT / FACULTY, SCHOOL, DEPARTMENT

Characterization of the fusion protein of the human parainfluenza virus type 3

TITRE DE LA THÈSE / TITLE OF THESIS

Ken Dimock
DIRECTEUR (DIRECTRICE) DE LA THÈSE / THESIS SUPERVISOR

CO-DIRECTEUR (CO-DIRECTRICE) DE LA THÈSE / THESIS CO-SUPERVISOR

EXAMINATEURS (EXAMINATRICES) DE LA THÈSE / THESIS EXAMINERS

Veronika Von Messling

Sean Li

John Bell

Kirsten Mattison

Gary W. Slater
Le Doyen de la Faculté des études supérieures et postdoctorales / Dean of the Faculty of Graduate and Postdoctoral Studies

Characterization of the fusion protein of the human parainfluenza virus type 3

Neil McKenna

Thesis submitted to the

Faculty of Graduate and Postdoctoral Studies

In partial fulfillment of the requirements for the degree of

Doctor of Philosophy in Microbiology and Immunology

Department of Biochemistry, Microbiology and Immunology

Faculty of Medicine

University of Ottawa

Your file Votre référence
ISBN: 978-0-494-46517-2
Our file Notre référence
ISBN: 978-0-494-46517-2

Abstract

Human parainfluenza virus type 3 (HPIV3), a member of the family *Paramyxoviridae*, is an enveloped, negative-sense single stranded RNA virus, and an important cause of upper and lower respiratory tract disease in children. Infection by HPIV3 requires fusion of the viral envelope with the plasma membrane of the host cell. Fusion occurs via the cooperative actions of the viral hemagglutinin-neuraminidase (HN) and fusion (F) glycoproteins. HN, the receptor-binding protein, binds sialic acid and undergoes a series of conformational changes that are believed to trigger characteristic conformational changes in the F protein that are necessary for membrane fusion. The specific objectives of this dissertation are to elucidate, in greater detail, features of HN-F interaction and F refolding during the entry process.

Mutations were introduced at position I474 of the F protein, in heptad repeat 2 (HR2), a carboxy-proximal sequence that forms a highly stable structure with the amino-proximal heptad repeat 1 (HR1), known as the 6-helix bundle (6-HB). Formation of the 6-HB is believed to release energy required for fusion of virion and host cell membranes. Mutation of I474 to small, polar residues produced F proteins that are uncleaved and non-fusogenic; 6-HB formed by peptides based these mutants were thermodynamically unstable. Mutation of I474 to larger polar or nonpolar side chains, or to smaller polar side chains, resulted in F proteins that were cleaved and fusogenic to wild-type levels, although 6-HB stability was variable. The ability of HR2 peptides to inhibit virus infection and glycoprotein-driven fusion mirrored 6-HB stability. Tagging of HN with FLAG and hexahistidine tags permitted Ni-affinity purification of HN. Cotransfection of HN and F, including F I474D, S, and E mutants, showed that stable HN-F complexes could be isolated when cell membranes were solubilized with octyl glucoside. A distinct

downregulation of HN expression was observed when HN and F were coexpressed in cells, likely as a co-translational or very early post-translational step.

A series of three-part chimeric F sequences consisting of fragments of HPIV3 and bovine PIV3 F coding regions were constructed. When expressed in the presence of the HPIV3 HN protein, the chimeric F proteins showed no differences in level of expression or fusogenicity. Also, there were no differences in the stability of homologous and heterologous HR1/HR2 complexes, and inhibition of HPIV3 infection by HR2 peptides of the HPIV3 and BPIV3 F proteins was similar.

HPIV3 resistant to inhibition by HR2 was produced by sequential passage of virus in increasing concentrations of a GST-HR2 fusion protein. Statistically significant resistance of populations as well as plaque-purified clones was demonstrated, although sequencing of resistant clones did not reveal mutations that could be clearly associated with resistance.

A model for HN and F in the fusion process is presented, based on data produced in this dissertation and on previously published evidence.

Acknowledgements

First and foremost, I would like to thank my supervisor, Dr. Ken Dimock, for his guidance, patience, and support, and allowing me to become independent in the lab but still being around to discuss anything science-related. Also appreciated was his desire to talk hockey and TV programs. His never-failing optimism was always noted and appreciated. Also deserving specific thanks is Dr. Reza Nokhbeh, for his infinite knowledge and assistance about all things microbiological, his endless patience with my questions, and most of all his friendship and sense of humour in the lab.

I would also like to thank my advisory committee, Drs. Doug Gray, John Baenziger, Steve Evans, and especially Dr. Earl Brown, whose willingness to discuss science and related issues in addition to the invaluable assistance he gave me with my various projects over the years. I would also like to thank Dr. Kathryn Wright, who was also a great source of reference for the science during my thesis, and for critical revision of this dissertation. Specific thanks also go out to Drs. Mark Wurth and Rebecca Dutch at the University of Kentucky for the circular dichroism analyses, as well as Yanqiu (Jenny) Wu and Dr. Natalie Goto of the Department of Chemistry at the University of Ottawa for their assistance with HPLC. Thanks also to the staff in BMI without whose help I would never have survived: Krystyna Chudzio, Linda Therrien, Carol Ann Kelly, Nicole Trudel, Joanne Barlow, and André Bergeron.

Also important are all the people who have come through the Dimock, Wright, Dillon, Sattar, and Brown labs over the years, as well as the BMI second and fourth floor people. Each has enriched my life in different ways, but specifically those whom I can consider life-long friends: David Alexander, Alain Haddad, Kris Chan, Ahmar Khan, Tamyo Mbisa, Audri Brewster, Jason Szeto, Franco Pagotto, Nelson Eng, Jason Tetro, Rich Kibbee, Fernando Mattias, Dion Shah, Evelin Loit, Dan MacDonald, Majid Mojibian,

and Mahmoud Aly deserve special mention. These people made my years in the lab tolerable.

Last, but not least, are my family, especially my parents Jim and Cec McKenna, whose unwavering support helped immensely, and my wife, Mona Shafey, with whom I have shared every moment of my life as an undergraduate and graduate student. I will never forget what she has done for me from the moment we first met.

TABLE OF CONTENTS

LIST OF FIGURES

LIST OF TABLES

Contributions of collaborators

Sequences encoding the untagged HPIV3 F protein containing I474V, A, G, S, D, and E mutations were constructed and characterized by Dr. Sharon Ebata as part of her Ph.D. dissertation, and are referenced in the text as such. GST-HR1 and GST-HR2 (wild-type, I474D, and I474E) were constructed by Christine Grisé. Plasmid pIBI-F-FLAG was constructed by Bogna Zolkiewska. The HPIV3 pIBI-F-FLAG plasmid with engineered *Nco*I, *Afl*II, *Sal*I, and *Bam*HI sites for construction of human/bovine chimeras was constructed by Drs. Kris H.K. Chan and Reza Nokhbeh. Circular dichroism-monitored thermal melts to assay 6-helix bundle stability were generated and analyzed by Drs. Mark A. Wurth and Rebecca E. Dutch at the University of Kentucky.

List of abbreviations

6-HB	Six-helix bundle
AMPV	Avian paramyxovirus
BFA	Brefeldin A
bHR1	BPIV3 F protein HR1
bHR2	BPIV3 F protein HR2
BPIV3	Bovine parainfluenza virus type 3
CPE	Cytopathic effects
Enf	Enfuvirtide (T-20, DP-178)
Env	Envelope glycoprotein (retrovirus)
ER	Endoplasmic reticulum
F	Fusion protein
GA	Golgi apparatus
GST	Glutathione-S-transferase
H	Hemagglutinin (measles virus)
HA	Hemagglutinin (influenza virus)
HIV	Human immunodeficiency virus
HN	Hemagglutinin-neuraminidase
HPIV2	Human parainfluenza virus type 2
HPIV3	Human parainfluenza virus type 3
HPLC	High-pressure liquid chromatography
HR1	Heptad repeat 1
HR2	Heptad repeat 2
hHR1	HPIV3 F protein HR1
hHR2	HPIV3 F protein HR2
IC_{50}	50% inhibitory concentration

LRT	Lower respiratory tract
M	Matrix protein
MLV	Murine leukemia virus
MOI	Multiplicity of infection
NDV	Newcastle disease virus
PBS	Phosphate-buffered saline
PCR	Polymerase chain reaction
PFU	Plaque forming units
PIV5	Simian parainfluenza virus 5 (also known as simian virus 5, SV5)
RSV	Respiratory syncytial virus
RT-PCR	Reverse transcription – polymerase chain reaction
S	Spike protein (SARS coronavirus)
SARS CoV	Severe acute respiratory syndrome coronavirus
SIV	Simian immunodeficiency virus
SDS-PAGE	Sodium-dodecyl sulphate-polyacrylamide gel electrophoresis
SV41	Simian virus 41
TBS	Tris-buffered saline
URT	Upper respiratory tract

Chapter 1 - General Introduction

One of the earliest stages of the enveloped virus life cycle is the fusion of virion and target cell membranes. This step is critical for all enveloped viruses, and is a attractive target for antivirals. Enveloped viruses rely on one or more envelope glycoproteins to promote the fusion of membranes. The paramyxovirus human parainfluenza virus type 3 (HPIV3) is a good model for virus entry, as it is a key human pathogen and the family *Paramyxoviridae* contains several other important pathogens; its entry mechanism is also very similar to the entry mechanisms employed by members of several other key virus families.

Human parainfluenza virus type 3 – taxonomy

Human parainfluenza virus type 3 (HPIV3) is taxonomically classified as follows: order *Mononegavirales*, family *Paramyxoviridae*, subfamily *Paramyxovirinae*, genus *Respirovirus*. The *Paramyxoviridae* share many similarities with other members of the *Mononegavirales*, including the *Rhabdoviridae* and the *Filoviridae*, such as cytoplasmic replication, sequential transcription of mostly non-overlapping mRNAs, a virion-encapsulated polymerase, and a negative-sense, single-stranded RNA genome tightly bound by a nucleocapsid protein (Lamb and Kolakofsky, 2001). Other important members of the *Paramyxoviridae*, their classification, host organisms, and associated disease are listed in table 1.

Table 1. List of paramyxoviruses and associated diseases.

Virus	Acronym	Genus	Primary host	Disease	Reference(s)
Human parainfluenza virus type 3	**HPIV3**	*Respirovirus*	Humans; other primates	URTI[1], LRTI[2]	(Henrickson, 2003; Chanock *et al.*, 2001)
Bovine parainfluenza virus type 3	**BPIV3**	*Respirovirus*	Cattle	URTI, LRTI	(Bailly *et al.*, 2000; Haanes *et al.*, 1997)
Human parainfluenza virus type 1	**HPIV1**	*Respirovirus*	Humans;other primates	URTI, LRTI	(Henrickson, 2003; Chanock *et al.*, 2001)
Sendai virus	**SeV**	*Respirovirus*	*Mus musclus*	URTI, LRTI; wasting, retarded growth	(Faisca and Desmecht, 2007)
Hendra virus	**HeV**	*Henipavirus*	Flying foxes; humans	Influenza-like illness	(Eaton *et al.*, 2006)
Nipah virus	**NiV**	*Henipavirus*	Flying foxes; horses; humans	Encephalitis, respiratory involvement	(Eaton *et al.*, 2006)
Measles virus	**MV**	*Morbillivirus*	Humans	URTI, rash	(Rima and Duprex, 2006; Barrett, 1999)
Peste-des-petits-ruminants virus	**PPRV**	*Morbillivirus*	Sheep; goats	URTI, LRTI, GI[3]	(Barrett, 1999)
Canine distemper virus	**CDV**	*Morbillivirus*	Canines; weasels, ferrets; other small mammals	URTI, LRTI, GI	(Cosby *et al.*, 2002; Barrett, 1999)
Human parainfluenza virus type 2	**HPIV2**	*Rubulavirus*	Humans	URTI, LRTI	(Henrickson, 2003; Chanock *et al.*, 2001)
Simian virus 5 (Simian parainfluenza virus 5)	**SV5 or PIV5**	*Rubulavirus*	Primates; canines	URTI, LRTI (particularly in canines)	(Chatziandreou *et al.*, 2004)
Mumps virus		*Rubulavirus*	Humans	Parotid gland swelling, fever	(Gupta *et al.*, 2005)
Menangle virus		*Rubulavirus*	Fruit bats; pigs	Stillborn piglets, flu-like illness	(Zhu *et al.*, 2003)
Newcastle disease virus	**NDV**	*Avulavirus*	Poultry	Severe URTI & LRTI, GI	(Alexander, 2000)
Human respiratory syncytial virus	**HRSV or RSV**	*Pneumovirus*	Humans	URTI, LRTI	(Lee *et al.*, 2005)
Bovine respiratory syncytial virus	**BRSV**	*Pneumovirus*	Cattle	URTI, LRTI	(Larsen, 2000)
Human metapneumovirus	**HMPV**	*Meta-pneumovirus*	Humans	URTI, LRTI	(Principi *et al.*, 2006)

[1]URTI = upper respiratory tract infection; [2]LRTI = lower respiratory tract infection;
[3]GI = gastrointestinal tract illness

Human parainfluenza virus type 3 – virus particle

The HPIV3 particle is a generally pleiomorphic, enveloped structure, approximately 150-250 nm in diameter, although larger particles have been described (Henrickson, 2003; Chanock *et al.*, 2001). The particle is bound by a double lipid bilayer, taken from the host cell plasma membrane, into which are incorporated two surface glycoproteins, the attachment protein, hemagglutinin-neuraminidase (HN), and the fusion (F) protein (Chanock *et al.*, 2001). Carried inside the envelope is the negative-sense, single-stranded RNA genome, although some non-infectious particles contain a positive-sense antigenomic RNA strand (Henrickson, 2003). The HPIV3 genome is 15,462 nucleotides in length and encodes 9 proteins (Chanock *et al.*, 2001). The genomic RNA is wound tightly in a nucleocapsid, associated with approximately 2,600 nucleocapsid (NP) protein molecules. The nucleocapsid also incorporates 300 phosphoprotein (P) and 40 large (L) polymerase protein molecules, the major components of the HPIV3 replicase complex (Chanock *et al.*, 2001). The nucleocapsid and the glycoproteins are bridged by the membrane-associated matrix (M) protein. HPIV3 nucleocapisds have left-handed helical symmetry, and are approximately 17-18 nm in diameter, 1 μm in length, with a pitch of 5.5 nm (Lamb and Kolakofsky, 2001). The HPIV3 genome, including gene lengths and protein sizes, is represented in Figure 1. The genome order is NP-P (which includes the alternately transcribed C, D, and V proteins)-M-F-HN-L. The HPIV3 particle is optimally infectious at physiological pH (7.4-8.0) and quickly loses infectivity at low pH (3.0-4.0), or in low humidity (Henrickson, 2003).

Figure 1. Schematic representation of the HPIV3 and BPIV3 genomes. Gene sizes, including untranslated regions (UTR) and open reading frames (ORF), ORF sizes, and protein lengths, are listed for HPIV3 (blue text) and BPIV3 (red text). The linear genome diagram is drawn to scale.

NP	P/C/D/V	M	F	HN	L	
1646	2013	1155	1851	1888	6795	Gene - nucleotides (incl. UTRs and ORF)
1646	1995	1149	1869	1888	6795	
1545	1806	1059	1617	1716	6699	Open reading frame - nucleotides
1545	1788	1053	1620	1716	6699	
515	603/199/131/80	353	539	572	2233	Gene product - amino acids
515	596/201/125/171	351	540	572	2233	

Human parainfluenza virus type 3 – disease, epidemiology, treatment and vaccines

HPIV3 infections are endemic throughout the year, but have an infection peak in the late spring in North America (Weinberg, 2006). Infections are very frequent among young children, particularly infants. The incidence rate of HPIV3 infection for infants less than 12 months old has been estimated to be as high as 66.9 per 100 population, decreasing in incidence to 16.7 infections per 100 population for children older than 48 months (Lee *et al.*, 2005).

HPIV3 replicates in respiratory epithelia, causing upper respiratory tract (URT) disease such as rhinitis and pharyngitis, progressing to the lower respiratory tract (LRT) in some cases (Chanock *et al.*, 2001). The most common LRT complication in HPIV3 infection is croup. HPIV3 infections are responsible for 65% of croup cases in the USA in an average year, with as many as 3 cases per 1000 population (Weinberg, 2006). Other LRT complications associated with HPIV3 include bronchitis, bronchiolitis, and bronchopneumonia (Weinberg, 2006; Chanock *et al.*, 2001). Physician-attended HPIV3 infections in children can be as high as 34 per 100 population; for children under the age of 59 months in the USA, 2,580,000 physician visits per year, and between 10,000 and 20,000 hospitalizations, are due to HPIV3 infection (Lee *et al.*, 2005; Hall, 2001). HPIV3 is second only to respiratory syncytial virus in hospitalizations for respiratory tract disease among infants (Lee *et al.*, 2005). Children are not the only population susceptible to HPIV3 infection. Adults are often reinfected since no long-lasting immunity from previous HPIV3 infections develops. Infection of adults is generally limited, with mild symptoms, although infections can be severe, particularly in the elderly and immunosuppressed. Mortality among these groups can be as high as 15-30% (Hall, 2001). HPIV3 is particularly dangerous to lung-transplant recipients, causing serious LRT disease in approximately 5% of patients within the first year of transplant (Vilchez *et al.*, 2003). 32% of HPIV3-infected

lung transplant recipients progress to allograft rejection within 18 months (Vilchez *et al.*, 2003).

Treatment options for HPIV3 infections are limited. Ribavirin has been used, with varying success rates, for suppression of viral infection in immunocompromised patients (Sparrelid *et al.*, 1997). Treatment is generally symptom-specific, with respiratory support available for patients suffering from serious LRT complications (Loughlin and Moscona, 2006). Prevention of HPIV3 infection by vaccination has been a focus for more than forty years, though mostly without success. Recent progress has been seen using the temperature-sensitive cp45 strain of HPIV3 as a vaccine candidate, which was, as of 2004, in phase 3 clinical trials, following a successful phase 2 trial (Belshe *et al.*, 2004; Belshe *et al.*, 2004).

Human parainfluenza virus type 3 – attachment and fusion

All enveloped viruses, including HPIV3, require fusion of their envelope with the target cell membrane as an early step in their life cycles, in order to release the viral genome for gene expression and replication. Enveloped viruses fuse through one of two primary mechanisms: endocytosis, acidification, and fusion with the endosomal membrane (e.g. orthomyxoviruses), or fusion at physiological pH with the cellular plasma membrane (e.g. paramyxoviruses). HPIV3 fusion is directed through the specific functions of the two envelope glycoproteins, HN and F. Paramyxovirus fusion is a complex process that is still not fully understood, though many key details in the fusion process are well-defined. Briefly, the earliest event in the paramyxovirus fusion process is virus attachment to sialic acid-containing cellular receptors by the HN protein (Villar and Barroso, 2006). This binding is believed to produce a conformational change in the HN protein, which is then transmitted to

the F protein through a physical interaction between the HN and the F proteins, producing conformational changes in the F protein. The conformational changes in the F protein are well-defined and include its refolding to form a six-membered bundle of anti-parallel heptad repeat α-helices, known as the six-helix bundle (6-HB) (Lamb *et al.*, 2006). Formation of the 6-HB in viral envelope fusion proteins is not unique to the family *Paramyxoviridae*. It characterizes a class of proteins known as the class I viral fusion proteins, which include the Env proteins of retroviruses, coronavirus spike proteins, influenza HA, and the GP of Marburg and Ebola viruses. The class I-directed fusion process is presented in much greater detail below. Refolding of the F protein is believed to release the energy and provide a protein conformation to mediate membrane-membrane coalescence. Following membrane fusion, the nucleocapsid of paramyxoviruses is released into the cytoplasm for transcription and replication. Detailed models for HN binding to sialic acid and parts of the F protein refolding process are well-characterized, but information about much of the pre- and post-fusion conformations of the F protein, the HN/F interaction, and refolding of the HN and F upon receptor binding remains unclear. A more detailed review of the data known about the roles of each glycoprotein in paramyxovirus membrane fusion is presented below.

The hemagglutinin-neuraminidase protein

Paramyxovirus HN proteins serve two key roles in the entry process. The first key role is binding of the HN protein to the cell-surface receptor, which for HPIV3 is known to be sialic acid-containing glycoproteins or gangliosides. More specifically, HPIV3 has been shown to bind to oligosaccharides containing terminal N-glycolylneuraminic acid (NeuGc) in α2-3Gal or N-acetylneuraminic acid (NeuAC) in both α3-3Gal and α2-6Gal linkages (Suzuki *et al.*, 2001); a recent study using a glycan array to screen HPIV3 binding also concluded specifically that HPIV3 HN binds to longer-chained glycans, notably tetrasaccharides or

longer, unless a trisaccharide α2-3-linked Gal is fucosylated or sulphated (Amonsen *et al.*, 2007). The terminal α2-3 sialic acid linkage is generally found in the upper respiratory tract, while α2-6 linkages are found in the lung (Nicholls *et al.*, 2007). The second key role of HN is as a sialidase, presumably in order to release nascent virions from host cell sialic-acid containing surface molecules and/or from host secretions that might prevent access to host tissues (Lamb and Kolakofsky, 2001).

The HN protein of HPIV3 is 572 amino acids in length. It is a type II membrane protein with a short cytoplasmic tail located at the amino terminus of the protein. A large, hydrophilic extracellular domain is found C-terminal to a trans-membrane domain of approximately 25-residues. The linear structure of the HPIV3 HN protein, including key features, is presented in Figure 2, panel A. Synthesis of the HN protein begins at the ER membrane, likely chaperoned by the GRP78-BiP resident ER chaperone (Ng *et al.*, 1992; Roux, 1990; Ng *et al.*, 1989). The extracellular domain contains four sites for high-mannose and/or complex N-linked glycosylation, which are believed to be important for proper protein processing, transport, and function (Tanaka and Galinski, 1995; Spriggs and Collins, 1990), and more specifically, for fusion promotion (Deng *et al.*, 1994). The HPIV3 HN protein assembles into tetramers through non-covalent monomer interactions, in contrast to the HN proteins of other paramyxoviruses. For example, the Newcastle disease virus (NDV) HN protein is covalently dimerized through a disulphide bridge between monomer C123 residues located in the putative "stalk" region of the protein (McGinnes and Morrison, 1994), a residue that is missing in HPIV3 HN. The covalently linked dimers of NDV form tetramers through non-covalent interactions. HN tetramers are transported to the cell surface, where they assume a binding-active state.

Figure 2. Linear representation of the features of the HPIV3 HN and F proteins. (A) A diagram showing the primary structure of the 572-residue HN protein. N-linked glycosylation sites are indicated by the CHO labels; active site residues are indicated by the residue number. Key structural features are highlighted and labelled. (B) A linear showing the primary structure of the 539-residue F protein. N-linked glycosylation sites are indicated by the CHO labels. Key features are highlighted and labelled.

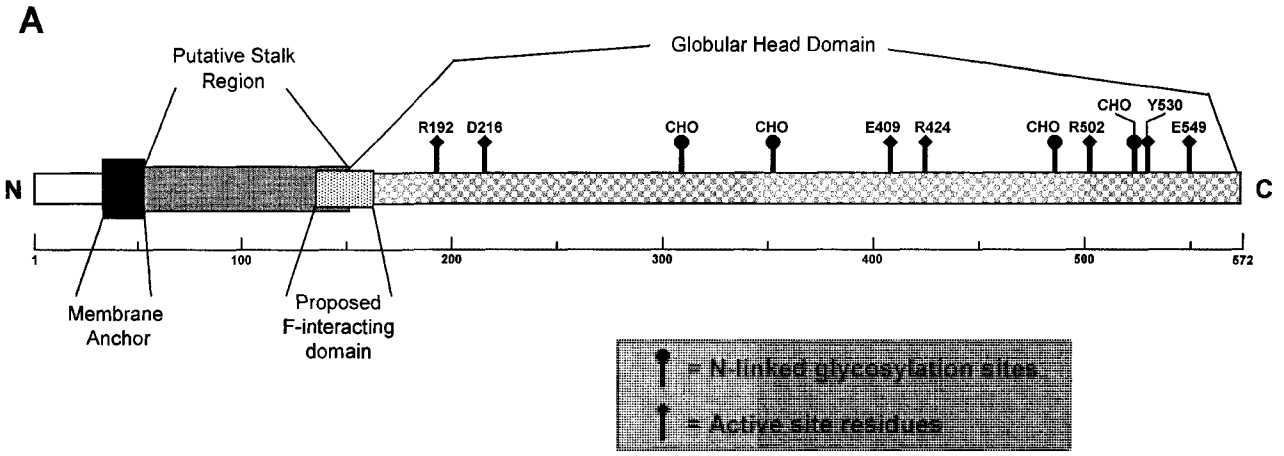
A
Putative Stalk Region
Globular Head Domain
R192
D216
CHO
CHO
E409
R424
CHO
R502
CHO
Y530
E549
N
C
1
100
200
300
400
500
572
Membrane Anchor
Proposed F-interacting domain
= N-linked glycosylation sites
= Active site residues

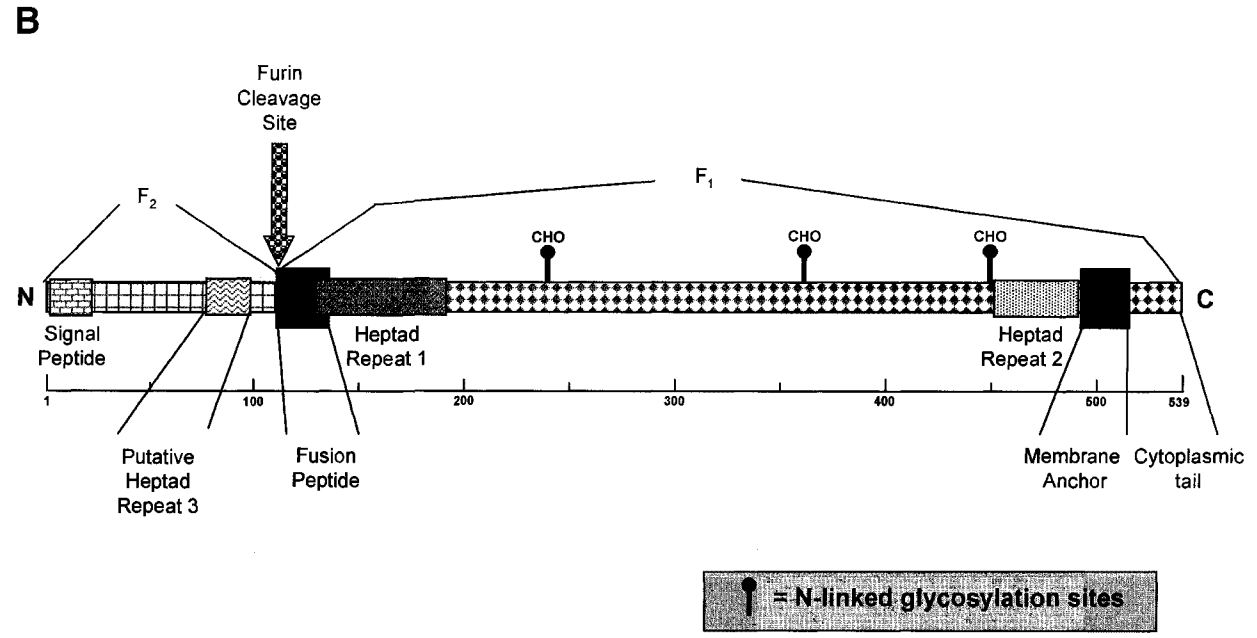
B
Furin Cleavage Site
F2
F1
CHO
CHO
CHO
N
C
Signal Peptide
Heptad Repeat 1
Heptad Repeat 2
1
100
200
300
400
500
539
Putative Heptad Repeat 3
Fusion Peptide
Membrane Anchor
Cytoplasmic tail
= N-linked glycosylation sites

The receptor-binding and neuraminidase activities are both located in the extracelluar domain of the HN protein, although there is some debate as to the exact locations of the two sites. The three-dimensional structures of the HPIV3 (Lawrence *et al.*, 2004), NDV (Ryan *et al.*, 2006; Crennell *et al.*, 2000), and simian virus 5 (PIV5) (Yuan *et al.*, 2005) HN extracellular "globular" domains, in their receptor-bound forms, have been published. The globular extracellular domains of the HN proteins are six-bladed β-sheet propellers. Note, however, that these structures lack the membrane-proximal "stalk", trans-membrane, and cytoplasmic domains. All three solved structures indicate very similar proteins, with near-perfect conservation of active site residues with each other and with influenza virus neuraminidase (NA); these residues have been proposed to act as both a primary sialic acid binding site and neuraminidase active site, differentiated only by the particular conformation of the HN protein (Yuan *et al.*, 2005; Lawrence *et al.*, 2004). The identified "active site" residues of the HN protein include R192, D216, E409, R424, R502, Y530, and E549 (Lawrence *et al.*, 2004). The three-dimensional structures of the paramyxovirus HN proteins also share basic structural similarity to influenza virus NA.

A second sialic acid binding site has been proposed in NDV HN, located at the membrane-distal end of the dimer interface of the HN globular domain, involving hydrophobic residues from each monomer (Zaitsev *et al.*, 2004). Sialic acid binding at this site is enhanced in the presence of the neuraminidase inhibitor Zanamivir, which inhibits sialic acid binding to the primary binding site (Porotto *et al.*, 2006b). This second binding site does not exist in all paramyxovirus HN proteins, including HPIV3 HN. Mutation of a single asparagine residue in HPIV1 HN (N523, a residue conserved in HPIV3), to glutamate, produced a second receptor binding site in human parainfluenza virus type 1 (HPIV1) HN, suggesting that a non-functional second binding site similar to the NDV HN site is present. An alternative, unidentified second sialic acid-binding site in HPIV3 HN, unrelated to the second binding site identified in NDV may exist (Porotto *et al.*, 2007),

although the function of such a receptor binding site in HN is unclear. It has been proposed that the dual, seemingly contrary, nature of the primary binding site (sialic acid binding and sialidase activities), may result in the need for a second, non-sialidase-active binding site to complement the primary site during fusion (Villar and Barroso, 2006). Recent speculation suggests that the primary site is used for initial binding, and the second site for fusion promotion (Porotto *et al.*, 2007).

The evidence for HN conformational change upon receptor binding may also explain the need for the second sialic acid binding site, since it is located at the dimer interface. Crystallization of the NDV HN in complex with its ligand resulted in a different dimer interface than that observed in the absence of ligand (Crennell *et al.*, 2000), however, different conformations of the dimer interface in the presence and absence of ligand were not observed for HPIV3 HN (Lawrence *et al.*, 2004). A tighter dimer interface in NDV HN was noted in the presence of ligand, suggesting that binding of sialic acid at the primary active site mediates refolding of the HN dimer such that the newly folded interface is in a proper conformation for the second site to become active, perhaps for tighter adhesion to the host cell and/or triggering the F protein for fusion. It should be noted, however, that the N523D mutation in HPIV1 HN did not enhance fusion (Bousse and Takimoto, 2006).

The stalk region of HN, defined as the 50-60 residue membrane-proximal region in the extracellular domain (Melanson and Iorio, 2006; Melanson and Iorio, 2004; Gravel and Morrison, 2003), may act as a stabilizer for the active tetramer (Yuan *et al.*, 2005). This region has also been predicted to be a key factor in the interaction between the HN and F proteins (detailed below in the section on HN-F interaction). There are few data that link the refolding in the HN head following receptor binding with the triggering of conformational changes in the F protein, although given the evidence for interaction between the stalk of HN stalk and the F protein, any such signal is likely to pass through this region. It has been speculated that the globular head of HN may also interact with the F protein (Yuan *et al.*,

2005), though there is little evidence to confirm this. The lack of evidence for a link between head and stalk rearrangements during receptor binding is an unfortunate side effect of the limitations of the existing three-dimensional structures of the HN protein, which do not include any stalk region residues.

HN-F interaction and triggering of the F protein following receptor binding

It has long been assumed that paramyxovirus attachment and fusion proteins interact, functionally and/or physically, due to the related nature of their activities during virus binding and entry. Early data showed a clear requirement for coexpression of HN (or the corresponding receptor-binding hemagglutinin (H) of morbilliviruses or G protein of henipaviruses) and F in cell-culture fusion models (Bagai and Lamb, 1995; Heminway *et al.*, 1994; Horvath *et al.*, 1992; Tanabayashi *et al.*, 1992; Hu *et al.*, 1992; Wild *et al.*, 1991; Ebata *et al.*, 1991). There were a few notable exceptions wherein the F protein, expressed on its own, could fuse cells, such as for the F proteins of PIV5 (Bagai and Lamb, 1995), peste-des-petits ruminants virus (PPRV) (Seth and Shaila, 2001), and for site-directed mutants of the NDV (Sergel *et al.*, 2000) and SER virus F proteins (Seth *et al.*, 2003). Even for these cases, coexpression of the F protein with the HN protein increased fusion over that observed when F was expressed alone. This functional interaction was also shown to be type-specific, requiring coexpression of HN and F proteins from the same virus (Yao *et al.*, 1997; Bagai and Lamb, 1995; Deng *et al.*, 1995; Tsurudome *et al.*, 1995; Bousse *et al.*, 1994; Wild *et al.*, 1991), with a few exceptional, specific cases where swapping the F proteins of the closely related Sendai and HPIV1 viruses (Bousse *et al.*, 1994), the human parainfluenza virus type 2 and mumps viruses (Tsurudome *et al.*, 1998), and the Hendra and Nipah viruses (Bossart *et al.*, 2002) was tolerated.

A physical interaction between the HN and F proteins has also been fairly well-established. Monoclonal antibodies against one of the glycoproteins coimmunoprecipitate the other glycoprotein of NDV and measles virus, among others (Deng *et al.*, 1999; Yao *et al.*, 1997; Stone-Hulslander and Morrison, 1997; Malvoisin and Wild, 1993), and similarly, GST-linked peptide fragments of NDV HN were shown to interact with sections of the NDV F protein (Gravel and Morrison, 2003). Cocapping experiments using HPIV2 and HPIV3 HN and F proteins indicated a type-specific colocalization at the plasma membrane surface (Yao *et al.*, 1997). Physical interaction of the HN and F proteins prior to plasma membrane presentation was suggested by several studies using F proteins tagged with an endoplasmic reticulum (ER) retention signal (KDEL), as retention of the F protein in the ER downregulated surface expression of the HPIV2 and HPIV3 HN proteins, in a non-type-specific manner (Tong and Compans, 1999; Tanaka *et al.*, 1996), although similar experiments using different ER retention tags (RRR or RRRRR), on PIV5 or HPIV3 HN proteins, or di-lysine (KK) tags on the F proteins, for Golgi retention, did not downregulate surface expression of the other glycoprotein (Paterson *et al.*, 1997). Interestingly, use of the poly-arginine tags to retain measles H or F in the ER was shown to retain the glycoprotein partner in a physical interaction, as shown by coimmunoprecipitation (Plemper *et al.*, 2001). While debated, the above evidence suggests that interaction of the HN and F proteins may in fact occur much earlier than presentation at the cell surface.

Localization of the fusion promotion activity of the HN protein has been well-studied. Early studies showed a functional separation between receptor binding and fusion activities using deletion mutants missing a short extracellular, membrane-proximal nine-residue stretch, which retained hemagglutination activity, while fusion promotion was abolished (Sergel *et al.*, 1993). Further confirmation of the role of the membrane-proximal extracellular domain in fusion promotion, referred to as the stalk of the HN protein, arose from studies using chimeric HN proteins. Chimeric HPIV1/Sendai proteins indicated that the

central 62% of HN was critical for fusion promotion (Bousse *et al.*, 1995). Chimeric HN proteins constructed of highly fusogenic and non-fusogenic NDV strains further localized the fusion promotion activity to the central 36% of the protein (Bousse *et al.*, 1995), while chimeric NDV/HPIV3 HN proteins identified an 82-residue "stalk" domain between the transmembrane and globular domains as critical for fusion promotion (Deng *et al.*, 1997; Deng *et al.*, 1995). The stalk has been reported to consist of one or two heptad repeat-type structures (Melanson and Iorio, 2004). Chimeric HPIV2/simian virus 41 (SV41) HN proteins indicated that the 58 membrane-proximal stalk residues were important (Tsurudome *et al.*, 1995), and Sendai/HPIV3 HN chimeras showed that fusion promotion was localized to the 89 membrane-proximal extracellular residues (Tanabayashi and Compans, 1996). Point mutations in HPIV3 HN at P111 (Porotto *et al.*, 2005; Porotto *et al.*, 2003), and NDV HN at L94 (Melanson and Iorio, 2004), both located in the stalk region, were shown to specifically inhibit fusion by affecting the triggering of F. Similarly, introduction of N-linked oligosaccharides into the stalk region inhibited HN-F interactions and membrane fusion, presumably though steric hindrance (Melanson and Iorio, 2006). A specific interaction between the HN stalk region and the F protein was shown using GST-and biotin-bound NDV HN and F peptides.,The HN stalk region physically bound to regions of the F protein including heptad repeat 2 (HR2); mutation of the HN stalk peptide to residues that inhibited fusion promotion in the full-length HN protein also abrogated the HR2-HN stalk interaction (Gravel and Morrison, 2003).

The globular head has often been dismissed as being unimportant for fusion promotion and interaction with the F protein; however, HN proteins containing head domain point mutations and HN chimeras, which bind effectively to sialic acid, have been shown to be fusion-deficient, perhaps suggesting that sequences critical for fusion promotion may also be localized to the globular head (Ferreira *et al.*, 2004; Tsurudome *et al.*, 1995). Recent results show head domain mutations that do not affect binding activity but affect

fusion promotion may be due to temperature-dependent HN multimerization defects, rather than to direct fusion promotion defects (Corey *et al.*, 2003). This may explain the lack of fusion promotion in these receptor binding HN protein mutants. Publication of a crystal structure of HN including the stalk might clear up a great deal of the uncertainty associated with the localization of a defined fusion-promoting domain.

Localization of an HN-interacting domain on the F protein is much less well-studied. Early analyses using chimeras of the HPIV2 and simian virus 41 (SV41) F proteins (Tsurudome *et al.*, 1998), localized HN-interacting domains of the F protein to four partially overlapping fragments, one of which in the extracellular head region between the two heptad repeats (for further details on the F protein and its functionality, see the section below). The second and third regions include the cysteine-rich sequences in the head region, and are overlapping. The fourth region ("M2") contains part of heptad repeat 2 (HR2) and the transmembrane domain. More recent analysis, using HR2 peptide-based pull-down assays, indicated a direct protein-protein interaction between HR2 and the stalk region of the HN protein (Gravel and Morrison, 2003), thereby confirming that the M2 region identified in the chimeras is involved directly in HN-F interactions. This does not preclude a role for other regions of the F protein in HN-F interactions, however, further characterization is necessary to determine conclusively what sections of the F protein are involved. It must also be kept in mind that certain paramyxovirus F proteins are able to fuse independently of HN and it is unclear as to how this is accomplished.

The fusion protein

The requirement for trimerization, cleavage activation, which exposes a highly hydrophobic fusion peptide, and formation of heptad repeat-based coiled coils, or six-helix bundles (6-HB), places paramyxovirus F proteins in a group of viral fusion proteins known

collectively as the "class I viral fusion proteins". In addition to the paramyxovirus F proteins, this group includes retrovirus fusion proteins (e.g. human immunodeficiency virus (HIV) Env/gp41), the orthomyovirus hemagglutinin protein (e.g. influenza virus $HA_{1,2}$), and filovirus fusion glycoproteins (e.g. Ebola $Gp_{1,2}$) (Weissenhorn *et al.*, 1999). Reviews of the properties of paramyxovirus F proteins and of the mechanism of action of class I fusion proteins are presented below.

The F protein of HPIV3 is a type I membrane protein of 539 amino acids, which, like the F proteins of all paramyxoviruses, has an N-terminal signal sequence, 18 amino acids in length, that is cleaved during translation (Lamb and Kolakofsky, 2001). F is synthesized as an inactive precursor (F_0) which is glycosylated during transit through the ER and the Golgi. There are three N-linked glycosylation sites on HPIV3 F populated by complex high-mannose oligosaccharides (Spriggs and Collins, 1990), which have been shown to be critical for infectivity (Tanaka *et al.*, 2006). Trimerization of F_0 into trimers occurs prior to exit from the ER (Russell *et al.*, 1994), and transport of F_0 to the Golgi apparatus occurs though the cell's secretory pathway. Upon entry into the *trans*-Golgi, F_0 is cleaved into the active, disulphide-linked $F_{1,2}$ form by the endogenous cellular subtilisin-like proprotein convertase, furin (Ortmann *et al.*, 1994). The cleavage site on HPIV3 F is located at amino acid position 110, C-terminal to a P-R-T-K-R protease recognition sequence. Interestingly, sequence conservation at the cleavage site among paramyxoviruses is quite high; furin is responsible for cleavage activation of the majority of paramyxovirus F proteins (Rockwell and Thorner, 2004; Panda *et al.*, 2004; Zimmer *et al.*, 2001; Bolt *et al.*, 2000; Li *et al.*, 1998; Bolt and Pedersen, 1998; Nakayama, 1997), with some notable exceptions, including those of HPIV1 and Sendai viruses, which are believed to be cleaved by tryptase Clara (Kido *et al.*, 1999). Similarly, many other class I viral fusion proteins are cleaved by furin, including HIV gp160, influenza HA_0, and the Ebola virus fusion glycoprotein (Rockwell and Thorner, 2004; Moulard and Decroly, 2000; Volchkov *et al.*, 1998; Stieneke-Grober *et al.*, 1992). Cleavage

of HPIV3 F_0 is not complete, as F_0 and $F_{1,2}$ exist in both infected cells and virions (Ebata, 1996). Cleavage of the F protein exposes the hydrophobic fusion peptide, approximately 25 residues in length, which has been shown to form α-helical structures, and is essential for F protein-mediated membrane fusion. When the F protein is activated, the fusion peptide is believed to bury itself in the target cell plasma membrane, acting as a second transmembrane domain; as a result, the F protein bridges the gap between host and viral membranes (Morrison, 2003). Addition of the PIV5 fusion peptide to a soluble protein was sufficient to convert the protein to a membrane-anchored protein (Paterson and Lamb, 1987). F proteins are transported to the cell surface, ready for incorporation into virus particles. As in virus envelopes, HN and F are also fusion-active at the cell surface, causing fusion of the host cell membrane with neighbouring cell membranes, producing large, multi-nucleated cells called syncytia. On both the cell surface and virion envelope surface, $F_{1,2}$ is assumed to become fusion active upon sialic acid binding by the HN protein.

Two 4-3 heptad repeats, structural motifs which have a propensity to form amphipathic α-helices which interact with each other to form coiled coils (Burkhard *et al.*, 2001), are found in the HPIV3 F protein and are critical for fusion activity. Heptad repeat 1 (HR1), approximately 60 residues in length, is located adjacent to the fusion peptide near the N-terminus of F_2. HR2, which is adjacent to the transmembrane domain near the C-terminus of F_2, is approximately 35 amino acids in length. The role of the heptad repeats is detailed below. Between the two heptad repeats is a stretch of protein containing nine cysteine residues that are perfectly conserved in F proteins of all members of the *Paramyxoviridae*. A small highly-conserved domain in this inter-HR stretch was recently shown to be critical in regulating folding, cleavage, and fusogenicity (Gardner *et al.*, 2007). The C-terminus includes the 20-residue trans-membrane domain and a 45-amino acid cytoplasmic tail. The cytoplasmic tail is important for F protein folding, transport, fusion activation and regulation, and is responsible for interaction with the matrix (M) protein. The

M protein interacts with the nucleocapsid, forming a bridge between the nucleocapsid and the envelope prior to viral release (Takimoto and Portner, 2004; Seth *et al.*, 2004; Waning *et al.*, 2004; Seth *et al.*, 2003; Waning *et al.*, 2002; Tong *et al.*, 2002; Lamb and Kolakofsky, 2001; Dutch and Lamb, 2001; Bagai and Lamb, 1996). The F_2 subunit of paramyxoviruses has a role in stabilization of the pre-fusion form of F as well as in triggering fusion (Gardner and Dutch, 2007; Yin *et al.*, 2006; Plemper and Compans, 2003). It has also been proposed that F_2 contains its own heptad repeat (HR-C or HR3), which interacts with HR1 (Chen *et al.*, 2001; Matthews *et al.*, 2000; Lambert *et al.*, 1996). A linear diagram of the F protein is presented in Figure 2, panel B. An alignment of the F protein sequences of several important members of the *Paramyxoviridae*, indicating regions of high similarity, is presented in Figure 3.

Interaction of F with cellular cytoskeletal components is poorly defined, although it was suggested over a decade ago (Sanderson *et al.*, 1995). However, RhoA, a regulatory GTPase of the Rho subfamily involved in cytoskeletal rearrangements (Ridley, 2006), was activated during respiratory syncytial virus (RSV) infection (Gower *et al.*, 2001), and signalling through the RhoA pathway was shown to be essential for syncytium formation (Gower *et al.*, 2005). Similarly, the other Rho subfamily GTPases, Cdc42 and Rac1, were shown to be important for fusion of cells expressing PIV5 and Nipah glycoproteins (Schowalter *et al.*, 2006). HIV gp41 also requires RhoA and/or Rac1 activity for fusion (Pontow *et al.*, 2004; del Real *et al.*, 2004).

Figure 3. Alignment of the F protein sequences of selected members of the family *Paramyxoviridae*. Features of the F protein are indicated by coloured asterisks above the sequence. Viruses and their abbreviations are: Genus *Paramyxovirinae*: **HPIV3** (human parainfluenza virus type 3), **BPIV3** (bovine parainfluenza virus type 3), **HPIV1** (human parainfluenza virus type 1), **Sendai** (Sendai virus or mouse parainfluenza virus type 1), **Hendra** (Hendra virus), **Nipah** (Nipah virus), **Measles_Edm** (measles virus, Edmonston strain), **CDV** (canine distemper virus), **PPRV** (peste-des-petits-ruminants), **Menangle** (Menangle virus), **HPIV2** (human parainfluenza virus type 2), **PIV5** (simian virus 5 or simian parainfluenza virus 5), **Mumps_JL** (mumps virus, Jeryl Lynn strain), **NDV** (Newcastle disease virus). Genus *Pneumovirinae*: **HRSV** (human respiratory syncytial virus), **BRSV** (bovine respiratory syncytial virus), **HMPV** (human metapneumovirus). Identical amino acids are shaded black, similar amino acids are shaded grey. The figure was produced using the Boxshade software program to illustrate a Clustal alignment.

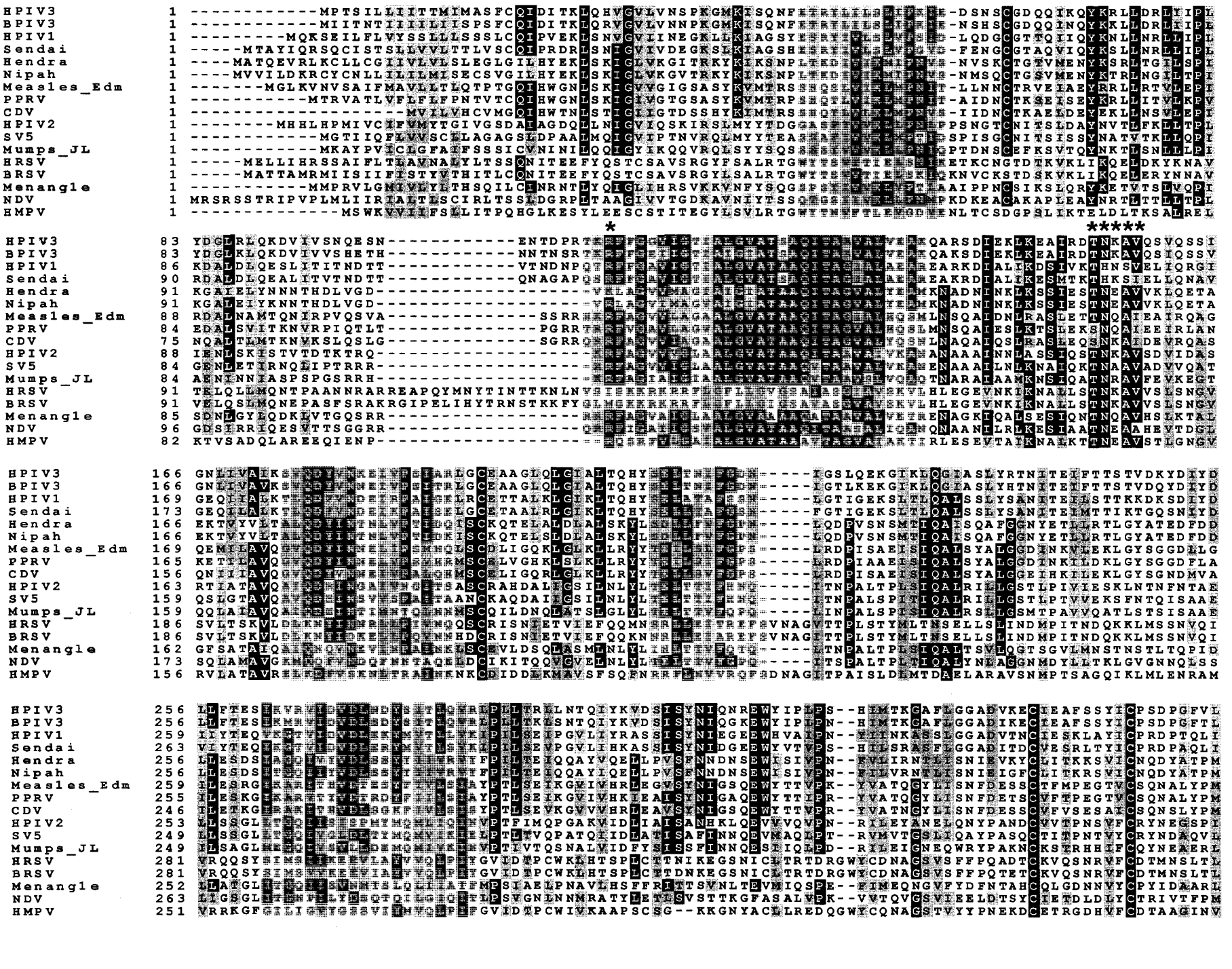
HPIV3
BPIV3
HPIV1
Sendai
Hendra
Nipah
Measles_Edm
PPRV
CDV
HPIV2
SV5
Mumps_JL
HRSV
BRSV
Menangle
NDV
HMPV

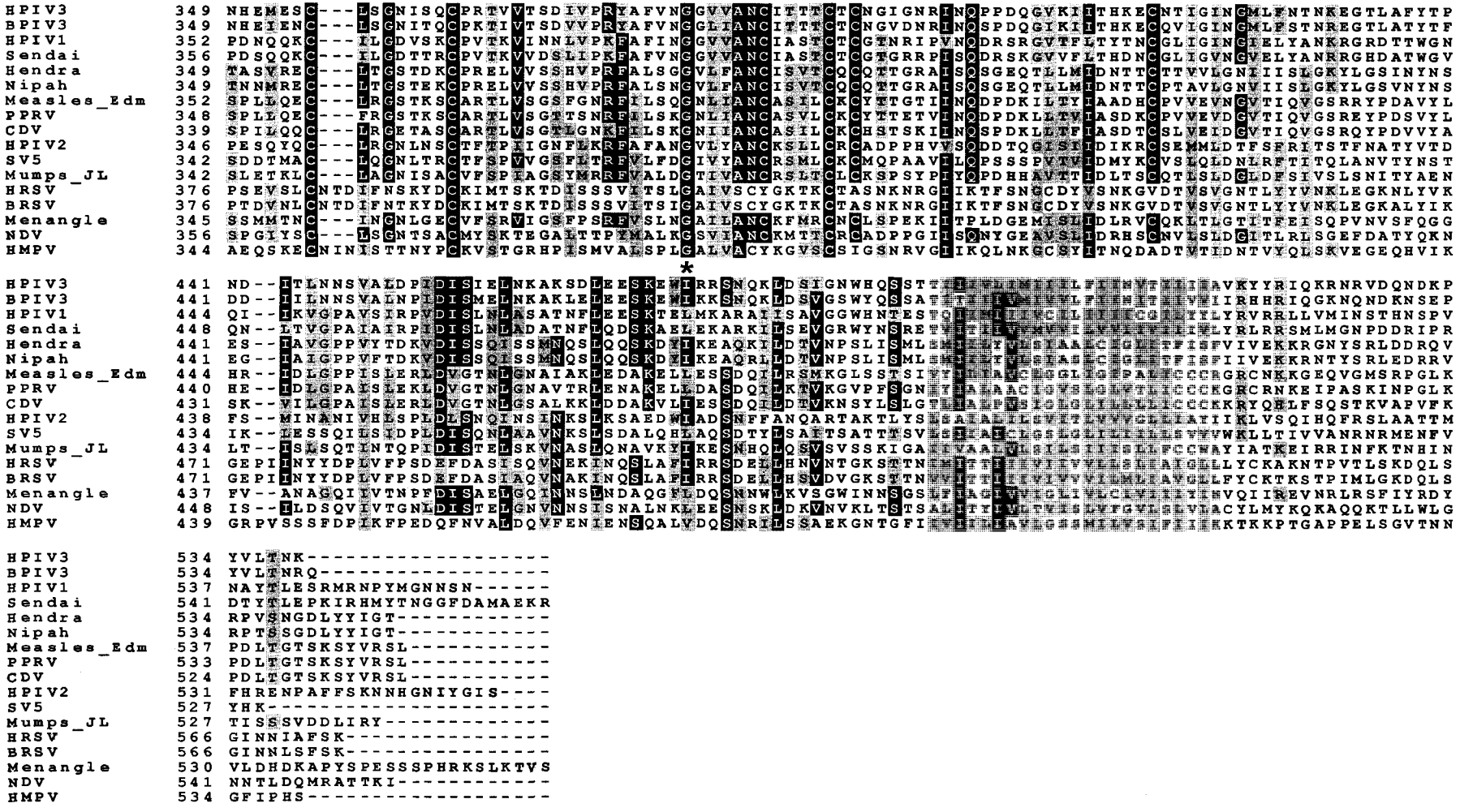

*—— Cleavage site

*—— Conserved binding pocket for I474 and homologues

*—— I474 and homologues

Class I fusion mechanism and properties (with emphasis on paramyxovirus F proteins)

All class I viral fusion proteins share three features: (1) a high-energy metastable trimeric protein conformation, in which the hydrophobic N-terminal fusion peptide has been released by cleavage; (2) a pair of characteristic extracellular 4-3 heptad repeats; and (3) a hydrophobic, protein-anchoring transmembrane domain (Russell and Luque, 2006). It is the characteristic behaviour of the heptad repeats during the fusion process that really defines the paramyxovirus F protein as a class I fusion protein. The three-dimensional structures of several class I viral fusion proteins have been determined but few conformational intermediates have been structurally characterized, leading to speculation about the key conformational changes required for fusion activity.

The first two three-dimensional structures of paramyxovirus F proteins, NDV F (Chen *et al.*, 2001) and HPIV3 F (Yin *et al.*, 2005), were derived for uncleaved, anchorless, secreted proteins. These structures included a 6-HB, which was speculated to exist only in stable, post-fusion forms of the F protein, as it had been predicted that uncleaved F proteins would be unable to achieve this conformation (Lamb *et al.*, 2006). A subsequent structure was obtained for the PIV5 F protein, which was stabilized using a heterologous membrane domain, showing what may be the key pre-fusion, and potentially pre-cleavage structure (Yin *et al.*, 2006). It has been proposed that the earlier structures, while uncleaved, actually represent post-fusion forms of the F proteins (Yin *et al.*, 2006; Russell and Luque, 2006), although it remains unclear how these post-fusion conformations were achieved in the absence of cleavage. It is possible that incubation temperatures, purification conditions, or improper protein modification arising from the use of insect cells to produce the proteins, were responsible for adoption of the post-fusion conformation. It is possible to speculate what conformational intermediates exist between the metastable, pre-fusion structure and the final, stable, post-fusion structure.

The importance of the 6-HB to membrane fusion mediated by paramyxovirus F proteins was demonstrated through early studies targeting the extracellular carboxy-terminal leucine zipper (HR2) for mutagenesis, which abolished fusogenicity while maintaining structural integrity and oligomerization of the F protein (Reitter *et al.*, 1995; Buckland *et al.*, 1992). Similarly, mutagenesis of HR1 produced fusion inactive F proteins without compromising structure or oligomerization (West *et al.*, 2005; Sergel *et al.*, 2001; Dutch *et al.*, 1999; Sergel-Germano *et al.*, 1994). However, the altered conformation of some HR1 mutants (Sergel *et al.*, 2001), suggests that HR1 plays an important role in proper folding of the F protein.

The observation that peptides based on HR1 and HR2 sequences arrest fusion protein function further supports the critical role of heptad repeats in the fusion process. The first peptides derived from class I fusion proteins that were studied were based on HIV gp41 sequences. When cells infected with HIV, or expressing HIV gp120 and gp41, were incubated with peptides based on HR1 sequences, gp41-mediated cell-cell fusion was inhibited (Wild *et al.*, 1994; Wild *et al.*, 1994; Wild *et al.*, 1993; Wild *et al.*, 1992). Mutational analysis of the gp41 peptides showed that their ability to inhibit fusion correlated with their ability to interact with the corresponding heptad repeat sequences of gp41 (Wild *et al.*, 1995). Peptides representing paramyxovirus HR1 and HR2 sequences were subsequently shown to inhibit paramyxovirus infection and F-driven fusion (Porotto *et al.*, 2006b; Bossart *et al.*, 2005; Wang *et al.*, 2005; Bossart *et al.*, 2005; Wang *et al.*, 2003; Yu *et al.*, 2002; San Roman *et al.*, 2002; Young *et al.*, 1999; Dutch *et al.*, 1999; Joshi *et al.*, 1998; Young *et al.*, 1997; Wild and Buckland, 1997; Yao and Compans, 1996; Lambert *et al.*, 1996), although HR2-based peptides generally exhibited stronger inhibitory properties than HR1-based peptides. In many of these studies, a thermostable 6-HB-like complex was formed between HR1 and HR2 peptides, made up of three HR1 and three HR2 molecules, as identified by circular dichroism and SDS-PAGE.

Formation of a 6-HB between HR1 and HR2 is a hallmark of class I fusion proteins. The three-dimensional structures of 6-HB indicate a core trimer of HR1 chains, surrounded by three HR2 chains, packed into the grooves of the HR1 trimer (Yin *et al.*, 2005; Eckert and Kim, 2001; Zhao *et al.*, 2000; Baker *et al.*, 1999; Malashkevich *et al.*, 1998; Chan *et al.*, 1997; Weissenhorn *et al.*, 1997; Tan *et al.*, 1997). Figure 4 is a representation of the HPIV3 6-HB in side, top-down, and bottom-up views, coloured in light (HR1) and dark (HR2) hues to distinguish monomers, based on the model of Yin *et al* (2005). Notable about this model of the HPIV3 6-HB is that the HR1-HR2 interactions are in fact intermonomer heptad repeat interactions. This structure, which is proposed to be a stable post-fusion conformation, also serves to explain the ability of HR peptides to inhibit the fusion process, as reviewed by Eckert and Kim (2001). The current model for fusion inhibition proposes the formation of an *in trans* 6-HB-like complex either between the HR1 sequence in the fusion protein and the exogenous HR2 peptide or between the HR2 sequence in the protein and the exogenous HR1 peptide, preventing the refolding necessary for the *in cis* HR1/HR2 complex to form. Further confirmation of this mode of inhibition comes from studies showing that individual HR peptides, but not pre-formed HR1-HR2 peptide complexes, are able to inhibit fusion (San Roman *et al.*, 2002; Young *et al.*, 1999). In a single study, complexed PIV5 HR1-HR2 peptides appeared to inhibit fusion, however, this may be due to partially uncomplexed peptides (Joshi *et al.*, 1998).

Figure 4. Model of the 6-helix bundle (6-HB) of the HPIV3 F protein. The 6-HB of the HPIV3 F protein structure presented by Yin *et al* (2005) is proposed to be the stable, post-fusion form of the 6-HB, and is reproduced here. (A) Side view. The viral membrane-proximal end is at the bottom of this panel. The head region of the F trimer would be above the bundle. (B) Top-down view. (C). Bottom-up view. Heptad repeat 1 (HR1) is lightly coloured and heptad repeat 2 (HR2) is darkly coloured; HR1 and HR2 from the same F protein monomer are presented as dark and light shades of the same colour. The 6-HB consists of antiparallel helices, with a core trimer of HR1 surrounded by HR2, and is made up of HR1-HR2 dimers from different F protein monomers. The figure was produced using the Deepview Swiss-PDB viewer.

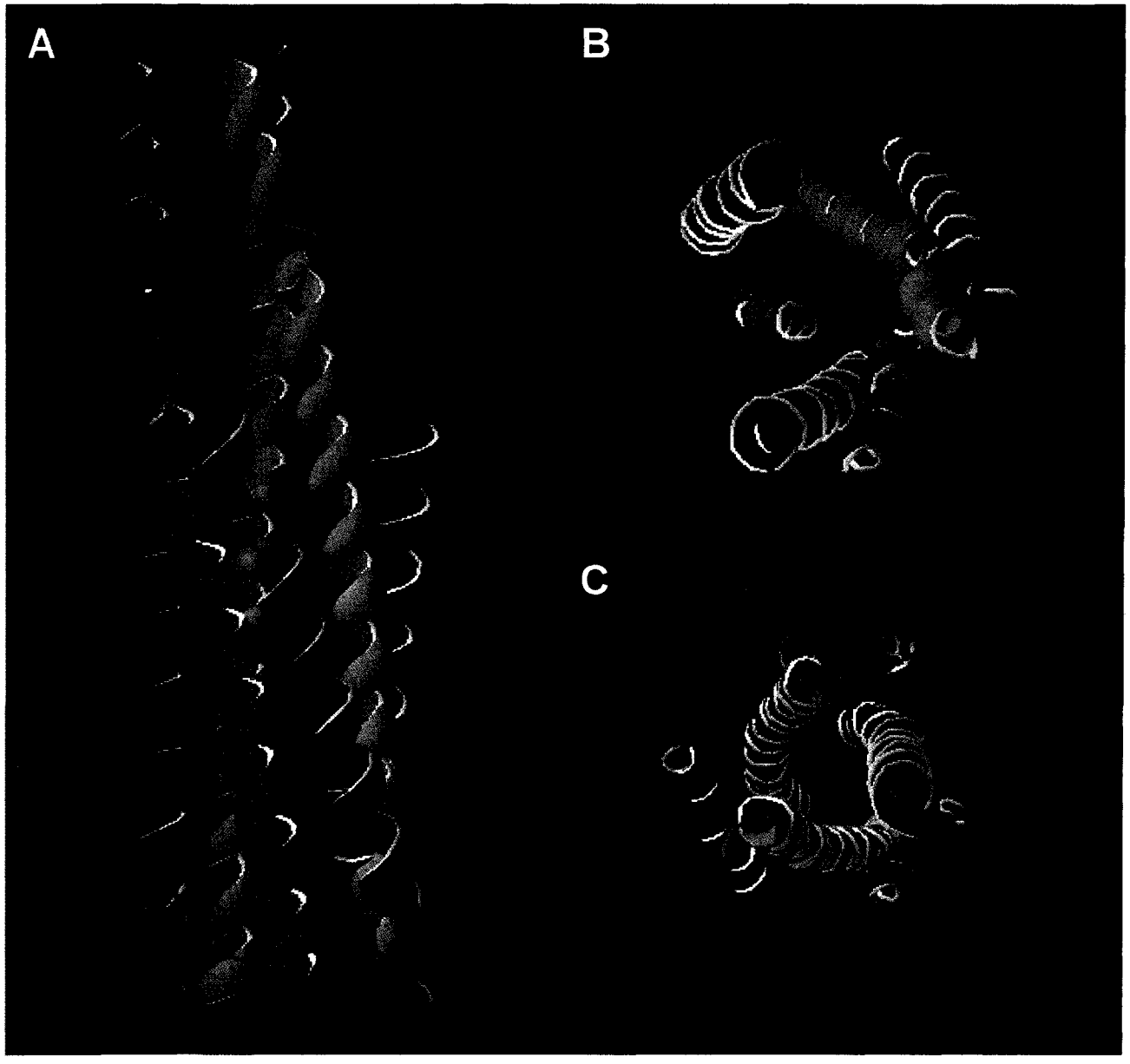
A
B
C

There is evidence for temporal separation of HR1 and HR2-based inhibition. In the presence of the HN protein, HR1 peptide is able to inhibit PIV5 F protein refolding at 4°C, while HR2 peptide is only able to inhibit refolding at 37°C (Russell *et al.*, 2001), suggesting that HR2 in the protein is "available" for HR1 peptide binding at an earlier step in the fusion process, while HR1 requires further conformational changes, presumably induced by a higher fusion-active temperature, to be available for binding by HR2 peptides. Similarly, conformational intermediates of other type I virus fusion proteins have been "trapped" using HR peptides (Earp *et al.*, 2005; Fass, 2003), suggesting that similar folding steps occur for all class I fusion proteins.

In the most recent models for F protein refolding (Russell and Luque, 2006; Lamb *et al.*, 2006; Morrison, 2003), the metastable, fusion-capable (cleaved) but pre-fusion form of the F protein is synthesized and presented on the cell surface as a mushroom-shaped trimer. HN binding to sialic acid results in conformational changes in HN that are transmitted, via a physical interaction between HN and F, to the F protein, through the HR2 domain (Gravel and Morrison, 2003). Conformational changes in the F protein can be monitored by changes in antibody-binding epitopes (Russell *et al.*, 2001). The first proposed event is the "stalk"-like HR2 swinging up and to the outside of the head domain of the F protein, exposing HR2 to HR1-based inhibition. In the pre-fusion conformation of class I fusion proteins, HR1 is not a contiguous helix but is predicted to be divided into multiple structures; in HA, it is a helix-loop-helix (Skehel and Wiley, 2002), and in PIV5 F, it is a combination of α-helix, β-strand, and turns (Russell and Luque, 2006). The pre-fusion form of HR1 has been referred to as a "spring-loaded" structure, ready to rapidly change conformation. Recent evidence indicates that proper folding of HR1 in the pre-fusion F structure is critical to both fusion as well as overall protein conformation (Luque and Russell, 2007). The pre-fusion F structure is then transformed, in a "spring-like" manner, into a triple-stranded coiled-coil made up of HR1 and the fusion peptide in a pre-fusion pre-

hairpin conformation similar to that published for influenza HA (Skehel and Wiley, 2002). Mutation of certain HR1 residues can enhance fusogenicity, presumably by enabling the "spring"-like activity of HR1 early in the fusion process (Luque and Russell, 2007). This new conformation exposes *in situ* HR1, which becomes available for HR2-based peptide inhibition. Peptides in which HR1 sequences are joined to the fusion peptide, which should generate a longer HA-stalk-like structure, exhibit increased fusion of unilamellar vesicles as compared to the fusion peptide itself (Peisajovich *et al.*, 2000; Ghosh and Shai, 1999; Epand *et al.*, 1999), suggesting that HR1 plays an important role in "assisting" the fusion peptide in membrane fusion. Following formation of the stalk-like HR1/fusion peptide structure, the fusion peptide inserts into the target membrane. At this stage, the F protein exists as a protein with each end buried in a membrane: the transmembrane domain in the virion membrane, and the fusion peptide in the target host cell membrane.

The remaining step is retraction of HR1 and HR2 to form the 6-HB, producing the minimum-energy conformation of the F protein; formation of the 6-HB has been proposed to release the free energy necessary to overcome energetic barriers to membrane fusion (Lamb *et al.*, 2006). HR2 residues 442, 447, 449 of PIV5 F have been shown to play a key role in the fusion-driving refolding of F to form 6-HB. Mutation of these residues, which bind tightly into an HR1 cleft in the 6-HB structure, disconnected 6-HB stability from fusogenicity, as some destabilized mutants were hyperfusogenic (Russell *et al.*, 2003). These residues may be part of a domain responsible for conformational switching from fusion-active to post-fusion forms of the protein. Folding of the F protein to form the 6-HB also pulls viral and cellular membranes into close enough proximity for fusion to proceed. Membrane fusion is proposed to occur through a series of complex, separate, but coupled steps, which include membrane dimpling, formation of a fusion stalk, expansion to form a single bilayer/hemifusion diaphragm (HD), expansion of the HD into a fusion pore, and subsequent pore enlargement (Chernomordik and Kozlov, 2003). It is believed that the key

energy barrier may be overcome at the fusion stalk stage using the energy released upon 6-HB formation.

Role of the HN and F glycoproteins in virus release

Following pore formation, the viral nucleocapsid is released into the cytoplasm, where it is replicated and transcribed. Following this, the HN and F glycoproteins are synthesized, and transported to the cell surface. The current model for viral budding implicates the M protein as the "organizer" protein, concentrating the glycoproteins at specific locations, possibly in lipid microdomains such as lipid rafts (Laliberte *et al.*, 2006), and acting as a bridge between the clustered glycoproteins and newly replicated nucleocapsids (Takimoto and Portner, 2004). While expression of the M protein alone of some paramyxoviruses induces budding of virus-like particles (Takimoto and Portner, 2004), the F protein of at least one paramyxovirus, Sendai virus, induces budding on its own (Takimoto *et al.*, 2001), although much higher efficiency budding is observed when M is coexpressed. The combination of nucleocapsid, M, and either HN or F resulted in release of PIV5 virus-like particles (Schmitt *et al.*, 2002). The cytoplasmic tails of HN and F are necessary for M interaction (Ali and Nayak, 2000) as well as for efficient budding and incorporation into virions (Waning *et al.*, 2002; Takimoto *et al.*, 2001; Fouillot-Coriou and Roux, 2000; Schmitt *et al.*, 1999; Cathomen *et al.*, 1998).

Specific objectives

The F protein of paramyxoviruses has been well-characterized as the effector of membrane fusion both in virus-cell fusion and in cell-cell fusion. The overall objective of this dissertation was to further characterize the role of the F protein in, and more specifically,

the regions of the F protein responsible for, the fusion process. Previous studies have shown the importance of the heptad repeats of the F protein to the fusion process. Of particular interest is HR2, which plays a key role in the formation of 6-HB, and can act, in peptide form, as a potent inhibitor of fusion; HR2 may also have a role in the physical interaction with the HN protein. With this information in mind, the first specific objective of this dissertation was to fully characterize the cleavage and fusogenicity of F proteins with mutations at position I474 of HR2, a residue which binds into a highly-conserved pocket on HR1 in the 6-HB. Peptides based on HR1 and HR2 sequences were produced and purified in order to assay 6-HB stability and their inhibitory properties. It was hypothesized that the fusion properties of mutant F proteins and the fusion inhibitory properties of mutant HR2 peptides would be directly related to the stability of 6-HB formed by the mutant HR2 sequences.

The second objective of this study was to develop an assay to probe for HN-F interactions by isolation of native complexes from cells expressing the two proteins. HN was the "bait" protein, tagged with hexahistidine so that nickel-agarose columns could be used to isolate HN-F complexes from cell lysates. The goal of these experiments was to assay the ability of fusion-negative F mutants to form complexes with HN, and to further map critical residues responsible for the HN-F interaction, with the hypothesis that sequences essential for HN-F complex formation and, therefore, for fusion, would be identified.

The third objective of this dissertation was to use chimeras constructed from the closely related human and bovine parainfluenza 3 F proteins to identify regions of the F protein specifically involved in fusion promotion via interaction with HN.

The final objective was to determine the mechanism of HR2-based inhibition of HPIV3 fusion by developing virus mutants resistant to HR2 peptide. The location of mutations conferring resistance to HR2 inhibition in HPIV3 might indicate specific regions of viral proteins involved in the fusion process.

Chapter 2 – Materials and Methods

Cells, viruses, bacterial strains, and culture conditions

Cell lines and culture conditions

HeLaT4 (human cervical adenocarcinoma epithelium-like, expressing the CD4 protein), MDBK (Madin-Darby Bovine Kidney), LLC-MK2 (Rhesus monkey kidney), and CV-1 and Vero (African green monkey kidney) cells were propagated in minimal essential medium (MEM) containing Earle's salts (Sigma, Oakville, ON) supplemented with 0.225% sodium bicarbonate, 10% fetal bovine serum, 2 mM L-glutamine, and 50 µg/ml gentamycin (Invitrogen, Burlington, ON). Cells were passaged at a splitting ratio of 1:5 to 1:10, on average every three days, incubated at 37°C unless otherwise noted. HeLaT4 cells were obtained from the NIAID Aids Research and Reference program (Rockville, MD). LLC-MK2 cells were obtained from Flow Laboratories (Rockville, MD). MDBK and CV-1 cells were obtained from ATCC. Vero cells were provided by Dr. Kathryn Wright (University of Ottawa).

Viruses and propagation

Human parainfluenza virus type 3 (HPIV3, Wash/47885/57, strain C243, ATCC VR-93) was originally obtained by Dr. Ken Dimock from Dr. D.A. McLeod at the Laboratory Centre for Disease Control (Ottawa, ON). Recombinant vaccinia virus strain vTF7-3, encoding the bacteriophage T7 RNA polymerase (Fuerst *et al.*, 1986) was obtained from ATCC, and the vTF7-3 parental vaccinia WR strain was obtained from Dr. Delsworth Harnish at McMaster University (Hamilton, ON). Urabe mumps virus vaccine strain Ur-1004 was obtained from Dr. Kathryn Wright (Brown *et al.*, 1996).

HPIV3 titre was determined by plaque assay by diluting virus in 10-fold steps for infection of cells. Infected LLC-MK2 monolayers were incubated under sterile 0.75%

agarose in MEM (MEM-agarose) overlays for 4 days, fixed using formol saline (15 mM NaCl, 4% (v/v) formaldehyde) and stained with crystal violet for visualization and counting of plaques. HPIV3 was grown in LLC-MK2 cells, and harvested for titration 4-5 days after infection, when significant cytopathology (cytopathic effect, CPE) was observed. Virus was harvested from crude supernatant following centrifugation at 12,000 rpm, 4°C, to pellet cell debris. Plaque purification of HPIV3 was performed by one-hour infection of LLC-MK2 monolayers, which were then covered by sterile MEM-agarose and incubated for 4-5 days at 37°C. Monolayers were stained with 25 µg/ml neutral red dye (Sigma), and a sterile inverted glass Pasteur pipet was used to excise the plaque. The excised agarose was then transferred to a fresh culture of LLC-MK2 cells in one well of a 12-well culture dish, and incubated for 3-4 days until CPE was evident.

Vaccinia vTF7-3 and WR were propagated in CV-1 cells. Cells were infected at an MOI of 0.1 and incubated 2-4 days until lace-like CPE was observed. Cells were then scraped, and subjected to three freeze-thaw cycles, followed by incubation with 0.025% (w/v) trypsin (0.5 mg/ml; Invitrogen, Burlington, ON) at 37°C for 30 minutes to disperse the virus. Vaccinia strains vTF7-3 and WR were titrated in the same manner as HPIV3 on either LLC-MK2 or HeLaT4 cells.

Mumps virus Ur-1004 was provided as a stock of known titre by Dr. Kathryn Wright (University of Ottawa). Titrations were performed by plaque assay using Vero cells, in the same manner as HPIV3.

Plaque reduction assays

Plaque reduction assays were performed at 37°C identically to the plaque assay described above, with the addition of a single step prior to infection where virus was incubated at room temperature in varying concentrations of HPLC-purified HR peptides or GST-HR proteins for 10 minutes, followed by infection of cells with this mixture. 50%

inhibitory concentration (IC_{50}) of heptad repeat and GST-heptad repeat peptides were calculated by extrapolation of inhibitory curves at the point of 50% inhibition.

Multiple-step growth curve

To produce a multiple-step growth curve for HPIV3, confluent LLC-MK2 cells, in 12-well dishes, were infected in triplicate at an MOI of 0.01. Cells were incubated at 37°C. Supernatants were removed and fresh medium placed on the cells, at time points of 0 (which represents one hour post exposure to virus), 12, 24, 48, 72, and 96 hours post-infection. Cell debris was removed from supernatants by centrifugation and the titre of virus in supernatants was determined, in duplicate, for each time point, by plaque assay on LLC-MK2 monolayers.

Bacterial strains, culture and induction conditions

Escherichia coli strains DH5α, SURE, and BL21(DE3) were grown on solid Luria-Bertani (LB) agar, and in liquid LB as described elsewhere (Ausubel *et al.*, 1999). Liquid cultures of *E. coli* were always incubated at 37°C, with shaking at 180-250 rpm. Protein expression was induced in BL21(DE3) by addition of 100 mM IPTG to fresh cultures when the OD_{600} reached 0.3-0.5, and the bacteria were harvested by centrifugation, 4-6 hours after induction.

Molecular biology – plasmid constructions, PCR amplifications, and sequencing

Plasmid constructions

FLAG epitope-tagged HPIV3 F protein was constructed by Bogna Zolkiewska by PCR amplification of a portion of the F coding sequence in the expression vector pIBI-F (Cote, 1989). pIBI-F plasmids expressing untagged F proteins containing mutations at position I474 were constructed by Dr. Sharon Ebata using Kunkel mutagenesis (Ebata,

1996). FLAG-tagged forms of the mutant F proteins were constructed by replacing an *Xba*I-*Nde*I fragment in pIBI-F-FLAG with the corresponding fragments containing the I474 mutations.

HPIV3 HN coding sequences were cloned into the pCITE-2a vector with assistance from Dr. Reza Nokhbeh, generating plasmid pCITE-HN. FLAG and His_6 tags were added to HN coding sequences by insertion of a double-stranded oligonucleotide between the *Pst*I and *Bam*HI sites of pCITE-HN. Sequences of all primers used in this dissertation are found in Table 2. The expression of HN and F sequences in pCITE-HN and pIBI-FLAG are under the control of the T7 RNA polymerase promoter.

Sequences representing HR1 and HR2 of the HPIV3 F protein were amplified by PCR as *Bam*HI-*Xho*I fragments, which were inserted between the *Bam*HI and *Xho*I sites of pGEX-4T-3 (GE Healthcare, Piscataway, NJ) by Christine Grisé, yielding plasmids encoding recombinant GST fusion proteins with C-terminal HR sequences that could be cleaved from GST using thrombin or factor Xa. Mutant HR2 and bovine parainfluenza virus 3 (BPIV3) HR1 and HR2 sequences were amplified and cloned using an identical approach.

5'-*Nco*I, 3'-*Bam*HI, and internal *Afl*II and *Sal*I restriction sites were introduced into the HPIV3 F coding sequences, in pIBI-F-FLAG, by Kris H.K. Chan and Reza Nokhbeh using site-directed mutagenesis. Introduction of identical sites into BPIV3 F sequences was performed by PCR amplification of short stretches of BPIV3 F sequences using primers that included the desired restriction sites and the 3' FLAG coding sequences, using pGEM-bPIV3 F as a template (kindly provided by Dr. Dongwon Yoo, University of Guelph, Guelph, ON). Three-part F gene chimeras were constructed by swapping *Nco*I-*Afl*II, *Afl*II-*Sal*I or *Sal*I-*Bam*HI fragments as required.

Table 2. List of oligonucleotides

Oligonucleotide	Sequence (5'-3')	Usage
HN-Flag-His_6 fwd	GCGACTATAAAGACGACGACGACAAA*CACCACCACCAC CACCAC***TAA**T[1]	Insertion of FLAG and His6 into HN
HN-Flag-His_6 rev	GATCATT**A***GTGGTGGTGGTGGTGGTG*TTTGTCGTCGTC GTCTTTATAGTCGCTGCA[1]	
XaFN(+)	ACACACGGATCC*ATCGAAGCTCGT*ACAGCGGCAGTTGC TCTG[2]	PCR-based constructs of GST-HR1 and HR2 fusions – HPIV3 F, I474 mutants, and BPIV3 F
XaFN(-)	ACACACCTCGAGT**CATCA**ACCTAATCTCGCAATTGATG G[2]	
XaBFN(+)	ACACACGGATCC*ATCGAAGCTCGT*ACCGCAGCAGTCG CTCTT[2]	
XaBFN(-)	ACACACCTCGAGT**CATCA**ACCTAATCTTGTGATTGAAG G[2]	
XaFC(+)	ACACACGGATCC*ATCGAAGCTCGT*TCTGTTGCACTTGA TCCAATT[2]	
XaFC(-)	ACACACCTCGAGT**CATCA**ATGCCAATTTCCAATGGAAT C[2]	
XaBFC(+)	ACACACGGATCC*ATCGAAGCTCGT*TCTGTTGCCCTTAA TCCGATT[2]	
XaBFC(-)	ACACACCTCGAG**TCATCA**ATACCAACTTCCAACAGAAT C[2]	
NcoI-fwd-bRgI	CACACACCATGGTCATCACAAACACAATCATA[3]	PCR-based constructs of bovine chimera regions
AflII-rev-bRgI	CACACACTTAAGCCCAGCTGCTTCACAACCTA[3]	
AflII-fwd-bRgII	CACACACTTAAGCTAGGAATTGCATTAACCCA[3]	
SalI-rev-bRgII	CACACAGTCGACTTTATAAATTTGAGTATTTG[3]	
SalI-fwd-bRgIII	CACACAGTCGACTCTATATCATACAACATACA[3]	
BamHI-rev-bRgIII	CACACAGGATCC**TCA**TTTGTCGTCGTCGTCTTTATAGTC TTGTC[3]	
AB138	TCAAAAGAGATTGGCAACAC	RT-PCR of HR2-resistant HPIV3 F
AB141	GAATTAACAAACATATTCGG	
AB147rev	TGCCCCTTTTGTCATGATGT	
BamHI-hF-rev	GGATCCTTTTTTATAATTTTAATATCTAAT	

[1]- the sequence encoding FLAG is underlined, the hexahistidine coding sequence is italicized, and the stop codon is in bold; [2]- the sequence encoding the *Bam*HI or *Xho*I restriction sites are underlined, the stop codon is in bold, and the sequence encoding the factor Xa recognition site is italicized; [3]- the sequence encoding the *Nco*I, *Afl*II, *Sal*I, or *Bam*HI restriction sites are underlined, and the stop codon is in bold.

All constructs were confirmed by sequence analysis performed by the University of Ottawa Biotechnology Research Institute (Ottawa, ON) or the Ontario Genomics Innovation Centre (Ottawa, ON).

RNA isolation, reverse transcriptase-PCR amplification, and standard PCR amplifications

PCR amplifications were performed as described elsewhere (Ausubel *et al.*, 1999), with modifications as needed. *Taq* DNA polymerase was variously obtained from Roche (Laval, QC), Invitrogen, or from Alp Oran (University of Ottawa). Thermal cycling was done using a Techne Progene thermal cycler (Burlington, NJ).

RNA was extracted from HPIV3-infected cells in 24-well, 12-well, and 6-well dishes, or 35 mm dishes, using the Trizol reagent (Invitrogen), as recommended by the manufacturer. All solutions coming into contact with RNA were treated with diethyl-pyrocarbonate (DEPC) prior to use. Reverse transcriptase (RT) reactions were performed on alcohol-precipitated RNA, using MMLV RT enzyme (Invitrogen) and RNase inhibitor (Invitrogen or Promega, Madison, WI) for cDNA sythesis. Both oligo-dT and 3' gene-end specific oligonucleotides were used to prime cDNA synthesis. cDNA was used as template for PCR amplification using primers designed to produce full-length or partial F gene products. Amplification of full-length F sequences was inconsistent so confirmatory sequence analysis was done with partial F gene products that were simultaneously amplified.

Protein expression analysis, purification and detection

Ttransfection and protein expression in cell culture

All transfections were done using HeLaT4 cells. Cells in 6-, 12-, or 24-well, or 35 or 100 mm dishes were transfected using Lipofectin (Invitrogen) according to the manufacturer's recommendations, and then infected with vaccinia virus vTF7-3 at a MOI of

5. For simplicity, throughout the dissertation, transfected and infected cells will be referred to as transfected cells, since no transfections in the absence of vTF7-3 infection were done in this study.

Expression and transport of wild-type and mutant F proteins to the cell surface were verified previously by Dr. S. Ebata using cell-surface and intracellular immunofluorescence microscopy and by cell-surface flow cytometry, using monoclonal antibodies specific for the HPIV3 F protein (Ebata, 1996).

Expression and transport of HN proteins to the cell surface was verified by guinea pig or human erythrocyte (RBC) hemadsorption using either glutaraldehyde-fixed guinea pig RBC (Research Diagnostics Inc., Flanders, NJ) or fresh human RBC. Blood was drawn from volunteers using heparin-sulphate vacutainers (kind gifts of Dr. Leo Filion) to prevent clotting, transferred on ice to centrifuge tubes, and centrifuged for 5 minutes at 2,000 x g to separate RBC from the plasma and buffy coat, which were removed. The RBC pellet was resuspended in cold TBS at a concentration of 0.5-1.0% (v/v) and kept on ice until required. For hemadsorption, briefly, HeLaT4 cells transfected with plasmids encoding HN were incubated overnight at 37°C, washed with tris-buffered saline (TBS - 25 mM Tris-HCl pH 7.2, 137 mM NaCl, 5.6 mM glucose, 5.0 mM KCl, 0.7 mM Na_2HPO_4), mixed with various volumes of prepared RBC in TBS, and incubated at 4°C for 30-45 minutes. Monolayers were then vigorously washed multiple times with cold TBS. Hemadsorption was visualized by light microscopy. Hemadsorption was considered positive if clumps of RBC were observed "stuck" to the HeLaT4 cells.

Brefeldin A (BFA; Sigma) was used as a Golgi apparatus-disturbing agent. BFA, dissolved in methanol at a concentration of 10 mg/ml, was applied to cells overnight at a concentration of 10 µg/ml. Control cells were treated with an equivalent volume of methanol only.

SDS-PAGE and western immunoblotting

Cell lysates were analyzed for protein expression by Western immunoblotting. Transfected cells were incubated overnight at 37°C. Cell lysates were prepared by lysis in 50mM phosphate buffer (pH 8.0) containing 100 mM NaCl and detergents at the indicated concentrations. Proteins in lysates were denatured by boiling for 5 minutes at 99°C in loading buffer containing 2-mercaptoethanol or dithiothreitol, and separated on discontinuous 9-12% polyacrylamide gels (SDS-PAGE) as described elsewhere (Ausubel *et al.*, 1999; Laemmli, 1970). Proteins were either stained using Coomassie blue or Gelcode Blue (Pierce, Rockford, IL), or transferred to PVDF membrane (Bio-Rad, Missisauga, ON) by overnight electrotransfer at 30 V in Western transfer buffer (25 mM Tris, 192 mM glycine, 20% (v/v) methanol). After protein transfer, membranes were incubated with 3% (w/v) BSA in TBS to block non-specific antibody binding. Membranes were then incubated with the primary antibody, usually a mouse monoclonal antibody specific for the FLAG epitope (M2, Sigma), diluted 1:10,000 in 3% BSA-TBS, for one hour at room temperature, with rocking. Binding of FLAG-specific antibody was visualized by two methods. Initially, one-hour incubation with alkaline phosphatase-conjugated goat anti-mouse antibodies in 3% BSA-TBS at a dilution of 1:10,000, together with the colourimetric nitroblue-tetrazolium (NBT)/5-Bromo-4-chloro-3-indolyl phosphate (BCIP) detection system (Pierce), was used to detect immunoreactive protein bands. Subsequently, the more sensitive enhanced chemiluminescence (ECL) method was used in concert with horseradish peroxidase-conjugated goat anti-mouse secondary antibodies (Sigma), diluted 1:10,000 in 3% BSA-TBS, incubated for one hour at room temperature. The ECL reagent was prepared by mixing 5 mL of "solution A" (100 mM Tris pH 8.5, 0.03 % (v/v) hydrogen peroxide) with 5 mL of "solution B" (100 mM Tris pH 8.5, 0.2 mM coumaric acid, 1.5 mM luminol). Membranes were incubated in the ECL reagent for 3-5 minutes, then exposed to film (Chronex film, Dupont, Wilmington, DE; X-OMAT film, Kodak, Rochester, NY; or Hybond ECL film, GE

Healthcare, Piscataway, NJ). Immunoreactive bands were visualized when film was developed.

Cleavage of F proteins was assessed by densitometric analysis of developed Western blots using AlphaEase software, using the spot densitometry analysis settings, according to the manufacturer's instructions (Alpha Innotech, San Leandro, CA).

Nickel affinity column chromatography

HeLaT4 cells transfected with plasmids expressing HN, F, and/or F mutants, in various combinations, were prepared for nickel (Ni) affinity column chromatography as follows. After overnight incubation, monolayers were scraped from the culture dishes, cells were pelleted by centrifugation at approximately 500 x g, washed once in TBS, and once in phosphate lysis buffer (50 mM sodium phosphate pH 8.0, 100 mM NaCl) containing no detergents. Cells were then lysed on ice in phosphate buffer containing 10 mM imidazole and 1 mM PMSF, in the presence of one of several different detergents: Nonidet P-40 (NP-40), 1 mM; Tween-20, 1 mM; Tween-80, 1 mM; Triton X-100, 1 mM; 1-O-n-dodecyl-β-D-glucopyranosyl(1-4) β -D-glucopyranoside (n-dodecylmaltoside), 10 mM; or 1-O-n-Octyl- β -D-glucopyranoside (octyl glucoside), 32 or 46 mM. All detergents were purchased from Roche Diagnostics (Laval, QC). Lysates were cleared by centrifugation at 12 000 x g, 4°C. Cell lysates were loaded onto 0.2 volumes of Ni-NTA superflow agarose (Qiagen, Mississauga, ON) that had been equilibrated with lysis buffer, in plastic Polyprep columns (Bio-Rad, Mississauga, ON). Columns were sealed and rotated at 4°C overnight. Columns were washed three times with five column volumes of wash solution (50 mM sodium phosphate pH 8.0, 300 mM NaCl, 50 mM imidazole, containing the appropriate detergent). Bound proteins were eluted with five column volumes of elution buffer (50 mM sodium phosphate pH 8.0, 300 mM NaCl, 250 mM imidazole, containing detergent), or with low pH elution solution (50 mM sodium phosphate pH 4.0, 300 mM NaCl containing detergent).

Equivalent volumes from each collected fraction were analyzed by SDS-PAGE and Western immunoblotting.

Peptides, purification, and testing of 6-helix bundles

Purification of GST-HR2 and HR2 by glutathione affinity chromatography and HPLC

Following induction of *E. coli* BL21(DE3) transformed with pGEX-4T-3 (GE Healthcare), or pGEX-4T-3 constructs encoding GST-HR1 or GST-HR2, cells were pelleted at 8000 x g, resuspended and lysed in Bugbuster reagent (EMD Biosciences, Madison, WI) according to the manufacturer's recommendations. GST proteins were bound to glutathione-sepharose 4B beads (GE Healthcare) at room temperature in sterile 15 mL centrifuge tubes, with rotation, for 1-2 hours. Beads were washed twice with phosphate-buffered saline (PBS, 137 mM NaCl, 2.7 mM KCl, 4.3 mM Na_2HPO_4, 1.4 mM KH_2PO_4). For purification of GST, GST-HR1 and GST-HR2, columns were then incubated at 4°C overnight in glutathione elution buffer (50 mM Tris pH 8.0, 10 mM reduced glutathione (Sigma)). Eluted proteins were quantified using the Bio-Rad Bradford-based protein assay kit. For purification of HR peptides, the peptides were released from GST by digestion for 14-16 h at 4°C with one unit of thrombin (Sigma) in 100 µL thrombin cleavage buffer (20 mM Tris-HCl pH 8.4, 0.15 M NaCl, 2.5 mM $CaCl_2$). Eluates were directly loaded onto a C4 column for reverse-phase HPLC (Varian, Palo Alto, CA) using a linear gradient of acetonitrile/water (from 90% water/10% acetonitrile to 90% acetonitrile/10% water) to purify peptides. Eluted peptides were dried under vacuum and resuspended in sterile PBS. Protein concentration was quantified by absorbance at 280 nm using the equation (Gill and von Hippel, 1989):

$$\text{mg/ml} = \frac{(0.5 \times \text{absorbance units}) \times (\text{dilution}) \times (\text{molecular weight of peptide})}{(\#\text{ of Trp residues} \times 5560) + (\#\text{ of Tyr residues} \times 1200)}$$

Assay of 6-HB formation

Formation of HR1- HR2 complexes was analyzed by multiple assays, depending on the degree of accuracy required. The simplest method was to mix crude GST-HR1- and GST-HR2-expressing *E. coli* Bugbuster lysates, followed by SDS-PAGE, without sample boiling. High MW complexes were visualized following Coomassie staining. Alternatively, GST-HR1 and GST-HR2 proteins in eluates from the glutathione-sepharose columns were mixed and analyzed by SDS-PAGE with Coomassie staining, or HR1 and HR2 peptides in eluates following thrombin cleavage were mixed and analyzed by electrophoresis in discontinuous tris-tricine SDS-polyacrylamide (16.5%) gels and silver staining (Ausubel *et al.*, 1999). Analysis of thermostability by circular dichroism (CD) of 6-HBs formed by HR1 and HR2 was carried out by Drs. Mark Wurth and Rebecca Dutch at the University of Kentucky. HPLC-purified HR1, and wild-type or mutant HR2 peptides, were mixed in equimolar (1 μM) amounts at 4°C for 30 min. The stability of each 6-HB was measured by monitoring the CD signal at 222 nm as the temperature was increased from 4-99°C at a rate of 1°C/min. CD spectra were recorded on a Jasco J-810 spectropolarimeter controlled with a Pelltier heating base. Baseline values for the individual peptides were recorded prior to thermal melts.

Quantitative contents-mixing fusion assays and fusion inhibition by HR peptides

Fusogenicity of wild-type and mutant F proteins was assayed in HeLaT4 cells, using a modified quantitative β-galactosidase reporter fusion assay (Bossart and Broder, 2004; Nussbaum *et al.*, 1994). Briefly, HeLaT4 cells were transfected with pCITE-HN-FLAG-His_6 and pIBIF-FLAG (encoding wild-type or mutant F proteins) in 24-well dishes, at an empirically optimized plasmid mass ratio of 10:1 (HN:F) (Ebata, 1996), and then infected with vTF7-3 at a MOI of 5 PFU/cell. Concurrently, HeLaT4 cells in 100-mm dishes were transfected with plasmid pG1NT7 (a gift of Dr. B. Moss, NIAID (Fuerst *et al.*, 1986)), in

which the β-galactosidase gene is under the control of the T7 RNA polymerase promoter, and infected with vaccinia virus WR at a MOI of 5 to prevent infection by vTF7-3 when cells were mixed. Cells were incubated 5-8 hours, and the pG1NT7-transfected cells were trypsinized, washed and added to monolayers of pCITE-HN/pIBIF-FLAG-transfected cells, in approximately equal numbers. Cells were incubated for 90 minutes at 37°C, washed, lysed with 0.5% NP-40, and the lysates were assayed for β-galactosidase activity using cholorophenol red β-D-galactoside (CPRG) (Roche). The rate of CPRG hydrolysis was measured spectrophotometrically at 540 nm. To assay fusion inhibition by GST-HR fusion proteins and by HR peptides, filter-sterilized GST-HR proteins or vacuum-dried and resuspended peptides were added to the pG1NT7-transfected cells immediately prior to their addition to the HN/F-transfected cells.

Generation of HR2 resistance in HPIV3

Development of resistance to HR2 of HPIV3 was done by serial passaging of HPIV3 in LLC-MK2 cells in the presence of increasing concentrations of GST-HR2 protein. All steps of the peptide selection were done in parallel with GST alone as a control. Initially, LLC-MK2 cells in 12-well dishes were infected with HPIV3 in the presence of 20 μM GST-HR2 (or GST), approximately 20 times the IC_{50} of GST-HR2 for HPIV3. With each passage, the concentration of GST-HR2 was increased by 10 μM, until the sixth and final passage, at which the concentration of GST-HR2 was 70 μM. For each passage, HPIV3, at an MOI of 0.1, was incubated in Optimem (Invitrogen) containing GST-HR2 protein for 10 minutes at room temperature. The mixture was then diluted approximately 1:3 with complete cell growth medium, and added to cells. Cells were incubated for 4-5 days, until visible CPE was noted. At each passage, the virus-containing supernatant was collected, centrifuged at 12,000 x g to remove cell debris, and virus titre was determined by plaque assay prior to further passage. Prior to plaque purification, supernatants were tested for population

resistance to peptide using the plaque reduction assay described above, in the presence of 10 μM GST-HR2.

Viruses were plaque purified from passages 4 and 6 as described above. Two plaque-purified HPIV3 clones were propagated in the presence of 70 μM GST or GST-HR2 and named 70-GST-6.70.1 and 70C-6.70.1, respectively. The remaining clones were propagated in the absence of peptide. Growth properties of the plaque-purified clones were analyzed using a multiple-step growth assay, as described above, and clones were individually tested for their resistance to 10 μM GST-HR2 using the plaque reduction assay.

Chapter 3 – Characterization of HPIV3 F protein mutants at position I474 of heptad repeat 2

Introduction

Fusion of the viral envelope with a cellular membrane is a critical early step in the life cycle of enveloped viruses. For members of the family *Paramyxoviridae*, such as HPIV3, the fusion and attachment glycoproteins are the effectors of virus entry; membrane fusion is mediated by the F glycoprotein following attachment to the host cell receptor by the HN glycoprotein. The HPIV3 F protein is synthesized as an inactive precursor (F_0) that trimerizes in the endoplasmic reticulum and is transported to the Golgi apparatus, where it is cleaved by the protease furin (Ortmann *et al.*, 1994), into a complex of disulphide-linked subunits ($F_{1,2}$), and subsequently transported to the cell surface. The F_1 subunit contains several structural motifs essential for fusion activity: (1) a hydrophobic fusion peptide at the N terminus immediately downstream of the cleavage site; (2) heptad repeat 1 (HR1), which abuts the fusion peptide, and (3) heptad repeat 2 (HR2), which is immediately upstream of (4) a carboxy-proximal transmembrane domain. Receptor binding is believed to result in conformational changes in the HN protein that induce a series of conformational changes in the F protein, leading to fusion of the viral envelope with the plasma membrane (Morrison, 2003).

Recently solved three-dimensional structures of paramyxovirus F proteins, in what are hypothesized to be pre-cleavage, pre-fusion (Yin *et al.*, 2005) and post-fusion (Yin *et al.*, 2006) conformations, provide evidence supporting a model of paramyxovirus membrane fusion (recently reviewed by Russell & Luque, 2006) in which the pre-fusion form of F is predicted to be a meta-stable mushroom-shaped molecule (Yin *et al.*, 2006). Once conformational changes in $F_{1,2}$ are triggered by receptor binding, several intermediates are believed to form, including a transient, energetically unfavourable structure in which HR1

adopts a triple stranded coiled-coil. This transient structure allows the fusion peptide to bury itself into the target cell membrane. Formation of the exposed HR1 coiled-coil is rapidly followed by formation of a coiled-coil trimer of HR1/HR2 dimers, known as the six-helix bundle (6-HB). The 6-HB is a defining characteristic of class I viral membrane fusion proteins, which include paramyxovirus F proteins, retrovirus envelope glycoproteins, and coronavirus spike proteins (Harrison, 2005; Earp *et al.*, 2005). The predicted pre-fusion structure of the simian parainfluenza virus 5 (PIV5) F protein suggests that HR1 is folded into the globular head of the trimer, that HR2 exists as a rigid, exposed stalk at the base of the head, and that the 6-HB is not formed until receptor binding-induced conformational changes occur (Yin *et al.*, 2006). The 6-HB, which is considered to be a post-fusion conformation, is energetically favoured, and its assembly is believed to be a critical step in the fusion process (Morrison, 2003; Baker *et al.*, 1999). The critical importance of HR1/HR2 interactions and 6-HB formation is supported by the fact that peptides derived from paramyxovirus HR2 sequences inhibit both infection by the homologous virus and membrane fusion mediated by F proteins (Porotto *et al.*, 2006a; Zhu *et al.*, 2005; Bossart *et al.*, 2005; Wang *et al.*, 2005; Wang *et al.*, 2003; Yu *et al.*, 2002; Bossart *et al.*, 2002; San Roman *et al.*, 2002; Lambert *et al.*, 1996). Also, HR1 and HR2 peptides have been shown to form 6-HB *in vitro* (Zhu *et al.*, 2005; Wang *et al.*, 2005; Liu *et al.*, 2004; Xu *et al.*, 2004a; Zhu *et al.*, 2003; Zhu *et al.*, 2002; Joshi *et al.*, 1998).

It has been proposed that the stability of the 6-HB is a critical determinant of F protein fusogenicity (Morrison, 2003). Here, an isoleucine located at a base heptad a-residue (I474) in HR2 of the HPIV3 F protein was targeted for mutagenesis. Based on the three-dimensional structure of the HPIV3 F protein published by Yin *et al.* (2006), I474 interacts with a TNxAV motif in HR1, which is well-conserved in F proteins of other members of the family *Paramyxoviridae*. It was hypothesized that mutation of I474 might disrupt formation of the 6-HB and subsequently affect fusogenicity of the F protein. While it

was not anticipated, some I474 mutations inhibited F_0 cleavage; as a result, an additional hypothesis was developed, that HR2 also acts as a key stabilizer for the pre-cleavage structure of F, which is recognized and cleaved by furin.

Results

Inhibition of HPIV3 infection and HPIV3 F protein-mediated fusion by HR2 peptides

A five-amino acid stretch, TNKAV, between residues 154 and 158 in HR1 of the HPIV3 F protein that is well-conserved in the F proteins of other members of the family *Paramyxoviridae,* was identified. Analysis of the three-dimensional structure of the HPIV3 F protein showed that this motif accommodates the side chain of I474 in HR2 (Yin *et al.*, 2005). Therefore, HPIV3 F proteins with mutations at residue I474 in HR2 were produced (Ebata, 1996), generating the following mutants: I474V, I474A, I474G, I474S, I474D and I474E. The effects of these substitutions on the ability of HR2 peptides to interfere with HPIV3 infection and with HPIV3 F protein-mediated cell-cell fusion were tested.

HR1 and HR2 peptides were produced as carboxy terminal fusions to GST (the wild-type HR1 and HR2 GST fusions, GST-HR1 and GST-HR2, were constructed by Christine Grisé), and were purified by glutathione elution from glutathione-agarose beads. HR1 and HR2 peptides were released from GST by cleavage with thrombin and purified by reverse-phase HPLC. GST-HR1 and GST-HR2, and HR1 and HR2 peptides were incubated with 50-100 PFU of HPIV3 for 10 minutes at room temperature and the virus/peptide mixtures were used to infect LLC-MK2 cells. The extent of plaque reduction was determined as compared to plaque formation in the absence of peptide. Wild-type HR2 (I474) showed a clear, dose-dependent inhibition of HPIV3 plaque formation (Figures 5 and 6, panels A and B) with a 50% inhibitory concentration (IC_{50}) value of approximately 890 nM for GST-HR2 and 8 nM for HR2 peptide alone, similar to IC_{50} values reported previously for HR2 peptides of HPIV3 and other paramyxoviruses (Porotto *et al.*, 2006a; Zhu *et al.*, 2005; Bossart *et al.*, 2005; Wang *et al.*, 2005; Wang *et al.*, 2003; Yu *et al.*, 2002; Bossart *et al.*, 2002; San Roman *et al.*, 2002; Lambert *et al.*, 1996). IC_{50} values required for plaque reduction for the various peptides are listed in Table 3. Note that the plaque reduction assay was approximately 100-fold more sensitive for purified HR2 peptides than for

Figure 5. Inhibition of HPIV3 infection and HN/F-driven cell-cell fusion by HR peptides. Panels A and B: Plaque reduction by HR peptides. HPIV3 (50-100 PFU) was incubated in the presence or absence of the indicated HR peptide (representing HR1 and HR2 sequences from the HPIV3 F protein) and then used to infect LLC-MK2 cells. Cells were fixed and stained, and plaques were counted 4-5 days post-infection. (A) Plaque reduction by peptides with non-polar amino acid substitutions at position I474. (B) Plaque reduction by peptides with polar amino acid substitutions at position I474. Panels C and D: Inhibition of cell-cell fusion by HR peptides. HeLaT4 cells expressing HPIV3 HN and F glycoproteins were mixed with HeLaT4 cells transfected with plasmid pG1NT7 (encoding β-galactosidase) in the presence or absence of the indicated HR peptide. (C) Fusion inhibition by peptides with non-polar amino acid substitutions at position I474. (D) Fusion inhibition by peptides with polar amino acid substitutions at position I474. Results obtained with wild-type HR1 and HR2 peptides are presented in all panels for comparison, and are bolded for emphasis. Data in all panels is the average of at least three separate experiments, using duplicate samples for each experiment, ± the standard deviation.

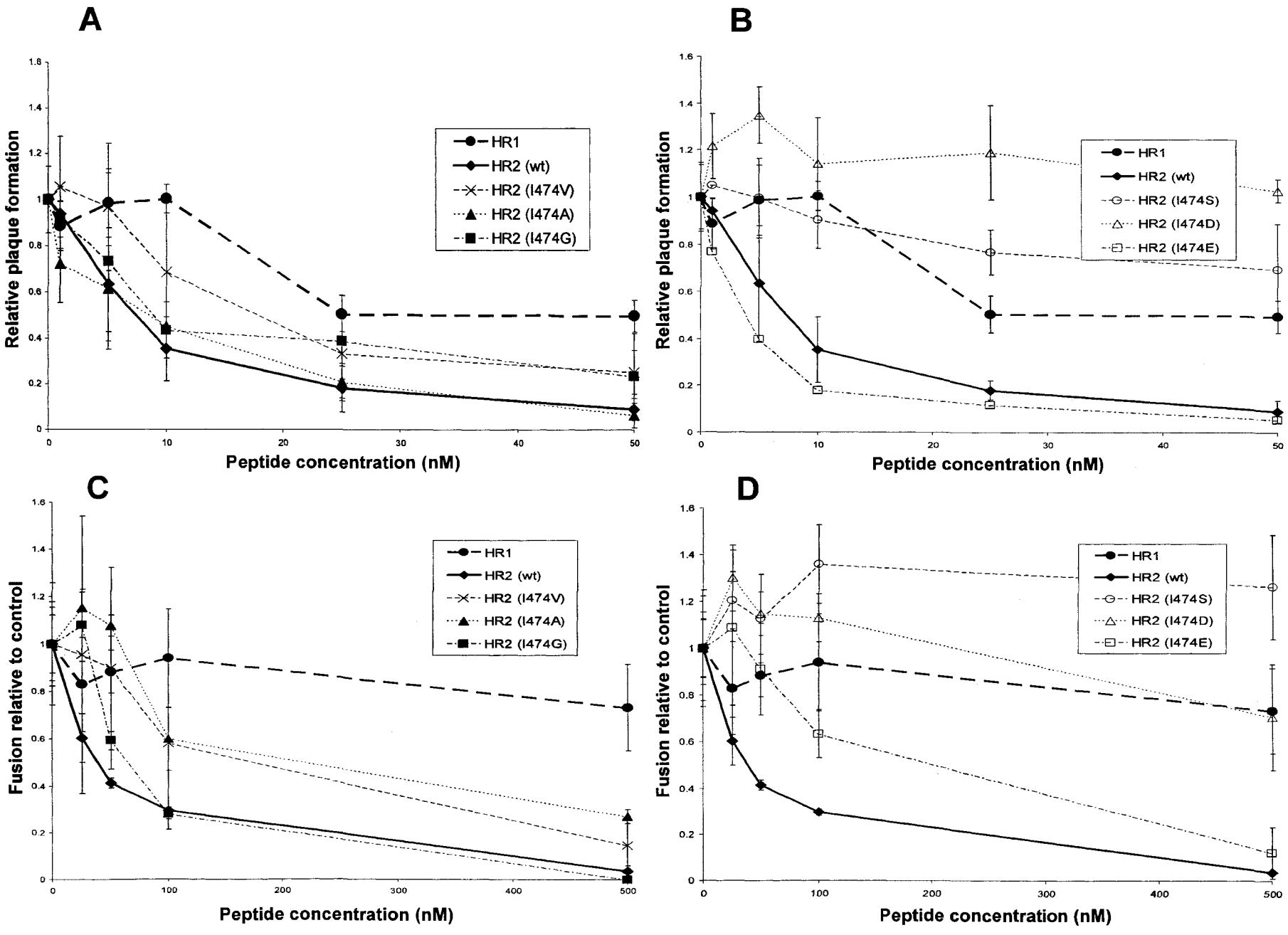
A
Relative plaque formation
Peptide concentration (nM)
HR1
HR2 (wt)
HR2 (I474V)
HR2 (I474A)
HR2 (I474G)
B
Relative plaque formation
Peptide concentration (nM)
HR1
HR2 (wt)
HR2 (I474S)
HR2 (I474D)
HR2 (I474E)
C
Fusion relative to control
Peptide concentration (nM)
HR1
HR2 (wt)
HR2 (I474V)
HR2 (I474A)
HR2 (I474G)
D
Fusion relative to control
Peptide concentration (nM)
HR1
HR2 (wt)
HR2 (I474S)
HR2 (I474D)
HR2 (I474E)

Figure 6. Inhibition of HPIV3 infection and HN/F-driven cell-cell fusion by HR peptides fused to GST (GST-HR). Panels A and B: Plaque reduction by GST-HR proteins. LLC-MK2 cells were infected with 50-100 PFU of HPIV3 after incubation with or without the indicated GST-HR protein (representing HR1 and HR2 sequences from the HPIV3 F protein) or GST alone, as a control. Plaques were fixed and stained, and counted 5 days post-infection. (A) Plaque reduction by GST-HR proteins with non-polar amino acid substitutions at position I474. (B) Plaque reduction by GST-HR proteins with polar amino acid substitutions at position I474. Panels C and D: Inhibition of cell-cell fusion by GST-HR proteins. HeLaT4 cells expressing HPIV3 HN and F glycoproteins were mixed with HeLaT4 cells transfected with plasmid pG1NT7 (encoding β-galactosidase) in the presence or absence of the indicated GST-HR protein. (C) Fusion inhibition by GST-HR proteins with non-polar amino acid substitutions at position I474. (D) Fusion inhibition by GST-HR proteins with polar amino acid substitutions at position I474. Results obtained with wild-type GST-HR2 proteins are presented in all panels for comparison, and are bolded for emphasis. Results for the GST-only control are presented in panels A and B only. Data in all panels is the average of at least three separate experiments, using duplicate samples for each experiment, ± the standard deviation.

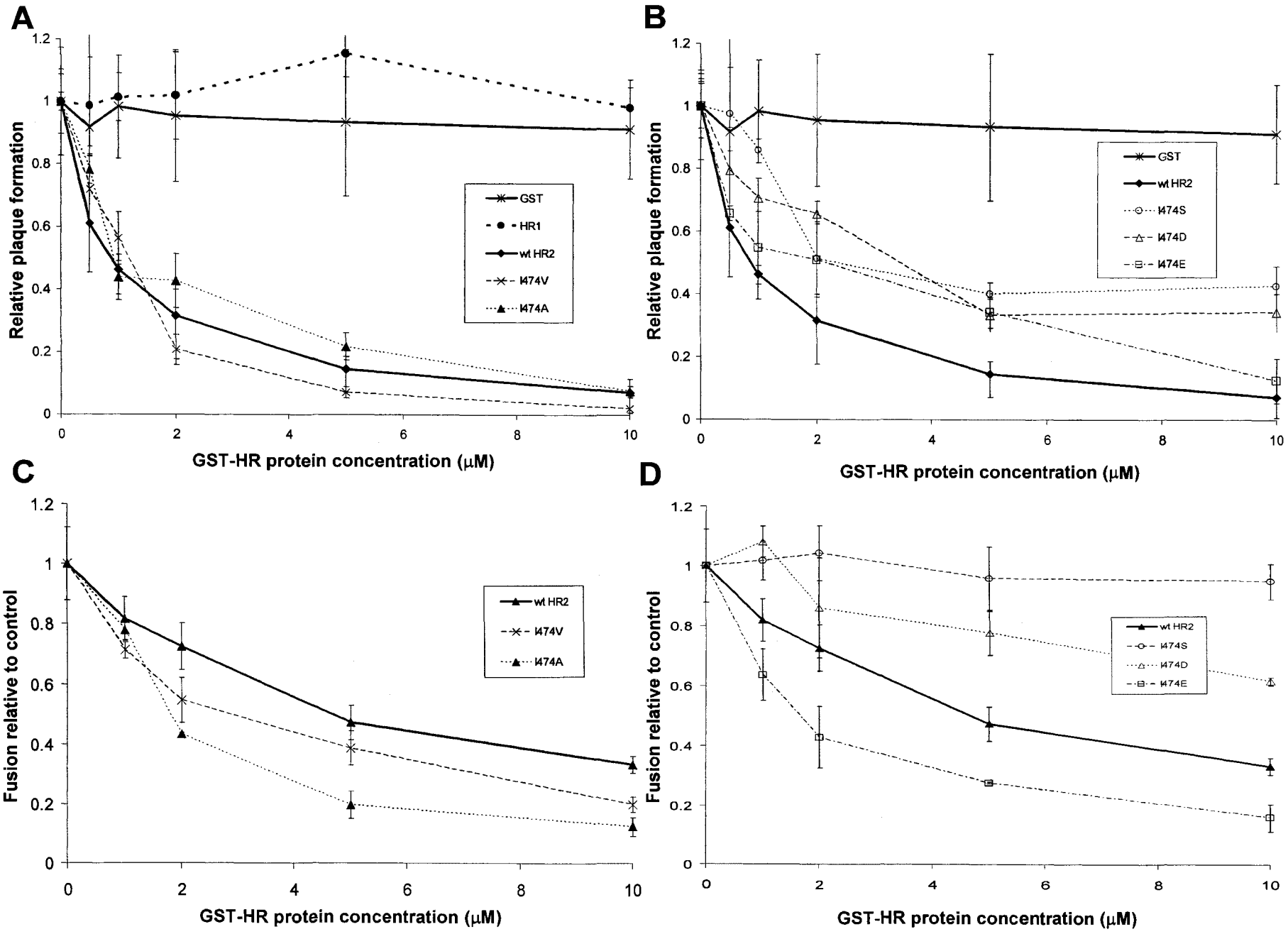
A
Relative plaque formation
GST-HR protein concentration (μM)
GST
HR1
wt HR2
I474V
I474A
B
Relative plaque formation
GST-HR protein concentration (μM)
GST
wt HR2
I474S
I474D
I474E
C
Fusion relative to control
GST-HR protein concentration (μM)
wt HR2
I474V
I474A
D
Fusion relative to control
GST-HR protein concentration (μM)
wt HR2
I474S
I474D
I474E

GST-HR2 proteins. Inhibition of plaque formation was HPIV3-specific since the wild-type HPIV3 HR2 peptide did not inhibit infection of Vero cells by mumps virus at concentrations up to 100 nM (see Figure 7). The HPIV3 HR1 peptide, but not GST-HR1, also inhibited plaque formation in a dose-dependent manner, however, the IC_{50} for HR1 was >50 nM (Figures 5 and 6, panels A). Most of the mutant HR2 peptides also showed dose-dependent inhibition of plaque formation. (Figures 5 and 6, panels A and B). I474S and I474D HR2 peptides inhibited poorly, and even at 50 nM, HPIV3 plaque formation was reduced by less than 30%. I474V, I474A, I474G and I474E peptides inhibited plaque formation similarly to the wild-type HR2 peptide.

HR1 and HR2 peptide inhibition of plaque formation by viruses containing type I membrane fusion proteins is believed to occur because binding of the peptides to cognate sequences in the F protein interferes with 6-HB formation *in situ* and blocks F protein-mediated membrane fusion (Eckert and Kim, 2001). The ability of HR1 and HR2 peptides to inhibit cell-cell membrane fusion mediated by the HPIV3 HN and F proteins was verified using a quantitative contents-mixing fusion reduction assay. Although the plaque reduction assay was approximately one order of magnitude more sensitive than the fusion assay for purified HR2 peptides, the sensitivity of the two assays was not appreciably different (within an order of magnitude of each other) for the GST-HR2 proteins; in both cases, the results obtained from the fusion reduction assay (Figure 5, panels C and D) corresponded well with the results of the plaque reduction assay. The HR1 peptide had little or no effect on cell-cell fusion (Figure 5, panel C).

While the extent of inhibition did not appear to directly correlate with polarity, bulkiness or charge of the substituted amino acid side chain at position 474, a subtle relationship between polarity and bulkiness of the residue was noted. If the amino

Table 3. Properties of wild-type and I474 mutant HR2 peptides

HR2 peptide	Fusion IC_{50} HR2 peptide (nM)	Fusion IC_{50} GST-HR2 (μM)	Plaque formation HR2 peptide IC_{50} (nM)	Plaque formation GST-HR2 IC_{50} (μM)	6-HB melting temperature (°C)[1]
Wild-type	45	4.70	8	0.89	>99
I474V	150	2.94	15	1.19	>99
I474A	200	1.82	8	0.96	77.5
I474G	60	nd[2]	9	nd[2]	78.0
I474S	>500	>10	>50	2.36	60.0
I474D	>500	>10	>50	3.50	57.0
I474E	175	1.65	5	2.15	72.5

[1]6-HB melting temperature of HPLC-purified HR1 and HR2 peptides determined by 50% dissociation as monitored by circular dichroism by MA Wurth and RE Dutch (University of Kentucky); [2]not determined

Figure 7. Inhibition of mumps virus strain Ur-1004 infection by the HPIV3 F protein HR2 peptide. Vero cells were infected with 100 PFU of mumps virus Ur-1004 after incubation with or without the HPIV3 HR2 peptide. Plaques were scored 4 days post-infection.

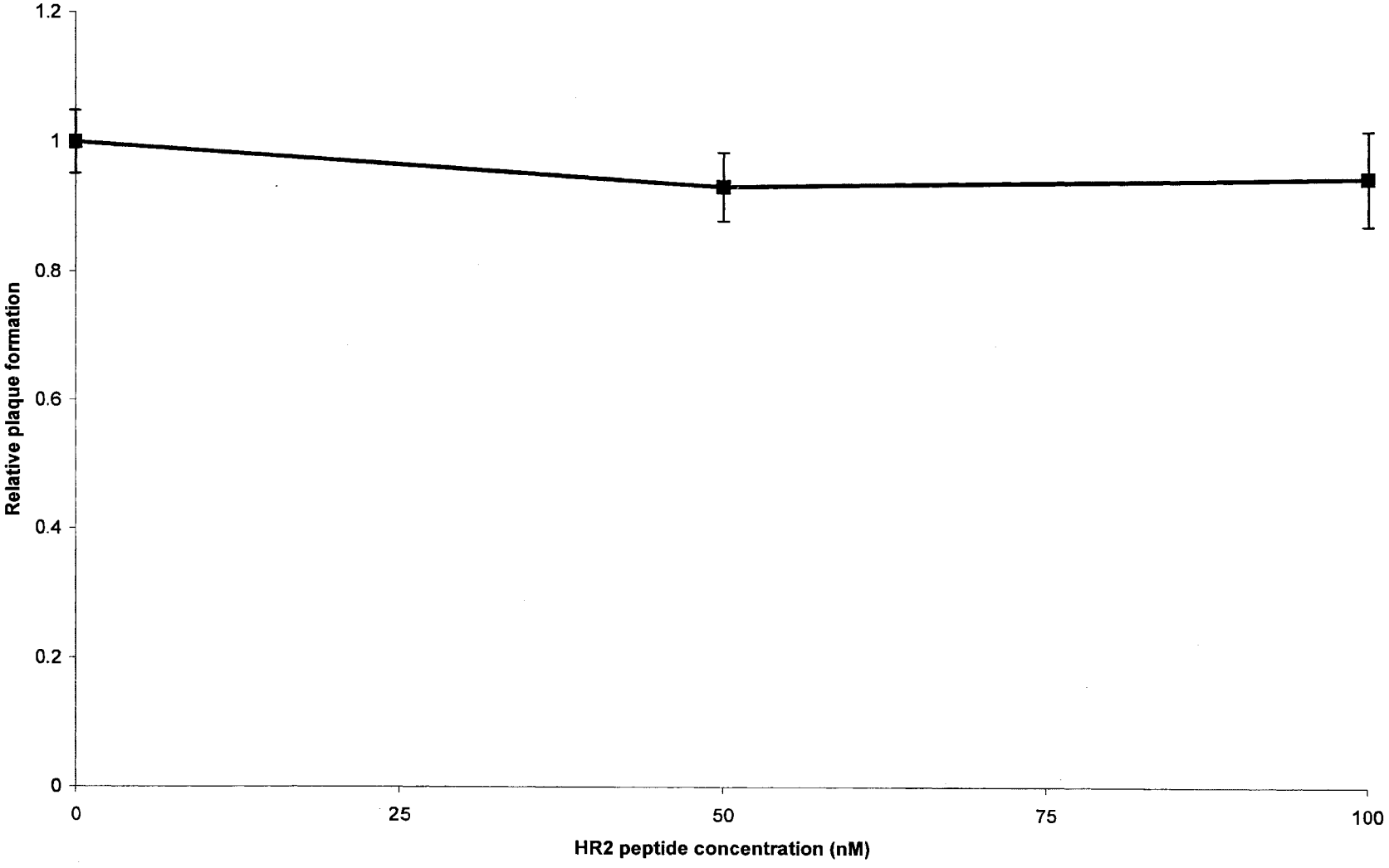
1.2
1
0.8
0.6
0.4
0.2
0
Relative plaque formation
0
25
50
75
100
HR2 peptide concentration (nM)

acid replacing I474 was hydrophobic, bulkiness did not affect fusion inhibition since the inhibitory properties of the I474V, I474A and I474G peptides were similar to those of the wild-type peptide (Figures 5 and 6, panels A and C). However, if the substituting amino acid was polar, inhibition of fusion and plaque formation was affected by the bulkiness of the amino acid side chain; peptides containing the I474S or the I474D mutations were not inhibitory at any concentration tested, while the inhibitory properties of the I474E peptide were similar to those of wild-type HR2 (Figures 5 and 6, panels B and D).

Inhibition of HPIV3 infection and HPIV3 F protein-mediated membrane fusion correlates with the thermal stability of the 6-HB

Tested next was whether the ability of HR2 peptides to inhibit HPIV3 plaque formation and HPIV3 F protein-mediated cell-cell fusion correlated with the stability of the 6-HB. Lysates of *E. coli* BL21(DE3) expressing either GST-HR1 or GST-HR2 were mixed, and the mixtures incubated on glutathione-agarose columns. After washing, columns were incubated with thrombin to cleave HR1-HR2 complexes from GST. Complexes were identified by tris-tricine SDS-PAGE at 4°C and silver staining. Figure 8 is a representation of one of these gels, and indicates (1) that complex formation is not complete under these conditions, and (2) that I474S and I474D HR2 sequences do not appear to form complexes that are stable enough to "survive" SDS-PAGE. I474G was not tested in this assay.

To gain a more thorough understanding of the stability of the 6-HB containing mutant HR2 sequences, thermal denaturation profiles of the 6-HB formed by HPLC-purified HR1 and HR2 peptides were determined. Peptides were mixed under conditions that allow 6-HBs to form, and thermal denaturation of HR1-HR2 complexes was monitored by circular dichroism (CD), which uses helicity as a measure of 6-HB formation (Dutch *et al.*, 1999).

Figure 8. Formation of 6-helix bundles by HR peptides. Lysates of *E. coli* BL21(DE3) expressing GST-HR1, or wild-type or I474 mutant GST-HR2, were mixed on ice prior to loading on glutathione affinity columns at 4°C. Columns were washed, and peptides were cleaved from GST overnight with one unit of thrombin at 4°C. Eluates were analyzed by tris-tricine PAGE at 4°C, with no heating of samples. Protein bands were visualized by silver staining, and photographed under transillumination. Bands of known identity are indicated on the figure.

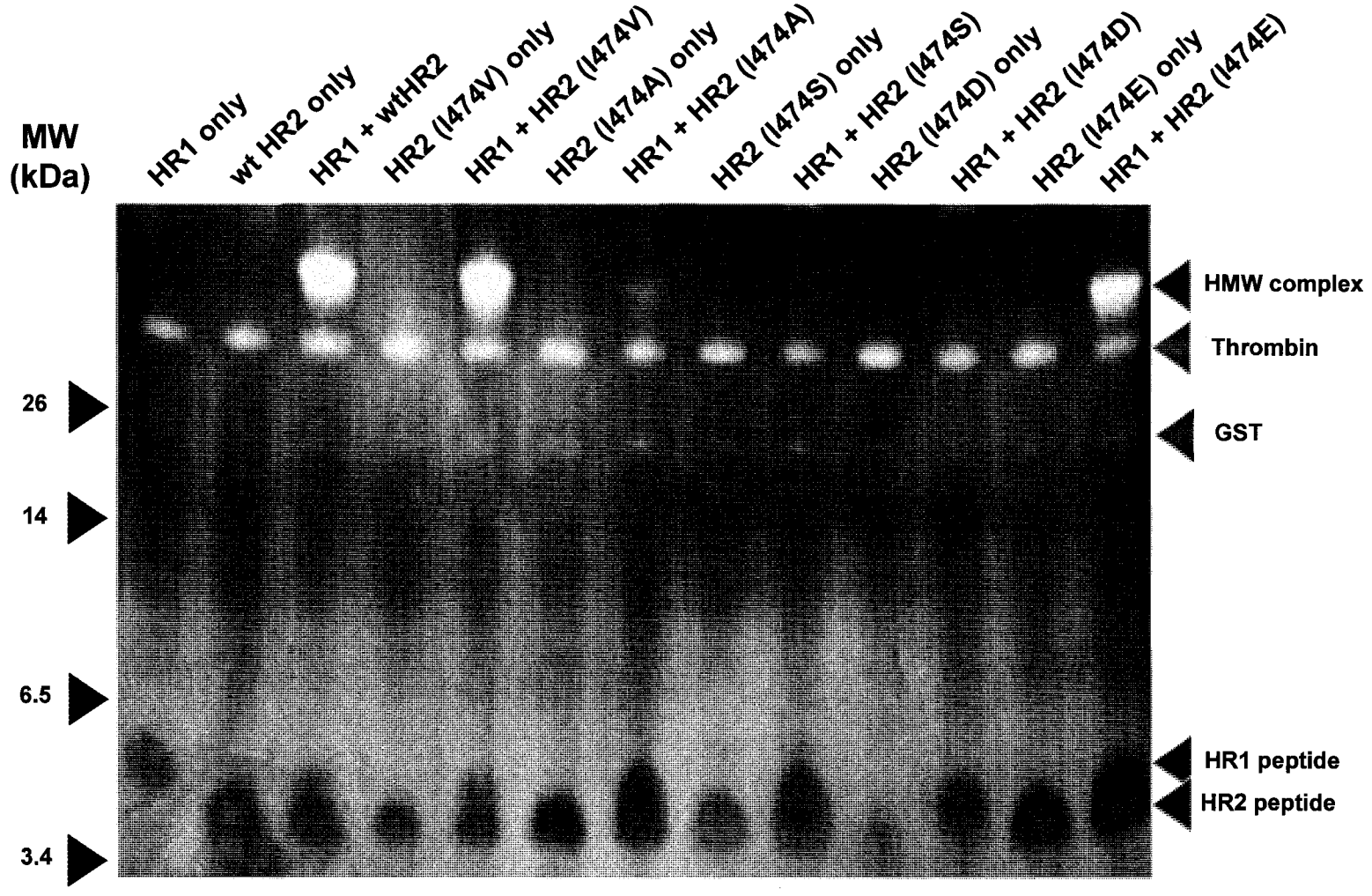
MW
(kDa)
HR1 only
wt HR2 only
HR1 + wtHR2
HR2 (I474V) only
HR1 + HR2 (I474V)
HR2 (I474A) only
HR1 + HR2 (I474A)
HR2 (I474S) only
HR1 + HR2 (I474S)
HR2 (I474D) only
HR1 + HR2 (I474D)
HR2 (I474E) only
HR1 + HR2 (I474E)
26
14
6.5
3.4
HMW complex
Thrombin
GST
HR1 peptide
HR2 peptide

These analyses were carried out by Drs. Mark Wurth and Rebecca Dutch (University of Kentucky). CD analysis confirmed that HR1-HR2 complexes were formed, as the melting temperatures of the HR1-HR2 mixtures were significantly greater than that of the HR1 peptide alone. The melting temperatures of the HR1-HR2 complexes are listed in Table 3 and representative thermal denaturation profiles of the HR1-HR2 complexes are shown in Figure 9. It was difficult to determine the absolute melting temperature for the wild-type 6-HB as the complex still retained partial helicity at temperatures greater than 99°C. This result indicates that the HPIV3 6-HB is one of the most stable paramyxovirus 6-HB yet characterized (Zhu *et al.*, 2005; Wang *et al.*, 2005; Liu *et al.*, 2004; Xu *et al.*, 2004a; Zhu *et al.*, 2003; Joshi *et al.*, 1998). Consistent with what was observed in the plaque reduction and fusion inhibition assays, the thermal stability of the 6-HBs formed with mutant HR2 peptides appeared to be subtly related to the bulkiness of polar amino acid side chains. Not surprisingly, the highest melting temperature was obtained for the 6-HB formed with the mutant HR2 peptide containing the I474V mutation. Replacing large, hydrophobic amino acid side chains with smaller hydrophobic side-chains, such as alanine or glycine, yielded HR1-HR2 complexes with lower melting temperatures. However, replacement of I474 with a polar amino acid further reduced the melting temperature of the 6-HB only if the side chain in question was less bulky than an isoleucine side chain. For example, HR2 containing glutamic acid at position 474 formed complexes with a higher melting temperature than complexes formed with HR2 containing serine or aspartic acid, which produced the least stable 6-HB. The ability of peptides to inhibit both F-mediated membrane fusion and HPIV3 infection, therefore, correlated with the thermal stability of the 6-HB.

Figure 9. Thermostability of the 6-HB. HPLC-purified HR1 and wild-type or mutant HR2 peptides were mixed at 4°C to allow 6-HBs to form. Thermal stability of 6-HBs was monitored by circular dichroism while increasing the temperature from 4-99°C. The thermal melting profile of HR1 peptide alone is presented for comparison. Representative 6-HB melting profiles for HR1 mixed with wild-type and all mutant HR2 peptides are presented. Experiment performed by Drs. M.A. Wurth and R.E. Dutch (University of Kentucky).

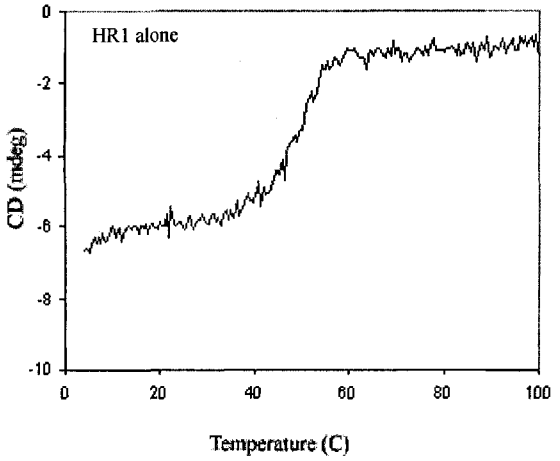
HR1 alone
CD (mdeg)
Temperature (C)

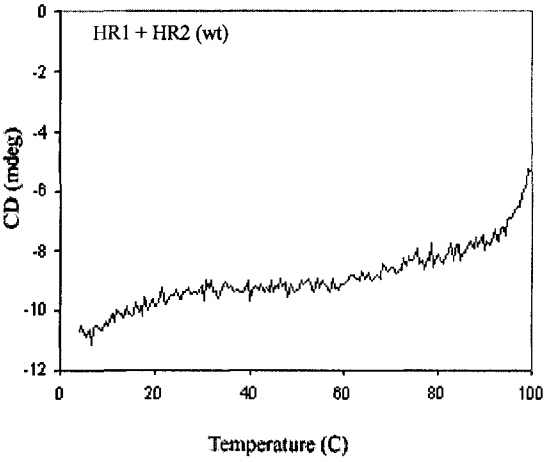
HR1 + HR2 (wt)
CD (mdeg)
Temperature (C)

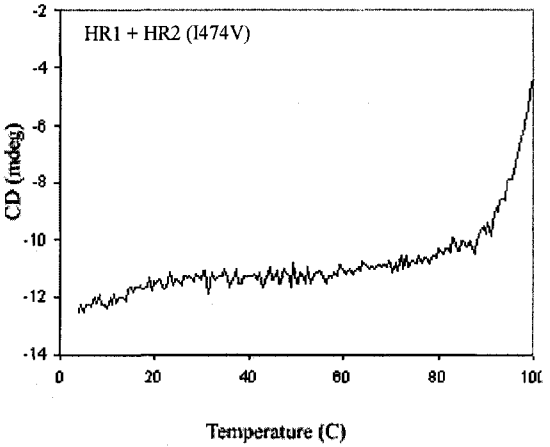
HR1 + HR2 (I474V)
CD (mdeg)
Temperature (C)

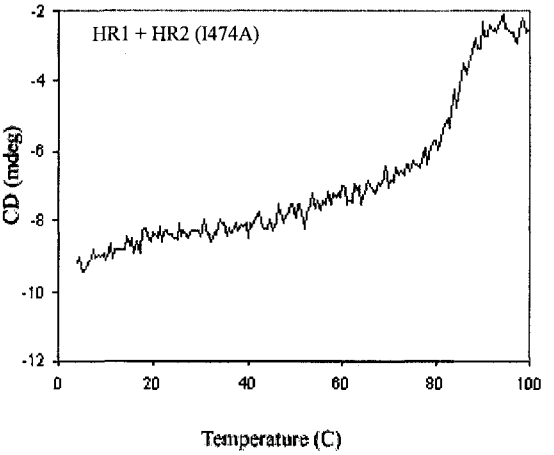
HR1 + HR2 (I474A)
CD (mdeg)
Temperature (C)

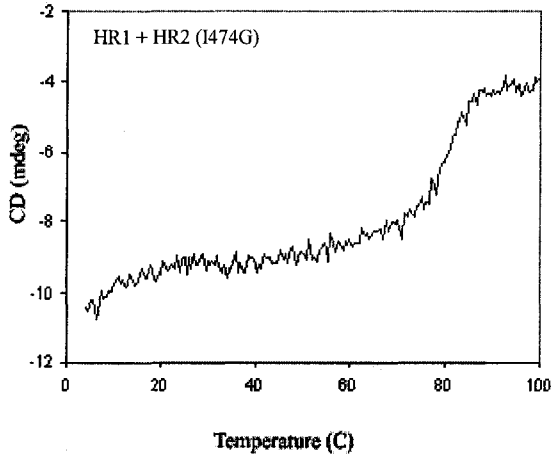
HR1 + HR2 (I474G)
CD (mdeg)
Temperature (C)

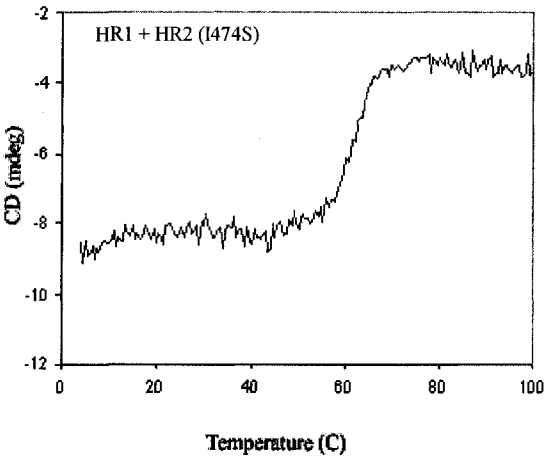
HR1 + HR2 (I474S)
CD (mdeg)
Temperature (C)

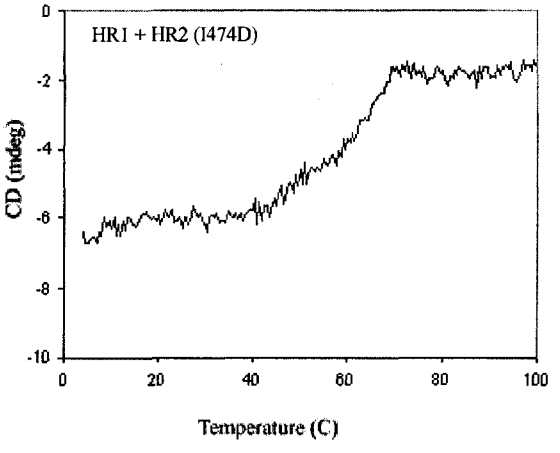
HR1 + HR2 (I474D)
CD (mdeg)
Temperature (C)

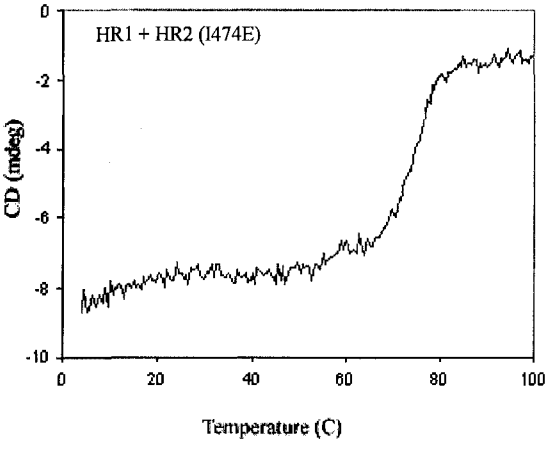
HR1 + HR2 (I474E)
CD (mdeg)
Temperature (C)

Some I474 mutations that allow for 6-HB formation produce F proteins that are uncleaved and non-fusogenic

To test whether mutations in HR2 that affect 6-HB stability have effects on HPIV3 F protein function, plasmids encoding F proteins carrying I474 mutations were constructed by Sharon Ebata (Ebata, 1996). Following transfection of HeLaT4 cells, surface expression of each F protein was monitored by flow cytometry and immunofluorescence microscopy (Ebata, 1996), using monoclonal antibodies that recognize different antigenic sites on the HPIV3 F protein (van Wyke-Coelingh and Tierney, 1989), and for fusogenicity in the cell fusion assay. To facilitate the analysis of F protein expression and proteolytic processing of F_0 into F_1 and $F_{2,}$ by western blotting, F protein sequences were tagged with the FLAG epitope, with assistance from Bogna Zolkiewska. Incorporation of the FLAG epitope had no apparent effect on cleavage or fusogenicity of the wild type F protein; the results of fusion assays performed with identical amounts of plasmid DNA expressing tagged and untagged F protein were similar, but since the untagged F protein could not be quantitated by western blot since there are no monoclonal anti-F antibodies in our laboratory that function in immunoblotting, direct comparisons are difficult. All mutant F proteins were expressed at the cell surface at levels similar to that of wild-type F protein, with the notable exception of I474G (Table 4) (Ebata, 1996). I474G appears to be expressed in much lower amounts than all of the other F proteins; it was not detected at the cell surface by flow cytometry and could only be detected intracellularly by immunofluorescence microscopy with prolonged exposure (Ebata, 1996). F proteins containing I474V, I474A and I474E substitutions were all cleaved to the same extent as the wild-type F protein; however, cleavage of the I474S protein was significantly inhibited, and cleavage of the I474D protein was abolished (Figures 10 and 11, Table 4). The fusion properties of the mutated F proteins mirrored their cleavage, as shown in Figure 10. The fusogenicity of F proteins with I474V, I474A and I474E mutations was similar to that of the wild-type F protein, but fusion mediated by the

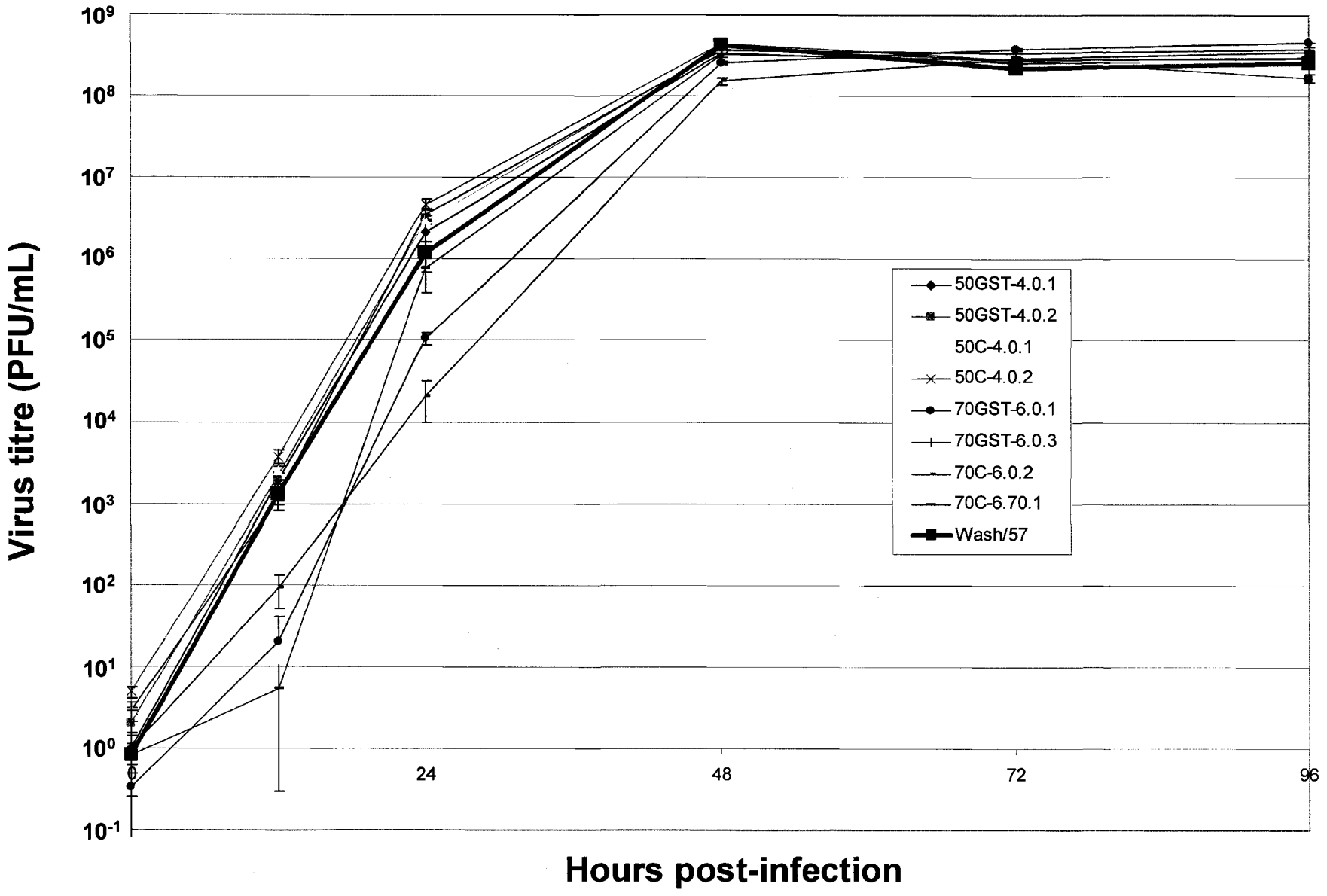
Virus titre (PFU/mL)
10^9
10^8
10^7
10^6
10^5
10^4
10^3
10^2
10^1
10^0
10^-1
0
24
48
72
96
Hours post-infection
50GST-4.0.1
50GST-4.0.2
50C-4.0.1
50C-4.0.2
70GST-6.0.1
70GST-6.0.3
70C-6.0.2
70C-6.70.1
Wash/57

Figure 10. Cleavage and fusogenicity of wild-type and I474 mutant F proteins. Cleavage (dark bars). Lysates of HeLaT4 cells expressing FLAG-tagged wild type HPIV3 F protein or F proteins containing I474 mutations, as indicated, were subjected to SDS-PAGE. F_0 and F_1 were detected by western immunoblotting with a FLAG-specific monoclonal antibody and an HRP-conjugated rabbit anti-mouse antibody, and quantified by densitometric scanning. Data are presented as per cent cleavage relative to cleavage of the wild-type F protein (which was ~40% cleaved). Fusogenicity (light bars). HeLaT4 cells expressing wild type HPIV3 F protein, F proteins containing I474 mutations and/or the HPIV3 HN protein, as indicated, were mixed with HeLaT4 cells transfected with plasmid pG1NT7. Cell-cell fusion was quantified using a contents-mixing fusion assay (see text for details). Data are presented as per cent fusion relative to the amount of fusion mediated by the wild-type F protein in the presence of the HN protein. Cleavage results are the average of two experiments, ± the standard deviation. Fusion results are the average of three experiments, with duplicate reads of duplicate samples for each experiment ± the standard deviation.

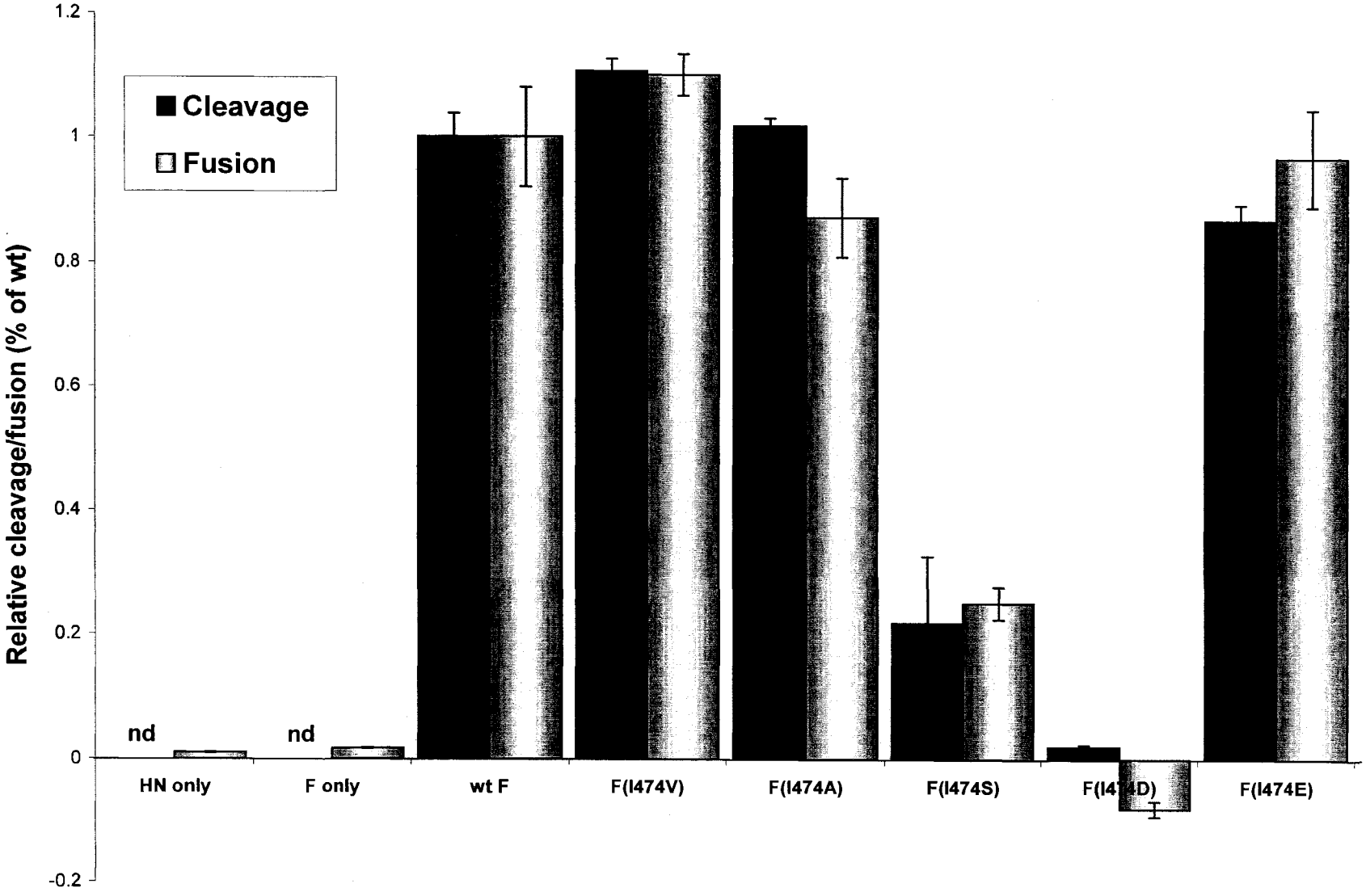
Cleavage
Fusion
Relative cleavage/fusion (% of wt)
1.2
1
0.8
0.6
0.4
0.2
0
-0.2
nd
nd
HN only
F only
wt F
F(I474V)
F(I474A)
F(I474S)
F(I474D)
F(I474E)

Figure 11. Cleavage of wild-type and I474 mutant F proteins. Lysates of HeLaT4 cells expressing FLAG-tagged wild type HPIV3 F protein or F proteins containing I474 mutations, as indicated, were subjected to SDS-PAGE, transferred to PVDF membranes, and immunoblotted. F_0 and F_1 were detected using a FLAG-specific monoclonal antibody and an HRP-conjugated rabbit anti-mouse antibody. An unidentified band of approximately 32 kDa was used as a loading control.

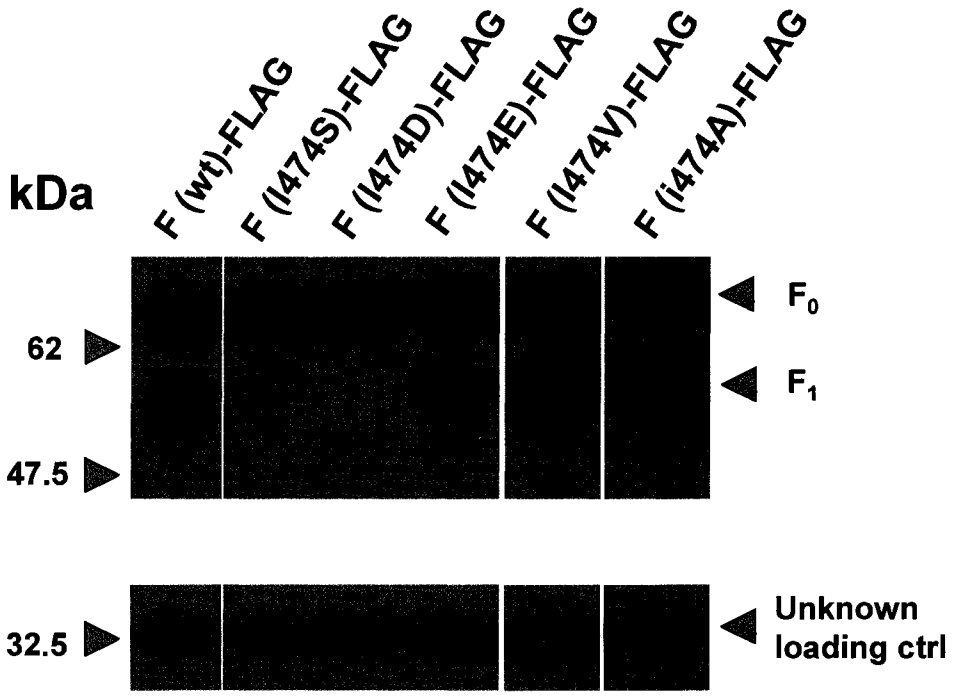
kDa
F (wt)-FLAG
F (I474S)-FLAG
F (I474D)-FLAG
F (I474E)-FLAG
F (I474V)-FLAG
F (i474A)-FLAG
62
47.5
32.5
F0
F1
Unknown
loading ctrl

Table 4. Surface expression, cleavage and fusogenicity of HPIV3 F proteins

F protein	MFI [1](A197)	MFI [1](B19)	Cleavage[2]	Fusogenicity[3]
control	1.6	1.6	n/a	n/a
wild-type	52.3	34.4	100	100
I474V	55.9	82.8	111	110
I474A	51.8	78.4	101	87.6
I474G	<1	<1	nd	nd
I474S	74.5	100.8	22	25
I474D	72.6	107.2	2	0
I474E	53.2	36.2	87	97

[1]MFI = mean fluorescence intensity determined by S. Ebata using the HPIV3 F-specific monoclonal antibody in parenthesis (Ebata, 1996; van Wyke-Coelingh and Tierney, 1989).
[2]Cleavage determined as a percentage of wild-type F protein cleavage.
[3]Fusogenicity determined as a percentage of fusion obtained with the wild-type F protein, using the quantitative fusion assay.

I474S protein was impaired and the I474D protein was completely inactive.

These results indicate that HR2, and, more specifically I474, plays a role in the formation and/or stabilization of an intermediate structure required for the proteolytic processing of F_0, in addition to a role in the formation of the 6-HB and fusion.

Discussion

The ability of wild-type and mutant HR2 peptides, and GST-HR2 proteins, derived from the HPIV3 F protein to inhibit both HPIV3 infection and HPIV3 glycoprotein-driven cell-cell fusion was demonstrated. The IC_{50} for plaque reduction by the wild-type HR2 peptide (8 nM) was similar to that determined by Lambert *et al.* (15nm), but noticeably lower than the values reported by Porotto *et al.* (500nm) and Yao and Compans (2 μM). The IC_{50} values of the HR2 peptides for both infection and fusion are also within the range of concentrations reported previously for other paramyxovirus HR2 peptides (Table 5). Previous studies indicated that the HR1 peptides of the RSV, NDV, and PIV5 F proteins were the only paramyxovirus HR1 peptides that inhibited cell-cell fusion and/or plaque formation (Zhu *et al.*, 2005; San Roman *et al.*, 2002; Russell *et al.*, 2001). For other type I fusion proteins, one report showed that HR1 of the SARS coronavirus (SARS CoV) spike protein (S) inhibited SARS CoV infection (Yuan *et al.*, 2004), although other reports have shown that HR1 of the SARS CoV S protein had no inhibitory effect (Bosch *et al.*, 2004; Bosch *et al.*, 2003). Earlier studies reported gp41 HR1-based inhibition of HIV fusion, though at 1000-fold higher peptide concentrations than HR2 (Wild *et al.*, 1994; Wild *et al.*, 1993; Wild *et al.*, 1992). No inhibition of cell-cell fusion by the HPIV3 HR1 peptide was observed; however, plaque formation was reduced when virus was incubated with the HR1 peptide, although at a considerably higher IC_{50} (25-50 nM) than for the HR2 peptide. The HR2 peptide also inhibited plaque formation and glycoprotein-driven fusion when fused to the C-terminus of GST at an IC_{50} of ~ 0.8 μM and ~ 5 μM, respectively, similar to a previous report for the HR2 region of the NDV F protein (IC_{50} of 1.25 μM and 2.90 μM, respectively (Yu *et al.*, 2002)).

Table 5. Paramyxovirus HR peptides: IC_{50} values for plaque formation and cell-cell fusion

Virus	Plaque formation IC50 (nM)	Cell-cell fusion IC50 (nM)	Reference
HPIV3	15 500 8[1]	500 40[1]	(Porotto *et al.*, 2006a; Lambert *et al.*, 1996)
NDV	2000-3000	1000-3000	(Zhu *et al.*, 2005; Yu *et al.*, 2002; San Roman *et al.*, 2002)
RSV	50 2900	n/a	(Wang *et al.*, 2003; Lambert *et al.*, 1996)
APMV	n/a	2000-4000	(Wang *et al.*, 2005)
Measles	42	n/a	(Lambert *et al.*, 1996)
Hendra	n/a	5-27	(Bossart *et al.*, 2005; Bossart *et al.*, 2002)

[1]this study

Inhibition of glycoprotein-driven fusion required more HR2 HPLC-purified peptide than did inhibition of plaque formation. Differences between peptides were more obvious when fusion inhibition was used as the readout, rather than plaque inhibition. Why this occurs is unclear. Perhaps, because for plaque reduction experiments, peptide was added to a small number of plaque-forming units (50-100 PFU), inhibition required a much lower concentration of peptide than for cell-cell fusion. It is not known exactly how many F molecules exist on a paramyxovirus particle, however, enveloped viruses of similar sizes can have as few as 75 fusion spikes, such as Env of HIV and SIV (Zhu *et al.*, 2006), or as many as 1200, such as the G protein of vesicular stomatitis virus (Thomas *et al.*, 1985), so one can assume that inhibition of 100 particles of HPIV3 would require less than 120,000 HR2 molecules. Much higher concentrations of peptide would be required to inhibit cell-cell fusion since transfected cells are likely expressing thousands of F molecules each, or more,

and each well contains hundreds of thousands of cells. No matter the explanation, it was possible to determine an IC_{50} for each peptide, and to identify HR2 peptides that were "poor" at forming stable 6-HB. With this in mind, it can be concluded that the quantitative fusion reduction assay is more discriminating than the plaque reduction assay. These results are somewhat in contradiction to other studies, where the concentrations of peptide required for inhibition of plaque formation was equal to, or greater than, those required for fusion reduction (Porotto *et al.*, 2006a; San Roman *et al.*, 2002). There was also an approximately 100-fold difference in the IC_{50} required for inhibition of virus infection and fusion when purified HR2 peptide is compared with the GST-HR2 fusion proteins, though efficient and reproducible fusion reduction was observed with both peptides and the GST-HR2 proteins. This difference is most likely due to steric hindrance of inhibition by the GST moiety. For the GST-HR2 proteins, there was also a similar difference between the IC_{50} values for fusion inhibition and plaque reduction, though this difference was not as pronounced as for the purified HR2 peptides. In spite of the concentration differences, due to the ease of production of recombinant GST proteins, rather than cleaved, HPLC-purified peptides, rapid screening of mutant HR sequences for inhibitory properties is made much easier by the use of GST-HR proteins.

Formation of a stable 6-HB is an integral component of the current model for class I viral fusion glycoprotein function. The HPIV3 HR1/HR2 complex formed *in vitro* is one of the most thermostable 6-HB characterized so far, with significant α-helical character retained at greater than 99°C. The published melting temperatures of 6-HBs for class I fusion proteins of paramyxoviruses and other viruses are listed in Table 6. The stability of the HPIV3 HR1/HR2 complex may be due to the lengths of the HR1 and HR2 peptides used in this study. The HPIV3 HR1 peptide is 18 residues longer (7 at the N-terminus, 11 at the C-terminus) than the 46 amino acid heptad repeat predicted by the

Table 6. Melting temperatures of 6-helix bundles formed by HR1 and HR2 peptides of class I viral fusion proteins

Virus	6-HB melting temperature (°C)	Reference
HPIV3	>99°C	This study
PIV5	>90°C	(Joshi *et al.*, 1998)
NDV[1]	91°C	(Zhu *et al.*, 2005)
Mumps	76°C	(Liu *et al.*, 2004)
APMV-2[2]	>90°C	(Wang *et al.*, 2005)
Measles	80-90°C	(Zhu *et al.*, 2002)
Nipah	85°C	(Xu *et al.*, 2004a)
Menangle	>90°C	(Zhu *et al.*, 2003)
SARS CoV	75°C >88°C >90°C	(Zhu *et al.*, 2004; Tripet *et al.*, 2004; Xu *et al.*, 2004b)
HIV-1	90°C	(Lu *et al.*, 1995; Blacklow *et al.*, 1995)

[1]NDV = Newcastle disease virus
[2]AMPV-2 = Avian paramyxovirus 2

LearnCOIL VMF program (http://learncoil-vmf.lcs.mit.edu/cgi-bin/vmf), which is often used to predict HR structures in other virus fusion proteins (Porotto *et al.*, 2006a; Zhu *et al.*, 2003; Malashkevich *et al.*, 2001; Zhao *et al.*, 2000; Singh *et al.*, 1999). This sequence was selected because it abuts the fusion peptide and terminates immediately prior to the first cysteine residue in F_1 (residue 192). Similarly, the HPIV3 HR2 peptide, with seven additional N-terminal residues and two additional C-terminal residues compared to the LearnCOIL prediction, was designed to begin with the first predicted heptad in this region and to end immediately upstream of the hydrophobic trans-membrane domain of the F protein. It is longer than HPIV3 HR2 peptides reported by others (Porotto *et al.*, 2006a; Lambert *et al.*, 1996). Perhaps the additional residues of the HR1 and HR2 peptides used in this study stabilize the HPIV3 6-HB. While there is a trend towards minimizing the length of HR2 peptides so as to identify the smallest inhibitory peptide, it may be advisable to consider longer peptides for non-drug-discovery applications, such as studies of 6-HB assembly, structure and properties.

Mutations in or near HR2 sequences of paramyxovirus F proteins can destabilize 6-HBs. For example, peptides bearing mutations just outside the α-helical domain of the HR2 region of the PIV5 F protein (L447 and I449), assembled into 6-HBs with reduced stability and had reduced fusion inhibition properties. This region has been proposed to be involved in F protein conformational transitions or switching (Russell *et al.*, 2003). Most of the mutations introduced at position 474 in HR2 of the HPIV3 F protein yielded HR2 peptides that assembled, *in vitro*, into 6-HBs with reduced thermostability. Some of the HR2 peptides had a reduced ability to interfere with F glycoprotein-mediated membrane fusion and with HPIV3 infection that correlated, although not perfectly, with 6-HB stability. I474D and I474S HR2 peptides formed 6-HB with melting temperatures below 60°C and were unable to inhibit plaque formation. 6-HBs formed with I474A, I474G and I474E peptides exhibited intermediate melting temperatures but IC_{50} values similar to those of the wild-type HR2

peptide. These observations are consistent with the idea that HR2 peptides are inhibitory because of a dominant-negative interaction between exogenous HR2 peptide and the HR1 sequence in the F protein (Eckert and Kim, 2001), an interaction that is modeled by the *in vitro* formation of a 6-HB, and with the hypothesis that the extent of fusion inhibition correlates with 6-HB stability.

The varying degree of 6-HB destabilization produced by I474 mutations suggests a "hierarchy" of tolerance for substitution at position I474. Substitution at I474 of HPIV3 F with hydrophobic residues yielded HR2 peptides that inhibited F-mediated cell-cell fusion, and HPIV3 infection, like the wild-type peptide, even though the I474A and I474G peptides formed 6-HBs with intermediate melting temperatures. However, HR2 peptides with polar amino acid substitutions differed widely in their abilities to form 6-HBs and to inhibit cell-cell fusion and HPIV3 infection. The results suggest that bulkiness of a polar amino acid side chain may compensate for reduced hydrophobicity. HR2 peptides with smaller, non-polar amino acid substitutions (e.g. I474A, I474G) or bulky, polar residues (e.g. I474E) formed 6-HBs *in vitro* that were somewhat destabilized, with melting temperatures of 75-85°C, yet retained inhibitory properties. F proteins carrying these same mutations were fusogenic, with the notable exception of the F protein containing the I474G mutation, which was not detected at the cell surface. If the substituting residue was smaller and polar (e.g. I474D, I474S), the 6-HBs formed *in vitro* were unstable and unable to inhibit plaque formation and cell-cell fusion.

A TNxAV motif was noted in HR1, consisting of residues T154, N155, A157 and V158. This TNxAV motif may accommodate the I474 side chain (Figure 12, panel C) in the 6-HB. An analysis of other published paramyxovirus 6-HB supports this hypothesis. In PIV5 and RSV HR1/HR2 complexes, TNxAV motifs are found opposite the amino acids that correspond to I474 in the HPIV3 F protein; L467 in the PIV5 F protein and I506 in the RSV F protein. The TNxAV motif is well conserved in F protein sequences across the family

Figure 12. Three-dimensional representation of the TNxAV pocket in pre-cleavage and post-fusion forms of the paramyxovirus F protein. (A) The PIV5 F protein in a stable pre-fusion, pre-cleavage form, as both a trimer and a single monomer (Yin *et al.*, 2006). Residue L467, which corresponds to I474 in the HPIV3 F protein, is located in the stalk region, and is drawn as a space-filling residue. The F_0 cleavage site is indicated by white arrows, demonstrating the spatial separation between L467 and the cleavage site. (B) The HPIV3 F protein in what is believed to be a stable, post-fusion (but uncleaved) form (Yin *et al.*, 2005). The current model for F protein function predicts that there is a major conformational transition from the structure depicted in panel A to this structure. I474 is highlighted as a space-filling residue and can be seen in the base of the stalk-like region. (C) Structural conservation of the TNxAV pocket for I474 and its homologues. I474 in the HPIV3 F protein and T154 and A157 residues in the PIV5 and RSV F proteins are labeled. The figure was produced using the Deepview Swiss-PDB viewer.

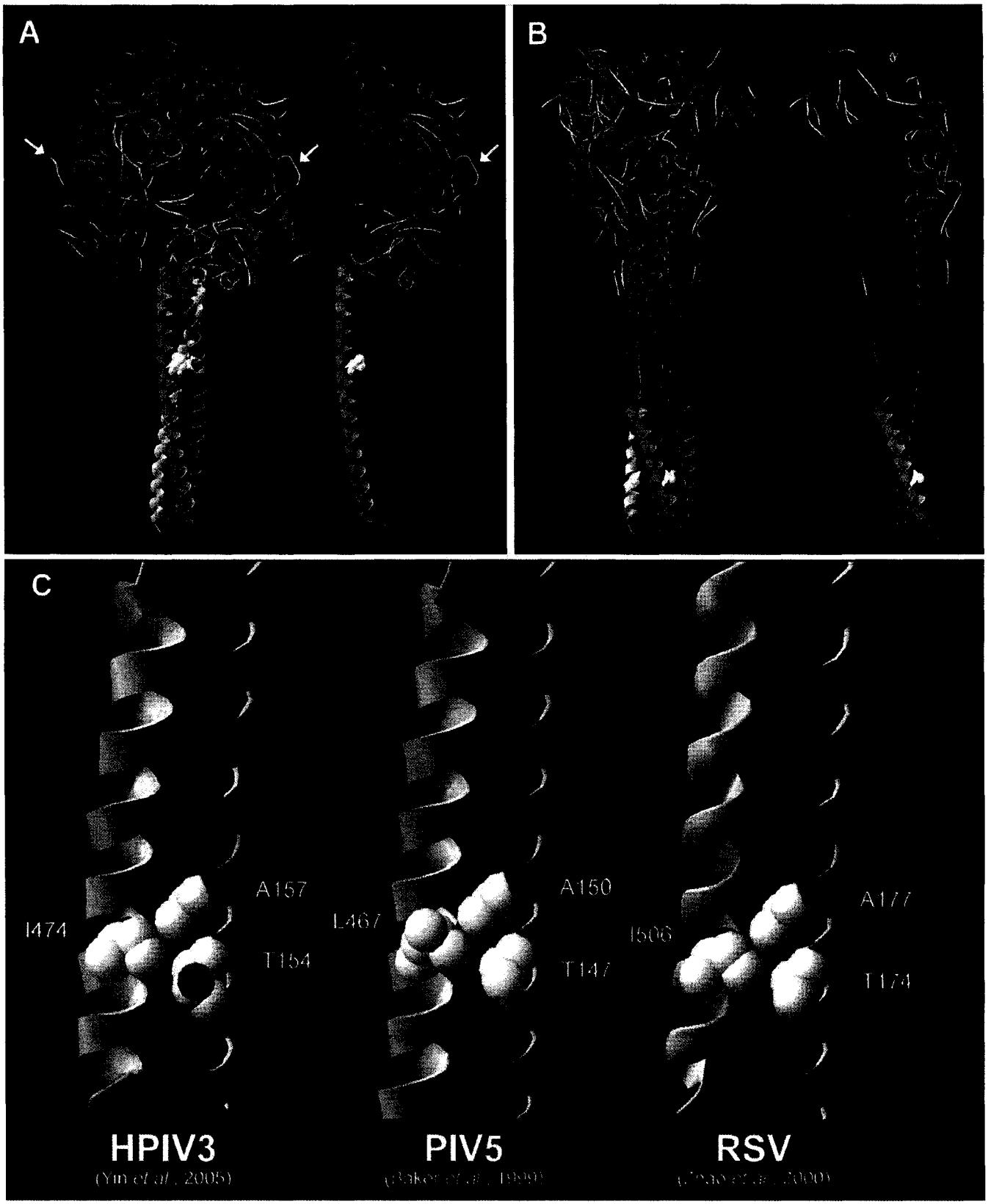
A
B
C
I474
A157
T154
HPIV3
(Yin et al., 2005)
L467
A150
T147
PIV5
(Baker et al., 1999)
I506
A177
T174
RSV
(Tsao et al., 2000)

Paramxoviridae (Figure 13), suggesting that this is a key point of contact between HR1 and HR2, and a tempting target for small-molecule inhibition of paramyxovirus fusion: similar conservation of another stretch of the F protein, a cavity located between the neck and head regions of F, has been exploited to design a substituted aniline that inhibited measles virus fusion in a highly effective manner (Sun *et al.*, 2006; Plemper *et al.*, 2005; Plemper *et al.*, 2004; Plemper *et al.*, 2003). The TNxAV motif may represent a "pocket" that is filled by bulky hydrophobic amino acids, such as isoleucine (HPIV3, RSV), leucine (PIV5) or valine (I474V mutation), stabilizing the 6-HB. Smaller, hydrophobic residues may be tolerated, bracketed by the alanine and the aliphatic end of the threonine residue in the pocket. A large, polar side chain, as in glutamic acid, may also be tolerated partly due the hydrophobic character of its long aliphatic chain and/or through a hydrogen bond between the carboxyl oxygen of the glutamic acid and the hydroxyl group of the threonine. Small polar amino acid side chains are not tolerated, likely due to either the lack of hydrophobic character in their sidechains, or the inability to form stabilizing bonds within the pocket.

The effects of I474 mutations on the function of the HPIV3 F protein were examined. While most of the mutant F proteins were functional, F proteins carrying I474S and I474D mutations were not cleaved, and, as a result, were unable to mediate cell-cell fusion. These observations suggest that an additional role for HR2 exists during the formation of, or stabilization of, a pre-cleavage F_0 structure. Gross misfolding of F_0 containing these mutations cannot explain the lack of cleavage because both proteins reach the cell surface and can be detected by monoclonal antibodies that recognize conformational epitopes. Similarly, the uncleaved I474D and I474S F_0 proteins form trimers, as demonstrated by cross-linking and non-denaturing SDS-polyacrylamide gel electrophoresis (Ebata, 1996). In the recently described structure of the pre-fusion form of the PIV5 F protein, there is no structure resembling the 6-HB, and no evidence of an interaction between HR1 and HR2 (Figure 12, panel A). Notable also, is the spatial separation between HR2 and the cleavage

Figure 13. The TNxAV pocket in HR1 sequences of members of the family *Paramyxoviridae*. Viruses and their abbreviations are: Genus *Paramyxovirinae*: **HPIV3** (human parainfluenza virus type 3), **BPIV3** (bovine parainfluenza virus type 3), **HPIV1** (human parainfluenza virus type 1), **Sendai** (Sendai virus or mouse parainfluenza virus type 1), **Hendra** (Hendra virus), **Nipah** (Nipah virus), **Measles_Edm** (measles virus, Edmonston strain), **CDV** (canine distemper virus), **PPRV** (peste-des-petits-ruminants), **Menangle** (Menangle virus), **HPIV2** (human parainfluenza virus type 2), **PIV5** (simian virus 5 or simian parainfluenza virus 5), **Mumps_JL** (mumps virus, Jeryl Lynn strain), **NDV** (Newcastle disease virus). Genus *Pneumovirinae*: **HRSV** (human respiratory syncytial virus), **BRSV** (bovine respiratory syncytial virus), **HMPV** (human metapneumovirus). Virus subfamilies are listed, in bolded italics, at the left of the figure. Identical amino acids are shaded black, similar amino acids are shaded grey. The figure was produced using the Boxshade software program to illustrate a Clustal alignment.

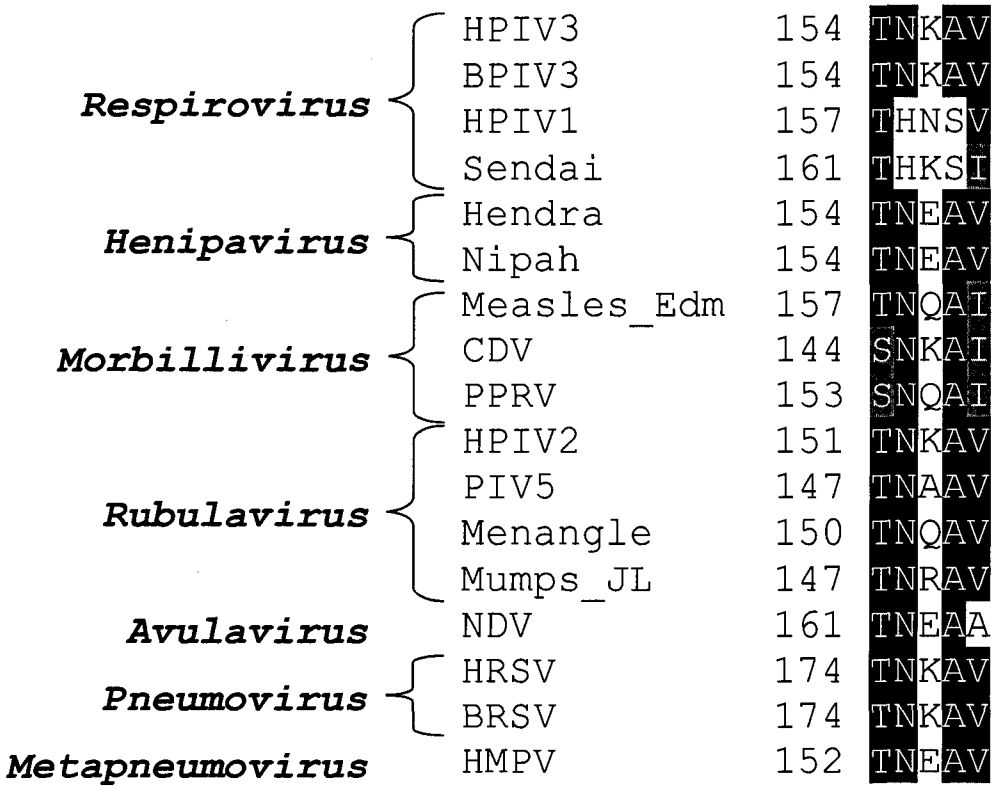
Respirovirus
HPIV3 154 TNKAV
BPIV3 154 TNKAV
HPIV1 157 THNSV
Sendai 161 THKSI
Henipavirus
Hendra 154 TNEAV
Nipah 154 TNEAV
Morbillivirus
Measles_Edm 157 TNQAI
CDV 144 SNKAI
PPRV 153 SNQAI
Rubulavirus
HPIV2 151 TNKAV
PIV5 147 TNAAV
Menangle 150 TNQAV
Mumps_JL 147 TNRAV
Avulavirus
NDV 161 TNEAA
Pneumovirus
HRSV 174 TNKAV
BRSV 174 TNKAV
Metapneumovirus
HMPV 152 TNEAV

site (indicated by the white arrows in Figure 12, panel A). HR2 peptides derived from the PIV5 F protein have been shown to adopt a helical conformation in tetrafluoroethylene (Joshi *et al.*, 1998) and helical HR2 monomers could possibly interact with each other in the prefusion trimer, given their close proximity (Figure 12, panel A). However, HPIV3 HR2 peptides have never been seen to form multimers, *in vitro*, whether as GST-fusion peptides in crude *E. coli* lysates, after affinity column chromatography, or as cleaved, HPLC-purified peptides (see GST-HR2 alone lanes in Figures 8 and 23), nor do they show any helical character in aqueous solution. Also, no evidence for a trimer-stabilizing HR2-HR2 interaction has been reported for any class I fusion glycoprotein. Therefore, if the I474D and I474S mutations destabilize a transient structure dependent on HR2 for stability, this is not reflected in the assembly and surface presentation of the F_0 trimer; since I474D and I474S mutations do not affect trimerization, surface presentation, or proper folding of the F protein (Ebata, 1996), it certainly appears as though the globular head domains stabilize the trimer, and HR2 plays a role in stabilization of the pre-cleavage intermediate of the F protein. The I474G mutation likely results in a F_0 protein that is misfolded to such an extent that it is degraded and difficult to detect in transfected cells.

Interestingly, cleavage and transport of another type I fusion protein, the murine leukemia virus (MLV) envelope glycoprotein (Env), is inhibited by coexpression of its homotypic HR1 peptide, although HR1 was shown to have no effect on fusion or on virus infection when provided exogenously (Ou and Silver, 2005). One interpretation of these results is that HR1 binding to HR2, intracellularly, prevents Env from adopting a conformation susceptible to proteolytic cleavage, or disrupts a cleavage-sensitive conformation of Env, because HR2 is exposed and accessible to HR1 prior to cleavage.

HR2 has been implicated in paramyxovirus HN-F interactions (Gravel and Morrison, 2003; Tsurudome *et al.*, 1998). As detailed below, HPIV3 complexes of HN and F proteins containing the I474D and I474S mutations could be isolated (see Figure_16 in Chapter 4).

Therefore, since F proteins with I474D and I474S mutations can interact with HN but are uncleaved, at least three intermediates, and, likely, transient conformations of the HR2 can be predicted: (1) a conformation in which HR2 contributes to HN-F interactions; (2) a cleavage-sensitive form of F, in which HR2 may be exposed and able to bind HR1; and (3) the classical, well-described, 6-HB. I474D and I474S mutants would appear to destabilize the second conformation, and partially destabilize the third, while allowing the first to form. Cleavage of F does not require coexpression of HN. The HN-F interaction-stabilizing conformation could be further investigated by using the known three-dimensional structures of pre-cleavage, and post-fusion F to target exposed residues for mutagenesis, in an effort to disrupt the HN-F interaction.

It is intriguing to speculate whether or not the I474S and I474D mutants would be fusion-competent, if only partially, if they were cleaved; it would seem likely, given that these proteins can form 6-HBs, even though the 6-HB are destabilized. One way to test this possibility would be to introduce an alternate cleavage sequence that might be sensitive to exogenously added protease, for example the Sendai F dibasic cleavage site that is sensitive to exogenously added trypsin (Luque and Russell, 2007).

One line of investigation that might provide additional information, is to monitor the kinetics of 6-HB formation by surface plasmon resonance. The kinetics of 6-HB formation is an understudied area for all of the class I fusion proteins.

The evidence presented in this chapter reveals a key role for HR2 in the formation of an F protein structure that is required for proteolytic processing of F_0 and functionality of the F protein. This could be due to a localized change in structure, but with a significant enough effect on the overall conformation of F to abolish cleavage. Stabilization of a pre-cleavage structure is a novel role for HR2, in addition to its well-defined role in 6-HB formation and its proposed role in interactions with the HN protein.

Chapter 4 – Investigation of the HPIV3 HN-F interaction

Introduction

Paramyxovirus envelopes include two integral glycoproteins, the receptor-binding hemagglutinin-neuraminidase (HN) and the fusion glycoprotein (F). These two proteins have been shown to functionally interact; for the majority of the paramyxoviruses, cell-cell fusion occurs only when HN and F are coexpressed in cells (Heminway *et al.*, 1994; Horvath *et al.*, 1992; Hu *et al.*, 1992; Wild *et al.*, 1991; Ebata *et al.*, 1991), although there are exceptions. The F proteins of PIV5 (Bagai and Lamb, 1995) and peste des petits ruminants virus (Seth and Shaila, 2001), and site-directed mutants of the NDV (Sergel *et al.*, 2000) and SER virus (Seth *et al.*, 2003) F proteins mediate fusion in the absence of the HN protein, though in each case, coexpression of HN significantly increased the amount of fusion. This functional interaction between HN and F is also type-specific, generally requiring coexpression of HN and F from the same virus (Yao *et al.*, 1997; Bagai and Lamb, 1995; Deng *et al.*, 1995; Tsurudome *et al.*, 1995; Bousse *et al.*, 1994; Wild *et al.*, 1991), again, with a few exceptions, as described in the general introduction. Evidence for a physical interaction between HN and F exists. For NDV, measles virus, HPIV2, Sendai virus, and PIV5, monoclonal antibodies directed against one of the viral glycoproteins can coprecipitate the other (Deng *et al.*, 1999; Yao *et al.*, 1997; Stone-Hulslander and Morrison, 1997; Malvoisin and Wild, 1993), and cocapping experiments showed that HPIV2 HN and F colocalize in cells in the presence of antibody (Yao *et al.*, 1997). Intracellular trapping experiments also suggested that HPIV3 (Tong and Compans, 1999; Tanaka *et al.*, 1996), HPIV2 (Tong and Compans, 1999), and measles virus (Plemper *et al.*, 2001) glycoproteins physically interact with each other. A direct interaction between peptides derived from the stalk region of the HN protein and HR2 of the F protein of NDV was demonstrated (Gravel and Morrison, 2003), as previously proposed based on studies with chimeric HN and F

proteins (Tsurudome *et al.*, 1998; Tanabayashi and Compans, 1996; Deng *et al.*, 1995; Tsurudome *et al.*, 1995). However, the measles virus hemagglutinin (H) and F proteins associate with each other when mutations that abrogate fusion promotion and the interaction of NDV HN and F were introduced into similar regions of the stalk domain of the H protein. These results suggest that a region of the measles H protein other than the stalk may be involved in H-F interactions (Corey and Iorio, 2007).

The isolation of native HN-F complexes without the use of immunoprecipitations has not been reported. Notably, most of the above studies employed monospecific antibodies to precipitate HN-F complexes, which may alter HN-F interactions. Complex formation between HN and F is accepted to be a critical requirement for paramyxovirus membrane fusion to occur, or at least for promotion of membrane fusion. The objective of the work described in this chapter was to develop an assay that would provide a rapid, simple method for isolation of native HPIV3 HN-F complexes, which could then be used to elucidate regions on the two protein that are critical for their interaction. Specifically, the HN protein was tagged with a hexahistidine sequence, with the idea that F, complexed with HN, could be purified from cell lysates using nickel-agarose chromatography columns.

Results

Construction of FLAG- and hexahistidine-tagged HN protein, and purification using Ni affinity column chromatography

To purify HN from cell lysates using Ni-affinity chromatography, a plasmid encoding the HPIV3 HN protein with a carboxy-terminal hexahistidine tag (HN-His_6) under control of the T7 promoter was constructed by Catherine Zaborowska. HeLaT4 cells expressing HN-His_6 were lysed in phosphate lysis buffer containing various detergents. The cell lysates were passed over Ni-agarose columns and the binding and elution of the HN-His_6 protein was monitored by SDS-PAGE and immunoblotting of column fractions. No binding of HN-His_6 to the column was observed (results not shown). It was noted that a cysteine residue (C571) is located two residues upstream of the HN translational stop signal. It was hypothesized that the hexahistidine tag may be inaccessible to Ni ions because of the secondary structure of the HN protein. A second plasmid, *pCITE-HN-FLAG-His_6*, was constructed in which the HN-His_6 coding sequences were modified so that a hydrophilic spacer (FLAG, DYKDDDDK) was inserted between the carboxy terminal amino acids of HN and the hexahistidine tag to shift the tag further away from C571 and to allow for HN to be detected by immunoblotting using anti-FLAG monoclonal antibodies. This proved to be a judicious decision. Expression of the doubly-tagged protein was verified by SDS-PAGE separation and immunoblotting of cell lysates with FLAG-specific antibodies (see Figure 14, panel A). Surface expression and functionality of tagged HN was visually confirmed using human and guinea pig erythrocyte hemadsorption (results not shown). After much of this work was completed, it was shown that C571 is in fact involved in disulfide bonding with C159 (Lawrence *et al.*, 2004). Successful binding of FLAG- and hexahistidine-tagged HN to Ni agarose columns, and elution of the protein, was examined. Cells expressing HN-FLAG-His_6 were lysed with nonidet P-40 (NP-40), *n*-dodecyl-β-D-maltoside (dodecyl maltoside),

Figure 14. Isolation of native complexes of the HPIV3 HN and F proteins. HeLaT4 cells expressing HN-FLAG-His_6, F-FLAG, or both, were lysed using octyl glucoside, and lysates were passed over Ni affinity columns. Columns were extensively washed, and bound proteins were eluted using imidazole. Column fractions were collected and analyzed by SDS-PAGE. FLAG-tagged proteins were detected by immunoblotting. (A) HN-FLAG-His_6 fully binds to and elutes from Ni affinity colums.Results from two separate experiments with HN-FLAG-His_6, performed six months apart are shown. (B) F-FLAG does not bind to Ni affinity columns. (C) HN-FLAG-His_6/F-FLAG complexes bind to and can be eluted from Ni affinity columns. Immunoblots in panels A and B were developed using the enhanced chemiluminscence (ECL) reagent system; the immunoblot in panel C was developed using the NBT/BCIP colourimetric detection system.

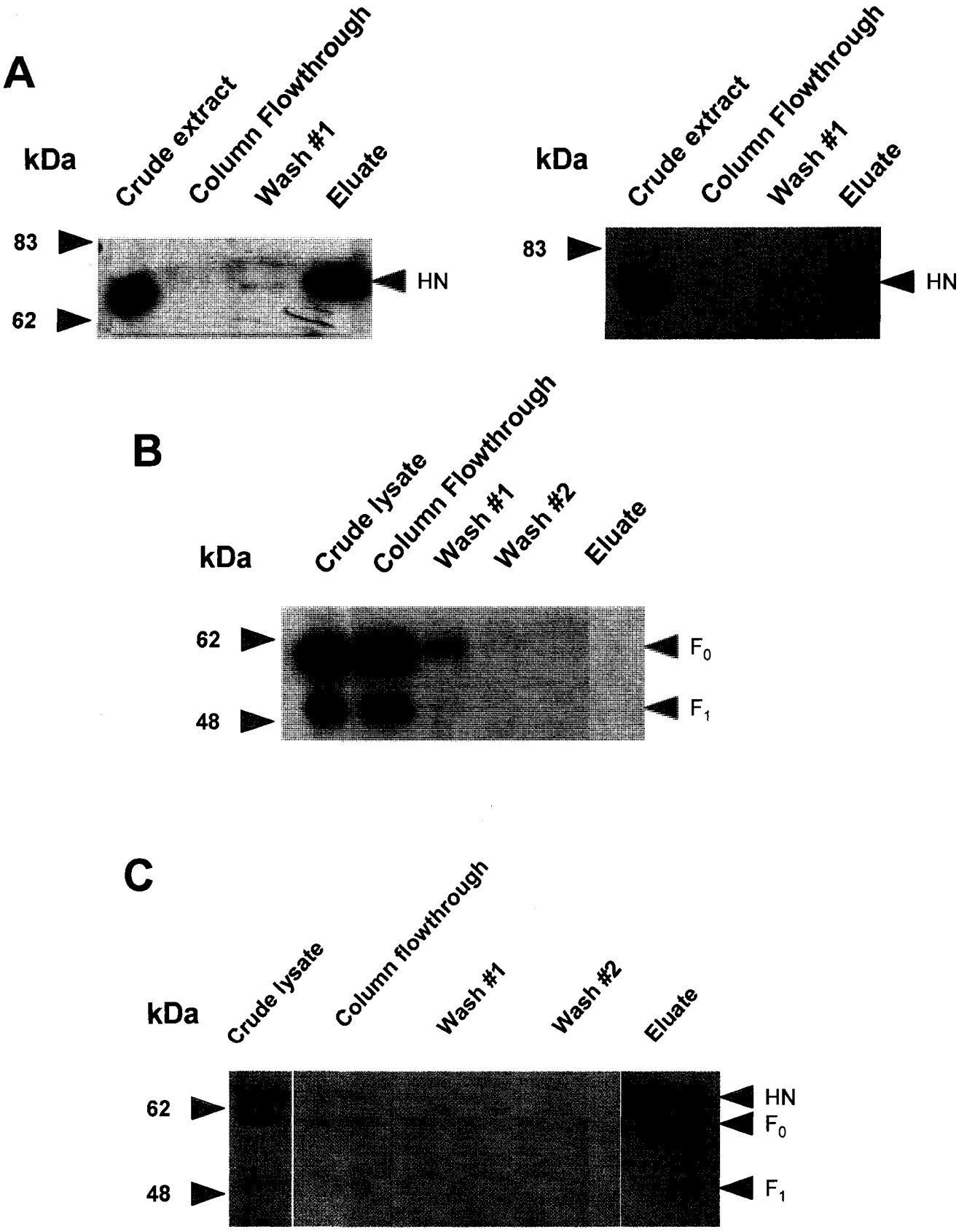
A
kDa
Crude extract
Column Flowthrough
Wash #1
Eluate
83
62
HN
kDa
Crude extract
Column Flowthrough
Wash #1
Eluate
83
HN
B
kDa
Crude lysate
Column Flowthrough
Wash #1
Wash #2
Eluate
62
48
F0
F1
C
kDa
Crude lysate
Column flowthrough
Wash #1
Wash #2
Eluate
62
48
HN
F0
F1

polyoxyethylene (20) sorbitan monolaurate (Tween-20), polyoxyethylene (20) sorbitan monooleate (Tween-80), or n-octyl-β-D-glucopyranoside (octyl glucoside), all at concentrations suggested by suppliers. Lysates were incubated with Ni-agarose columns at 4°C for 2-4 hours, the columns were washed extensively, and bound proteins were eluted using 150 mM imidazole. Crude lysate, column flow-through, wash, and eluate fractions were collected and analyzed by immunoblotting. Quantitative binding and elution of HN-FLAG-His_6 was observed for all detergents tested. The results of binding and elution of HN-FLAG-His_6 in lysates prepared with octyl glucoside are shown in Figure 14, panel A. Solubility of HN was found to be optimal at an octyl glucoside concentration of 32 mM (see below) and this concentration of octyl glucoside was subsequently used to prepare all cell lysates described in this chapter, unless otherwise noted. In each octyl glucoside experiment, HN was near-quantitatively bound to and eluted from the Ni agarose columns. The ability to bind HN was highly reproducible, and the results of two separate experiments, performed six months apart, are presented in Figure 14, panel A.

Solubility of the HN and F proteins is highly dependant on the detergent used to lyse cells

To optimize recovery of HN protein and HN-F complexes by Ni-affinity chromatograpy, the solubility of HN-FLAG-His_6 and F-FLAG proteins in octyl glucoside was examined. HeLaT4 cells, expressing HN-FLAG-His_6 or F-FLAG, were lysed with different detergents. Control cell lysates, in which the HPIV3 glycoproteins are considered to be completely solubilized, were produced by lysing the cells in phosphate buffer, pH 8.0, containing 1% SDS (Figure 15, panel B). Cells were also lysed in

Figure 15. Solubility of the HPIV3 HN and F proteins in octyl glucoside. (A) HeLaT4 cells, transfected with plasmids encoding HN-FLAG-His_6 or F-FLAG were scraped from culture dishes, washed, and lysed with phosphate buffer containing various concentrations of octyl glucoside, as indicated. Supernatants (S) were removed following centrifugation of lysates, and both supernatants and pellets (P) were mixed with SDS-PAGE loading buffer. Equal proportions of supernatants and pellets were subjected to SDS-PAGE. Proteins were transferred to PVDF membranes, and FLAG-tagged proteins were detected by immunoblotting. (B) HeLaT4 cells, transfected and treated identically to those in panel (A), were lysed with phosphate buffer containing 1% SDS, or 0.5% Triton X-100 and analyzed as described above.

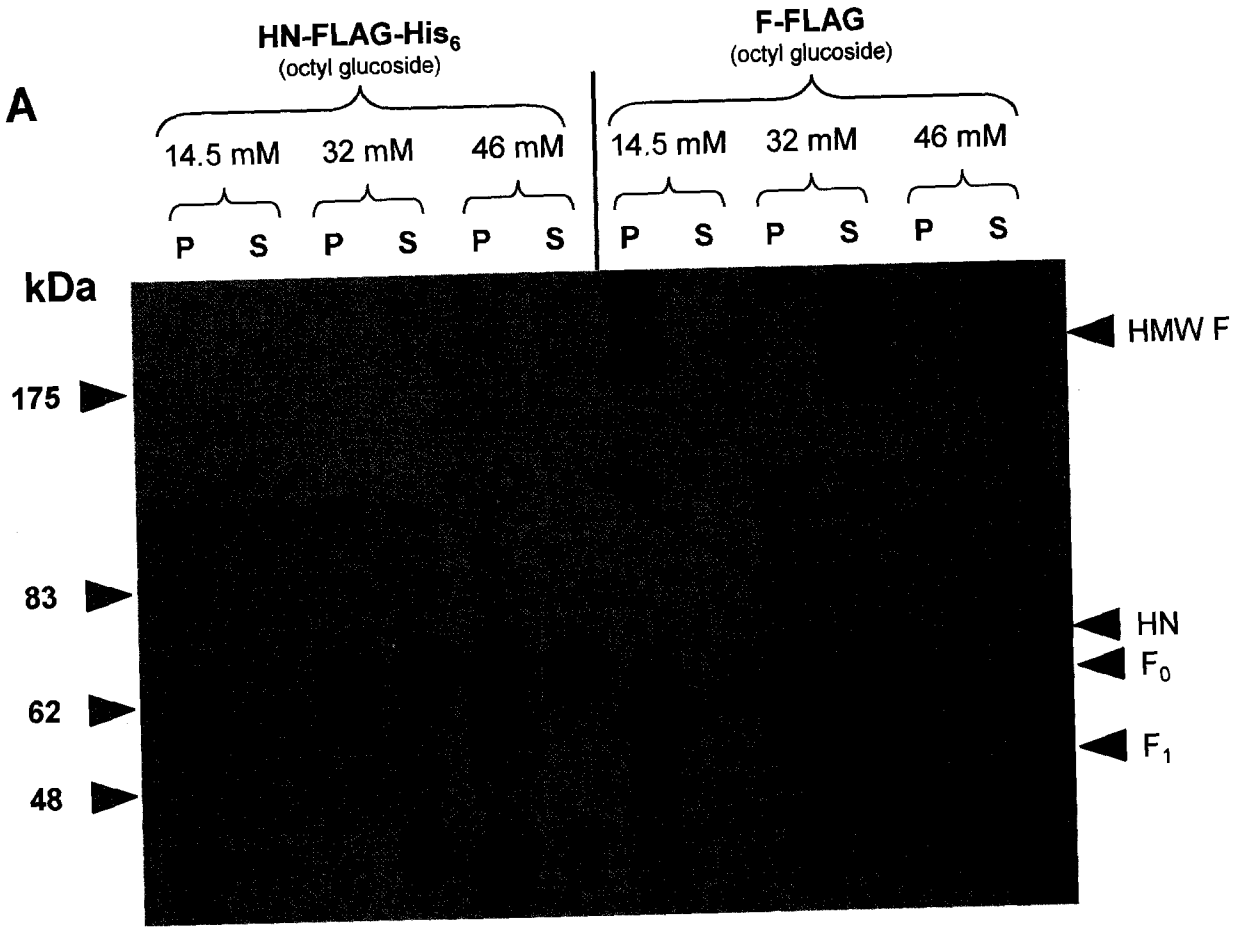
A
HN-FLAG-His6
(octyl glucoside)
F-FLAG
(octyl glucoside)
14.5 mM
32 mM
46 mM
14.5 mM
32 mM
46 mM
P S P S P S P S P S P S
kDa
175
83
62
48
HMW F
HN
F0
F1

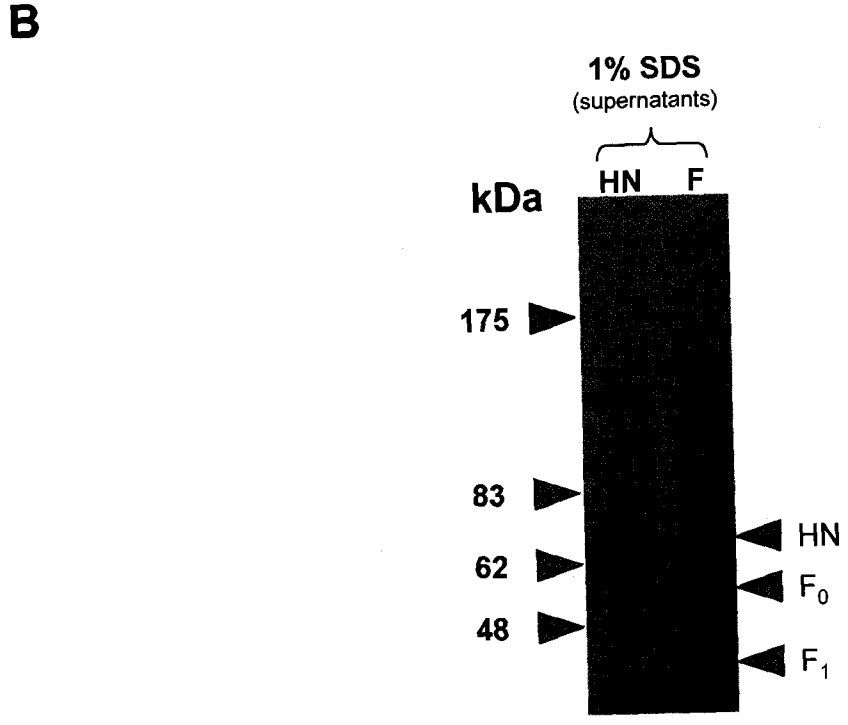
B
1% SDS
(supernatants)
HN F
kDa
175
83
62
48
HN
F0
F1

phosphate buffer, pH 8.0, containing different concentrations of octyl glucoside. The concentrations of octyl glucoside tested, 14.5 mM, 32 mM, and 46 mM (which was recommended by the supplier), span, and exceed, the critical micellar concentration of 15-25 mM (Mukerjee and Chan, 2002; Wasylewski and Kozik, 1979). Lysates were centrifuged for 5 min at 12,000 x g, 4°C. The soluble supernatants and pellets, solubilized in SDS-PAGE loading buffer, were analyzed by SDS-PAGE and immunoblotting for the FLAG tag, The optimal concentration for solubilization of the HPIV3 HN protein in octyl glucoside was between 32-46 mM (Figure 15, panel A); however, approximately 50% of the HN protein remained insoluble, and in the pellet, even at the optimal concentrations. Similarly, the solubility of the F protein appeared to be maximal at 32 mM, although not quantitative, and in fact, quite poor at 46 mM. The high molecular weight (HMW) bands in octyl glucoside lysates of cells expressing HPIV3 Fare believed to be F trimers that do not dissociate during SDS-PAGE. These HMW bands do not appear when cells are solubilised with SDS (Figure 15 panel B), NP-40, and Triton X-100 (not shown).

Cleavage or fusion activity of the F protein are not required for HN-F complex formation

Since HN-FLAG-His_6 and F-FLAG were both functional, as evidenced by extensive cell fusion in cells expressing the two glycoproteins, and because HN-FLAG-His_6, but not F-FLAG (see below), bound to Ni agarose columns, the possibility that HN and F proteins would copurify as a complex was tested. HeLaT4 cells expressing HN-FLAG-His_6 and F-FLAG were lysed using various detergents and analyzed by Ni-agarose chromatography, SDS-PAGE and immunoblotting. If F-FLAG was detected in the eluate, this was interpreted to mean that the HN-F complex was stable in the detergent used for cell lysis. If no F-FLAG was detected in the eluate it was assumed that HN-F complexes had dissociated. When transfected cells were lysed with 32 mM (not shown) or 46 mM octyl glucoside (Figure 14,

panel C), both HN and F were detected in the eluate. It is interesting to note that the complexes contained both cleaved $F_{1,2}$-FLAG, as well as uncleaved F_0-FLAG. Also notable is the fact that the colorimetric detection system was used for this single experiment, rather than the more sensitive enhanced chemiluminescence (ECL) detection method. As detailed below, later attempts to repeat purification of the wild-type F protein with HN were difficult, due to downregulation of HN expression when F and HN are coexpressed.

HN-F complexes were not detected when NP-40, Tween-20, Tween-80 or dodecyl maltoside were used to lyse cells (results not shown). The instability of HN-F complexes in dodecyl maltoside was unexpected, because this detergent was used to lyse cells for coimmunoprecipitation of the HN and F glycoproteins of human parainfluenza virus type 2 (Yao *et al.*, 1997) and NDV (Deng *et al.*, 1999).

No FLAG-tagged F protein was detected in the eluates following Ni agarose chromatography of lysates prepared from cells expressing only F-FLAG (Figure 14, Panel B). This result confirms that F-FLAG present in eluates of octyl glucoside lysates of cells expressing both HN-FLAG-His_6 and F-FLAG is likely to be in HN-F complexes, and not binding non-specifically to the Ni agarose column.

As detailed in Chapter 3, mutation of the F protein at position I474 in HR2 produced a series of F proteins that differed in fusogenicity, cleavage, and 6-HB stability. To determine if the mutated F proteins could complex with HN, HeLaT4 cells were cotransfected with plasmids encoding FLAG-tagged F proteins bearing I474S, D and E substitutions and with *pCITE-HN-FLAG-*His_6. Following octyl glucoside lysis, lysates were analyzed by Ni agarose column chromatography, SDS-PAGE and Western blotting with a FLAG-specific antibody. The results (Figure 16) indicate that all three altered F proteins can form HN-F complexes. However, low levels of HN expression in cells expressing F, and poor recovery of the HN protein called the reliability of the assay into question. The effect of F protein protein expression on HN expression was investigated in greater detail, as

Figure 16. Isolation of HN-F complexes containing I474 mutant F proteins. Octyl glucoside lysates of HeLaT4 cells expressing HN-FLAG-His_6 and I474 F mutant F-FLAG proteins, as indicated, were passed over Ni affinity columns, and after washing, proteins were eluted using imidazole. Column fractions were analyzed by SDS-PAGE and FLAG-tagged proteins were detected by immunoblotting. HN-F complexes were isolated in all cases. (A) HN and F(I474S) complexes. (B) HN and F(I474D) complexes. (C) HN and F(I474E) complexes.

A – F(I474S)

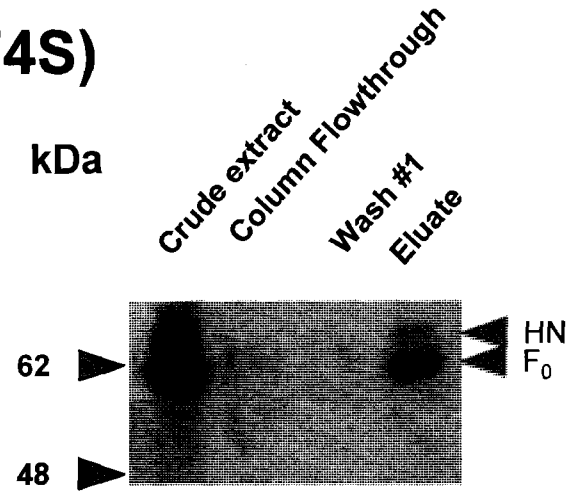

B – F(I474D)

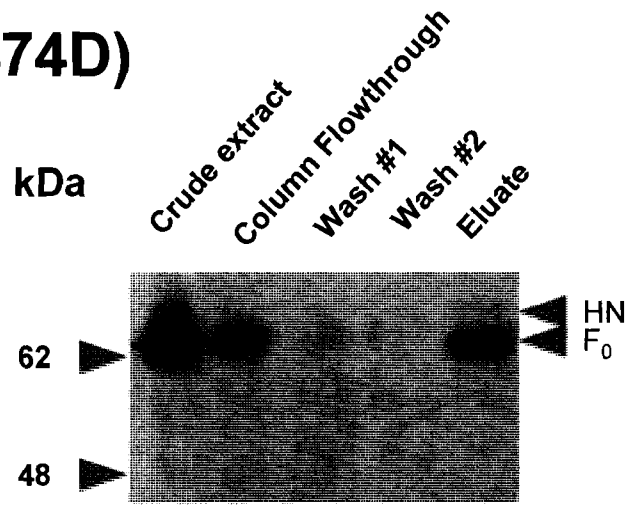

C – F(I474E)

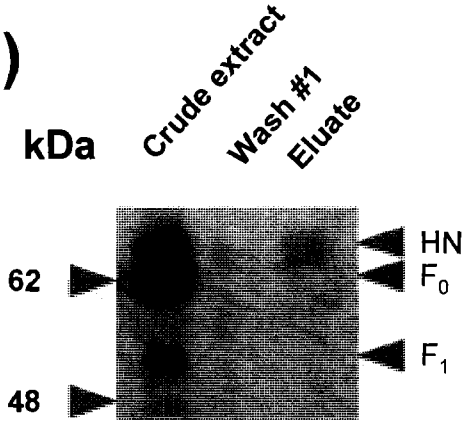

described below.

Expression of HN is consistently downregulated when coexpressed with F protein

It was previously demonstrated that expression of high levels of the F proteins of HPIV1 and Sendai virus resulted in the downregulation of expression of the homologous HN proteins, at a co- or post-translational stage (Bousse *et al.*, 1997). A similar reduction in the amount of the HPIV3 HN protein was seen in HeLaT4 cells coexpressing HN and wild-type or mutated HPIV3 F proteins, as compared to cells expressing HN alone (Figure 17, panel A). This effect was consistent, and although the degree of HN downregulation varied somewhat from experiment to experiment, it did not appear to be dependent on the plasmid DNA preparation, the source, passage, or relative health of the HeLaT4 cells, or on the stock of vTF7-3 used for the experiments. The downregulation of HN was such that purification of complexes was made near to impossible, since HN was used as the "bait" protein in this study.

To investigate the mechanism of HPIV3 HN downregulation in transfected cells expressing the HPIV3 F protein, HN expression in the presence of brefeldin A (BFA) was examined. BFA causes the Golgi apparatus to form vesicles that are absorbed into the endoplasmic reticulum (ER) of eukaryotic cells (Dinter and Berger, 1998; Sciaky *et al.*, 1997; Klausner *et al.*, 1992). The rationale for the use of BFA to disrupt ER exit of HN and F was twofold: firstly, to help solve the ongoing controversy of the subcellular location of the first interaction between HN and F, disruption of ER exit and isolation of complexes would be useful; secondly, though Bousse and colleagues (1997) indicated that downregulation of HN by F was occurring early after translation, it was unclear if this same situation was occurring in cells expressing HPIV3 HN and F. If HN downregulation was occurring beyond the ER, disruption of ER exit by BFA could limit the downregulation of HN expression by F

Figure 17. Downregulation of HPIV3 HN protein expression by coexpression of the HPIV3 F protein. (A) Lysates of HeLaT4 cells, expressing HN-FLAG-His_6 alone or coexpressing HN-FLAG-His_6 and wild-type or mutant F-FLAG, were analyzed by SDS-PAGE. FLAG-tagged proteins were detected by immunoblotting. Experiments were performed approximately six months apart. Panels B and C: Lysates of brefeldin-treated HeLaT4 cells, expressing F-FLAG (B), HN-FLAG-His_6 (C) or co-expressing HN-FLAG-His_6 and F-FLAG (C), were analyzed by SDS-PAGE and FLAG-tagged proteins were detected by immunoblotting.

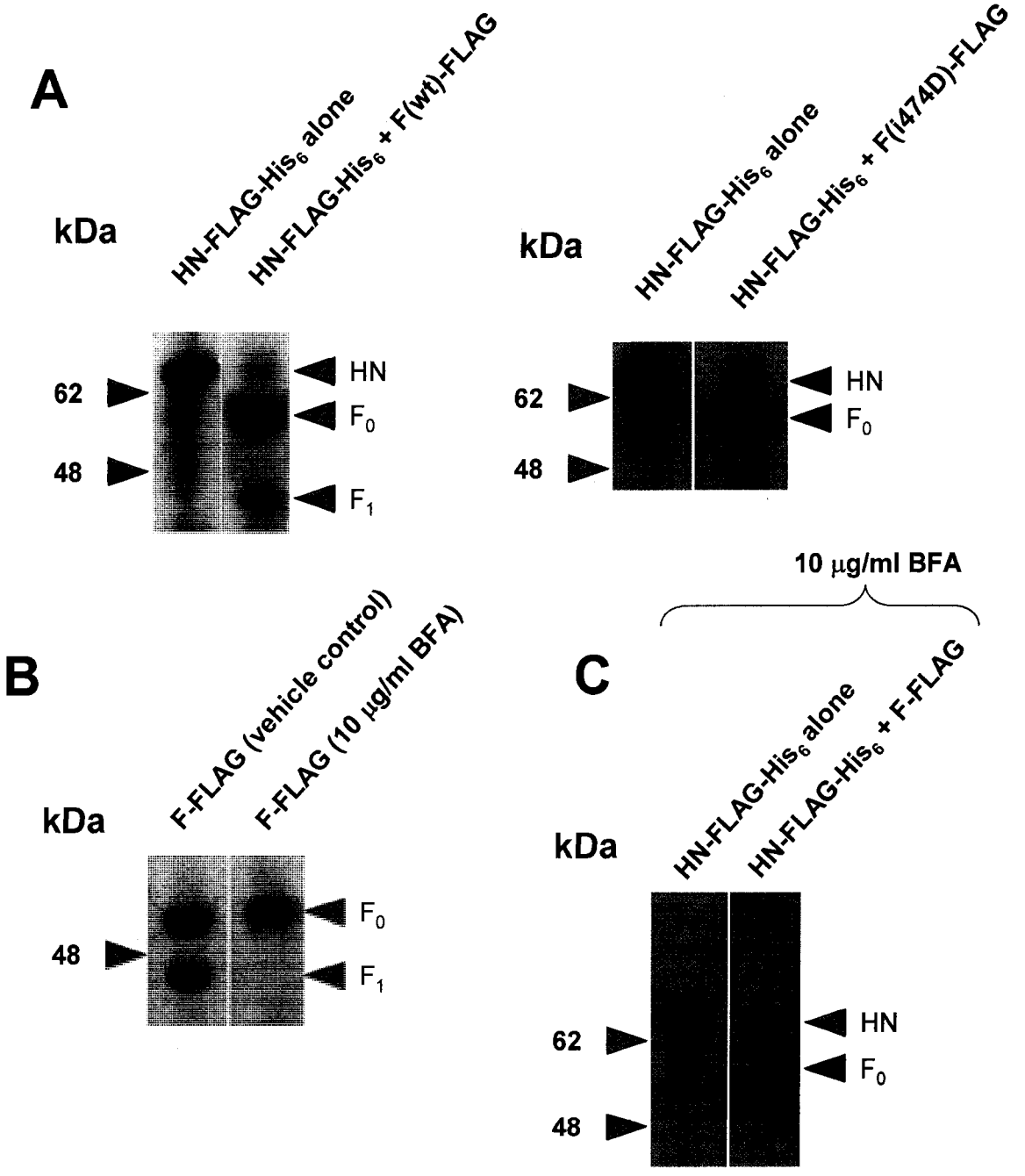
A
kDa
HN-FLAG-His6 alone
HN-FLAG-His6 + F(wt)-FLAG
62
48
HN
F0
F1
kDa
HN-FLAG-His6 alone
HN-FLAG-His6 + F(i474D)-FLAG
62
48
HN
F0
B
kDa
F-FLAG (vehicle control)
F-FLAG (10 μg/ml BFA)
48
F0
F1
10 μg/ml BFA
C
kDa
HN-FLAG-His6 alone
HN-FLAG-His6 + F-FLAG
62
48
HN
F0

so that it might be possible to isolate HN-F complexes, as well as address the question of whether or not HN-F interaction takes place in the ER. The use of BFA was predicted to prevent cleavage of the F protein by furin, which is resident in the *trans*-Golgi (Scamuffa *et al.*, 2006; Nakayama, 1997), and thus a lack of F protein cleavage was considered to be a marker for BFA effects. HeLaT4 cells, expressing F-FLAG were treated overnight at 37°C with 10 µg/ml brefeldin A (BFA). Cell lysates were prepared and analyzed by immunoblotting for the FLAG epitope following SDS-PAGE (Figure 17, panel B). BFA had the desired effect, as the F protein was not cleaved in BFA-treated cells. No effect was seen on HN-FLAG-His_6 expression in cells treated with BFA (Figure 17, panel C, first lane), compared to untreated cells (not shown); however, the downregulation of HN was observed in BFA-treated cells in which HN and F were coexpressed. It is evident from these results that purification of HN-F complexes from HeLaT4 cells expressing both proteins is near-to-impossible, given the extent of the downregulation of HN expression, and its incomplete solubilisation in octyl glucoside.

HN-F complexes do not assemble when separate cell lysates containing HN or F proteins are combined

In an effort to overcome the problems caused by the downregulation of HN in cells expressing both HN and F proteins, lysates of HN-expressing cells and F-expressing cells were mixed. Octyl glucoside lysates and NP-40 lysates were prepared and mixed in different combinations. On occasion both HN-FLAG-His_6 and F-FLAG were bound to Ni agarose colums, however, results were generally negative, and this approach was felt to be unreliable. HN-FLAG-His_6 was also bound to Ni agarose and used in an attempt to capture F-FLAG from cell lysates, without success.

Discussion

This study is the first to describe direct isolation of "native" paramyxovirus HN-F complexes. The methods used to isolate the HN-F complexes did not rely on antibody-based precipitations, a step that may disrupt or otherwise affect HN-F interactions. An obvious application of the assay is to investigate the structural basis of HN-F glycoprotein interaction, particularly in view of the three-dimensional crystal structures of paramyxovirus HN (Ryan *et al.*, 2006; Yuan *et al.*, 2005; Lawrence *et al.*, 2004; Crennell *et al.*, 2000) and F (Yin *et al.*, 2006; Yin *et al.*, 2005; Chen *et al.*, 2001) proteins. It is unfortunate that the observed downregulation of HN expression in cells that also express the F protein, in addition to the incomplete solubility of HN in octyl glucoside, made isolation of HN-F complexes unreliable. Despite several attempts to modify the isolation procedure, including optimization of detergent concentrations and mixing of lysates from cells separately expressing HN and F, it was not possible to reliably replicate the early successes observed in HN-F complex isolation. If methods can be improved so that HN-F complexes can be reproducibly isolated, this assay has the potential to be extremely useful in the study of HN-F interactions and their role in paramyxovirus entry.

The results presented in this study identify several interesting features of HN-F interactions. First, both cleaved, active F_1 and the inactive F_0 precursor copurify with HN. It is unclear if F_2 is also isolated in the complexes, as there was no way to detect F_2 by immunoblotting, as the FLAG tag is located on the F_1 moiety. F_1 and F_2 are covalently linked by a disulphide bond (Lamb and Kolakofsky, 2001), which would suggest that F_2 is also pulled down. Isolation of $F_{1,2}$ and F_0 in complex with HN mirrors studies in which mAbs against NDV HN coprecipitated both cleaved and uncleaved forms of F (Deng *et al.*, 1999; Stone-Hulslander and Morrison, 1997), but is not consistent with results obtained for measles virus (Corey and Iorio, 2007; Malvoisin and Wild, 1993), HPIV2, Sendai virus, and

PIV5 (Yao *et al.*, 1997), in which F_0 was not coprecipitated with HN. The mild detergent conditions used in this study may account for the isolation of HN-F complexes containing both cleaved and uncleaved F protein. The published pre-cleavage (Yin *et al.*, 2006) and "post-cleavage"/post-fusion (Yin *et al.*, 2005; Chen *et al.*, 2001) structures of the F protein clearly indicate significantly different conformations, which may explain the differences in HN interactions with F_0 and $F_{1,2}$. Also, cleavage efficiencies may vary among paramyxovirus F proteins, which may affect the amounts of F_0 present in coimmunoprecipitates. It is also possible that differences in the ease with which HN-F complexes are disrupted is due to sequence differences among paramyxovirus glycoproteins. These results suggest that at least some of the F_0 protein present in HPIV3-infected cells, and possibly on virions (Ebata, 1996) is associated with HN.

The second observation is that fusion-negative F proteins (I474S, I474D) appear to form HN-F complexes, which also supports the idea that HN-F interactions occur before F_0 cleavage. These data support a model in which complexes of HN and F_0 form in the ER, and are transported through the Golgi apparatus to the cell surface. Evidence has been provided for intracellular complexing of HN and F based on ER-trapping of paramyxovirus glycoproteins by tagging the partner with ER retention tags such as KDEL (Tong and Compans, 1999; Tanaka *et al.*, 1996) or polyarginine (Plemper *et al.*, 2001), although there is one contradictory study that did not support this conclusion (Paterson *et al.*, 1997). The results of experiments using BFA, which blocks trafficking beyond the ER (Dinter and Berger, 1998; Sciaky *et al.*, 1997; Klausner *et al.*, 1992), supports a model in which HN and F interact early after translation. This is also consistent with the suggestion that downregulation of HN expression by F occurs cotranslationally or shortly after the two proteins are synthesized, and is not related to mRNA levels (Bousse *et al.*, 1997). It is unclear, though, whether downregulation of HN expression requires HN-F interaction.

The downregulation of HN expression was found to be unrelated to the preparation of HN and F plasmid DNA used, the cell passage and heaviness of cell growth, or the vTF7-3 stock used. In a previous study, similar results were obtained for HPIV1 and Sendai virus glycoproteins using both a vTF7-3-based expression system and the Semliki forest virus (SFV) expression system (Bousse *et al.*, 1997), indicating that this effect is not due to the use of the vaccinia virus expression system. The observed downregulation of HN expression when HN and F are coexpressed is unlikely to occur during paramyxovirus infection, and is likely an experimental artifact resulting from the high level of F protein expression in the experimental system used in this study. Expression of the F protein is strictly controlled in infected cells, through multiple mechanisms, which include transcriptional attenuation (Lamb and Kolakofsky, 2001), and transcription of a bicistronic M/F readthrough mRNA, which appears to reduce the amount of translatable monocistronic F transcripts by 35-80%, depending on the virus species (Rassa and Parks, 1998; Bousse *et al.*, 1997; Cattaneo *et al.*, 1987; Spriggs and Collins, 1986). Although several detergents were tested, HN-F complexes were only isolated when cells were disrupted with octyl glucoside. At the optimal concentration of octyl glucoside, approximately 50% of HN or F was solubilised. Together, the incomplete solubilitization of HPIV3 HN and F in octyl glucoside and the downregulation of HN expression account for the difficulties encountered in reproducibly isolating HN-F complexes.

The nickel affinity column chromatography assay developed here could be very useful, if it can be made more reproducible, to screen for structural elements that are essential for complex formation and/or fusion. Previous studies that screened for HN-F interactions between functionally altered proteins used coimmunoprecipitations to investigate homo- and heterotypic interactions between HN and F proteins (Corey and Iorio, 2007; Melanson and Iorio, 2006; Melanson and Iorio, 2004; Deng *et al.*, 1999; Yao *et al.*, 1997). This assay would be very useful to test interactions between mutant and chimeric

HN and F proteins, such as the tempting targets of the HN stalk and F HR2 regions, which are believed to be responsible for the HN-F interaction (Corey and Iorio, 2007; Melanson and Iorio, 2006; Melanson and Iorio, 2004; Gravel and Morrison, 2003; Deng *et al.*, 1999; Tsurudome *et al.*, 1998; Tsurudome *et al.*, 1995; Bousse *et al.*, 1994). The applicability of the assay to other important paramyxovirus glycoprotein interactions (e.g. NDV, measles, and mumps viruses) is also tantalizing to rapidly screen for compounds that disrupt these interactions, and thus interfere with fusion and virus infection.

Chapter 5 – Characterization of chimeras based on the human and bovine parainfluenza virus type 3 F proteins

Introduction

Chimeric proteins constructed from fragments of related or unrelated proteins have long been used to identify and characterize important functional regions on proteins. Of particular interest to this dissertation is the use of chimeric viral envelope glycoproteins to identify key features of the influenza hemagglutinin (Kozerski *et al.*, 2000; Melikyan *et al.*, 1999; Schroth-Diez *et al.*, 1998), the Env proteins of the regular and amylotrophic murine and feline leukemia retroviruses (MLV, A-MLV and FLV) (Nakamura *et al.*, 2001; Tailor *et al.*, 2000; Tailor and Kabat, 1997), and the human T-cell leukemia retrovirus (HTLV) (Kim *et al.*, 2000), the flavivirus E_2 glycoprotein of hepatitis C virus (Patel *et al.*, 2001; Patel *et al.*, 2000), the G protein of vesicular stomatitis virus (Schnell *et al.*, 1998), the SARS coronavirus spike protein (Broer *et al.*, 2006), and the gB and gD proteins of human herpes simplex virus type 1 (Cairns *et al.*, 2003; Browne *et al.*, 2003). Some key information about functional domains of the HN glycoprotein of paramyxoviruses has also been revealed using protein chimeras; for example the regions of HN involved in its assembly into the proper membrane topology (Parks and Lamb, 1993), the localization of the F-interacting domain to the 80-100 membrane-proximal residues of the stalk region (Tanabayashi and Compans, 1996; Deng *et al.*, 1995; Tsurudome *et al.*, 1995), and identification of the cytoplasmic domain as essential for incorporation into virions (Takimoto *et al.*, 1998) were elucidated using protein chimeras. Chimeric SER/PIV5 F proteins identified the cytoplasmic tail, trans-membrane domain, and the extracellular domain as key for F protein activation (Seth *et al.*, 2004). HPIV2/simian virus 41 (SV41) F protein chimeras revealed four regions of the F protein potentially responsible for HN/F interactions, including one region incorporating HR2, and two other regions in the central domain, one incorporating a short

central stretch of F_1, and the other including the cysteine-rich head region (Tsurudome *et al.*, 1998).

Bovine parainfluenza virus type 3 (BPIV3) is classified in the same genus as HPIV3, as a *Respirovirus,* and BPIV3 particles and nucleocapsids are similar in size to those of HPIV3. BPIV3 infections of cattle produce subclinical infections or infections with limited URT symptoms. Infections of cattle spread rapidly in high-density situations such as feedlot or transport activities. The primary complication of BPIV3 infection is the weakening of the immune system, leading to infections with bacterial respiratory pathogens such as *Pasteurella* sp., which produce severe bronchopneumonia, referred to as "shipping fever" (Bailly *et al.*, 2000; Haanes *et al.*, 1997). BPIV3 and HPIV3 genomes are organized identically, although the BPIV3 genome is 18 nucleotides longer (15,480 nucleotides) than the HPIV3 genome, with differences in the sizes of the P, M, and F open reading frames, as well as in the 5' untranslated region of the P gene, and the 3' and 5' untranslated regions of the P and F genes (Bailly *et al.*, 2000). The key genome differences are presented in Figure 1 (Chapter 1).

Inspired by the above studies, the objective of the experiments described in this chapter was to use three-part F protein chimeras consisting of fragments from HPIV3 F and BPIV3 F proteins to identify regions in the F protein responsible for fusion promotion by HN. HPIV3 and BPIV3 F proteins share 80% identity and 88.7% similarity at the amino acid level, although certain regions of the proteins have stretches of lower similarity, including the cytoplasmic tail, where they share 44% identity and 56% similarity. Tsurudome and colleagues produced chimeras of the HPIV2/SV41 F proteins which identified broad regions on the F protein involved in a functional interaction with HN. HPIV2 and SV41 F proteins share slightly less similarity than HPIV3 and BPIV3 F proteins: approximately 70% identity and 84% similarity at the amino acid level. Using the Tsurudome *et al.* study as a guide, it was hypothesized that the more closely related HPIV3 and BPIV3 F proteins would allow

more specific identification of short regions or individual residues involved in HN interaction and fusion promotion.

Results

Human/Bovine F protein chimeras – analysis and construction

Preliminary evidence produced by various members of the Dimock laboratory using plasmids expressing BPIV3 HN and F, attempting to optimize fusion prior to my arrival in the laboratory, indicated, using qualitative fusion assays (microscopic analysis), that BPIV3 F protein, when transfected in concert with HPIV3 HN protein, fused cells but at a lower level of efficiency than HPIV3 F protein. Based on these preliminary results, construction of HPIV3/BPIV3 F protein chimeras was begun with the purpose of identifying regions of the F protein involved in F protein function and interaction with the HN protein.

To produce chimeras of the HPIV3 and BPIV3 F proteins, restriction enzyme recognition sequences for *Nco*I and *Bam*HI were introduced into plasmid pIBI-F-FLAG, by site-directed mutagenesis, to bracket the HPIV3 F coding sequences, by Drs Kris Chan and Reza Nokhbeh. *Afl*II and *Sal*I sites were engineered into the HPIV3 F coding sequence; the *Afl*II site resulted in a single Q198K change, but no change in the BPIV3 sequence, while the *Sal*I site had no effect on the HPIV3 F coding sequence. Similar sites were produced by PCR amplification of the BPIV3 F coding sequences in plasmid pGEM-BPIV3F, with no effect on the amino acid sequence. These restriction sites made it easy to exchange corresponding regions of the two F proteins. An alignment of each protein is presented in Figure 18 and a summary of fragment size, and percentage identity and similarity is found in Table 7. Important regions of the F protein contained in each fragment are listed in Table 8. The first letter of the chimeric F protein nomenclature indicates the virus from which region I (*Nco*I-*Afl*II fragment) was derived, the second letter represents region II (*Afl*II-*Sal*I fragment), and the third, region III (*Sal*I- *Bam*HI fragment). For example, HBH is a chimeric protein made up of regions I and III from HPIV3 F, and region II from BPIV3.

Figure 18. Alignment of the F proteins of HPIV3 and BPIV3. Amino acid pairs where *Afl*II and *Sal*I sites were introduced to allow construction of chimeric coding sequences are indicated by the yellow and green highlighting, respectively. Indicated above the sequences are heptad repeat 1, heptad repeat 2, and the transmembrane domain. Identical amino acids are shaded black, similar amino acids are shaded grey. The figure was produced using the Boxshade software program to illustrate a Clustal alignment.

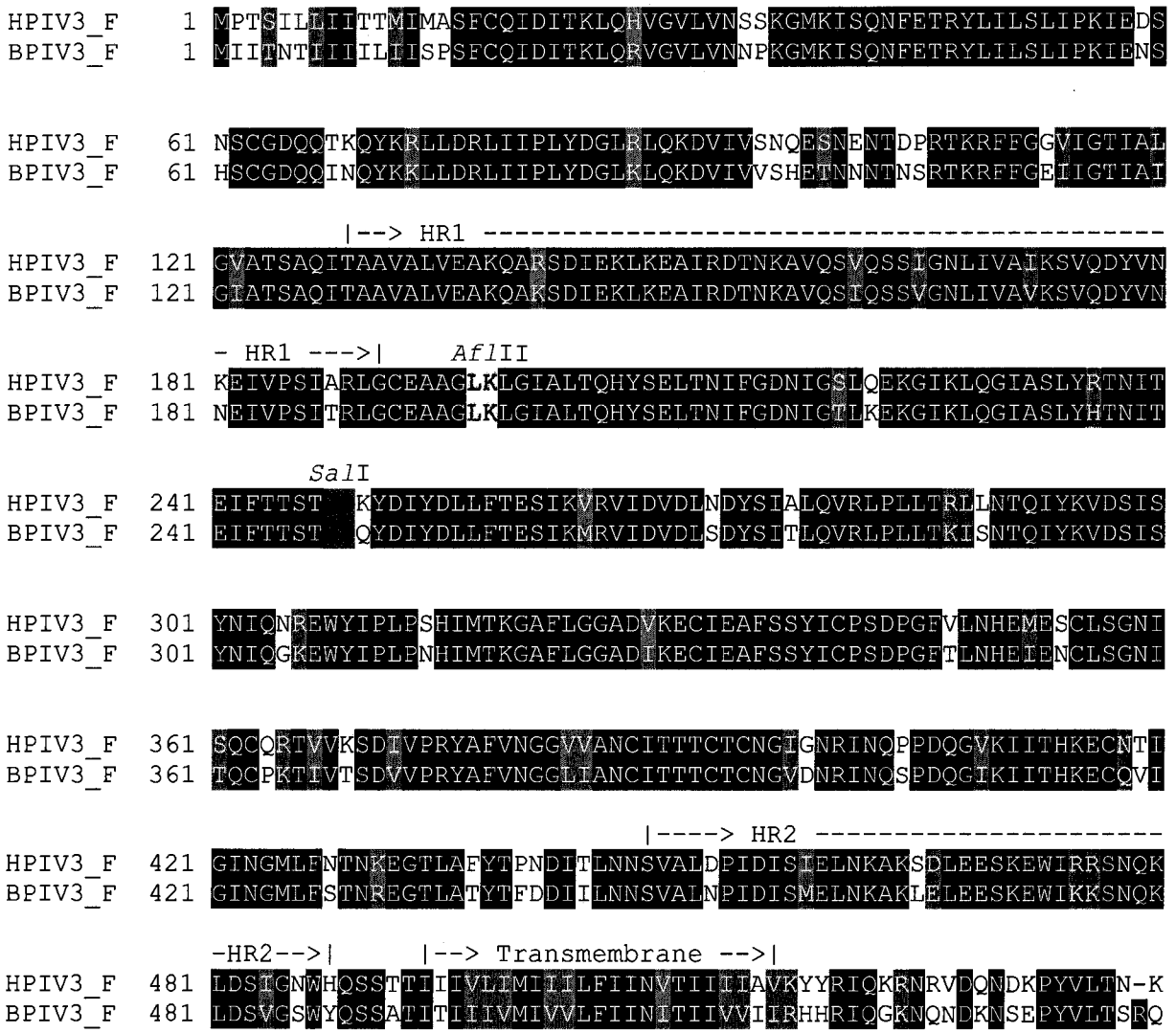
HPIV3_F 1 MPTSILLIITTMIMASFCQIDITKLQHVGVLVNSSKGMKISQNFETRYLILSLIPKIEDS
BPIV3_F 1 MIITNTIIIILIISPSFCQIDITKLQRVGVLVNNPKGMKISQNFETRYLILSLIPKIENS
HPIV3_F 61 NSCGDQQTKQYKRLLDRLIIPLYDGLRLQKDVIVSNQESNENTDPRTKRFFGGVIGTIAL
BPIV3_F 61 HSCGDQQINQYKKLLDRLIIPLYDGLKLQKDVIVVSHETNNNTNSRTKRFFGEIIGTIAI
|--> HR1 ----------
HPIV3_F 121 GVATSAQITAAVALVEAKQARSDIEKLKEAIRDTNKAVQSVQSSIGNLIVAIKSVQDYVN
BPIV3_F 121 GIATSAQITAAVALVEAKQAKSDIEKLKEAIRDTNKAVQSIQSSVGNLIVAVKSVQDYVN
- HR1 --->| AflII
HPIV3_F 181 KEIVPSIARLGCEAAGLKLGIALTQHYSELTNIFGDNIGSLQEKGIKLQGIASLYRTNIT
BPIV3_F 181 NEIVPSITRLGCEAAGLKLGIALTQHYSELTNIFGDNIGTLKEKGIKLQGIASLYHTNIT
SalI
HPIV3_F 241 EIFTTST KYDIYDLLFTESIKVRVIDVDLNDYSIALQVRLPLLTRLLNTQIYKVDSIS
BPIV3_F 241 EIFTTST QYDIYDLLFTESIKMRVIDVDLSDYSITLQVRLPLLTKISNTQIYKVDSIS
HPIV3_F 301 YNIQNREWYIPLPSHIMTKGAFLGGADVKECIEAFSSYICPSDPGFVLNHEMESCLSGNI
BPIV3_F 301 YNIQGKEWYIPLPNHIMTKGAFLGGADIKECIEAFSSYICPSDPGFTLNHEIENCLSGNI
HPIV3_F 361 SQCQRTVVKSDIVPRYAFVNGGVVANCITTTCTCNGIGNRINQPPDQGVKIITHKECNTI
BPIV3_F 361 TQCPKTIVTSDVVPRYAFVNGGLIANCITTTCTCNGVDNRINQSPDQGIKIITHKECQVI
|----> HR2 ----------
HPIV3_F 421 GINGMLFNTNKEGTLAFYTPNDITLNNSVALDPIDISIELNKAKSDLEESKEWIRRSNQK
BPIV3_F 421 GINGMLFSTNREGTLATYTFDDIILNNSVALNPIDISMELNKAKLELEESKEWIKKSNQK
-HR2-->| |--> Transmembrane -->|
HPIV3_F 481 LDSIGNWHQSSTTIIIVLIMIILFIINVTIIIIAVKYYRIQKRNRVDQNDKPYVLTN-K
BPIV3_F 481 LDSVGSWYQSSATITIIIVMIVVLFIINITIIVVIIRHHRIQGKNQNDKNSEPYVLTSRQ

Table 7. Size and sequence identity of F protein chimeric regions of BPIV3 and HPIV3

Region	Length (human)	Length (bovine)	% identity	% similarity
I	199	199	81.4%	88.4%
II	99	99	89.9%	94.9%
III	241	242	75.1%	87.1%
F protein	539	540	80.0%	88.7%

Table 8. List of key features of chimeric regions of HPIV3 and BPIV3 F proteins

Region	Key features	# of cysteines
I	Signal peptide, F_2, furin cleavage site, fusion peptide, HR1	3
II	Short central stretch	0
III	Cysteine-rich central region, HR2, trans-membrane, cytoplasmic tail	8

Quantitative fusion assays were carried out with several cell lines to identify cell lines that fused when the homologous pairs of HPIV3 or BPIV3 HN and F proteins were expressed. Fusion was observed only in HeLaT4 and Vero cells. The plasmid encoding the BPIV3 HN protein (pGEM4Zf-bovine HN) did not promote fusion with either of the BPIV3 or HPIV3 F proteins, at any plasmid ratio tested, in any cell line tested. However, when tested quantitatively, the HPIV3 HN protein promoted fusion with both the human F and the bovine F. All subsequent fusion assays were carried out using the HPIV3 HN protein.

Fusogenicity of the human/bovine chimeras

The rationale for swapping regions of the HPIV3 and BPIV3 F sequences was that region swapping might yield chimeric F proteins with differences in fusogenicity, which would allow for the identification of sequences in the F protein involved either in intermolecular interactions with HN or intramolecular interactions. Quantitative fusion assays were performed by expressing HPIV3 HN with HPIV3 F (pIBI-F-FLAG, used as a positive control), or with each of the eight FLAG-tagged chimeras (HHH, BHH, HBH, BHH, BBH, BHB, HHB, BBB), and using the contents-mixing quantitative fusion assay (Bossart and Broder, 2004; Nussbaum *et al.*, 1994). Results from a representative experiment are

presented in Figure 19. No obvious differences in fusogenicity were noted and statistical analysis (Student's t-test) showed that, while all F proteins mediated fusion that was significantly ($p<0.005$) greater than the negative control (no HN protein), there were no significant differences ($p>0.05$) in the fusogenicity of any of the chimeras compared to the positive control, nor between the chimeras and the HHH protein, which is unsurprising given that the parental HPIV3 and BPIV3 F proteins fuse cells, in concert with the HPIV3 HN protein, to statistically equivalent levels. Expression of each F protein in transfected cells was compared by Western blotting for the FLAG epitope in lysates of transfected HeLaT4 cells. A pair of sample western blots is presented in Figure 20. Although immunoblotting for another protein as a loading control was not done, a background band (unknown identity) for a protein with a molecular weight of approximately 45 kDa was used to control for amounts of protein loaded. No obvious difference in expression was noted. The size differences of the chimeric F proteins, which are summarized in Table 9, were reproducible from experiment to experiment, but cannot easily be explained by sequence differences. An amino acid is added to region III of the BPIV3 F sequence in the chimeric proteins, but it is negligible to the overall mass of the protein. Differences in glycosylation also do not explain the size differences. The high molecular weight bands found at >175 kDa are believed to be incompletely denatured F trimers, and amounts of this high molecular weight band vary.

Figure 19. Quantitative analysis of the fusogenicity of chimeric bovine/human PIV3 F proteins. HeLaT4 cells expressing wild type HPIV3 or BPIV3 F protein or F protein chimeras, and/or the HPIV3 HN protein, as indicated, were mixed with HeLaT4 cells transfected with plasmid pG1NT7. Cell-cell fusion was quantified using a contents-mixing fusion assay (see text for details). Chimeric F proteins are named using the parental virus origin of each specific region of the three-part chimeras, where "H" indicates HPIV3 F protein origin, and "B" indicates BPIV3 F protein origin. Data are presented as per cent fusion relative to the amount of fusion mediated by the wild-type F protein in the presence of the HN protein, and are means of duplicate samples from triplicate wells of a representative experiment, ± the standard deviation.

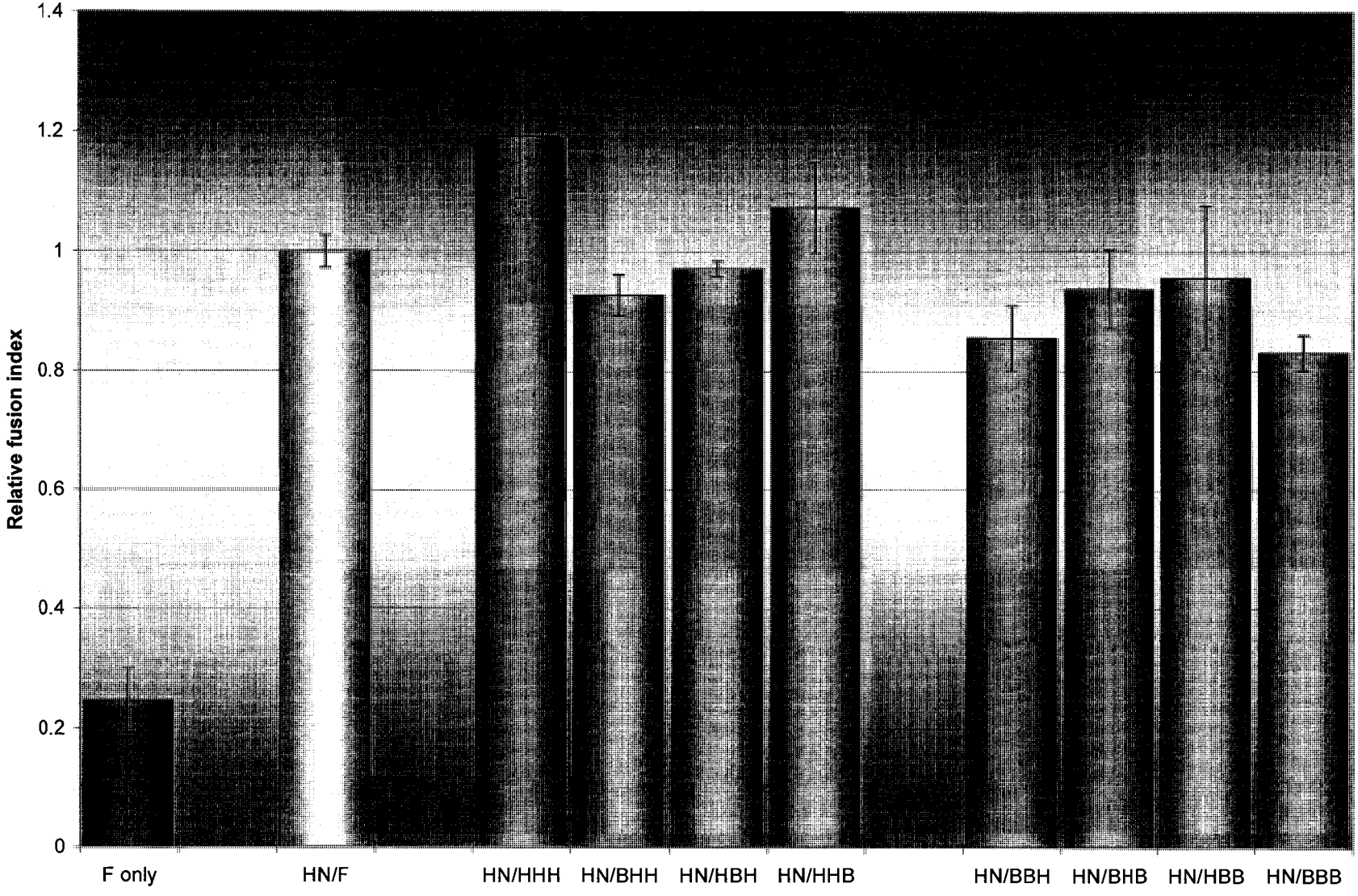
Relative fusion index
1.4
1.2
1
0.8
0.6
0.4
0.2
0
F only
HN/F
HN/HHH
HN/BHH
HN/HBH
HN/HHB
HN/BBH
HN/BHB
HN/HBB
HN/BBB

Figure 20. Expression of chimeric bovine/human PIV3 F proteins. Lysates of HeLaT4 cells expressing chimeric FLAG-tagged F proteins, were analyzed by SDS-PAGE and FLAG-tagged proteins were detected by immunoblotting. Two representative immunoblots are presented. In the upper blot, HHB appears to be incompletely denatured, and in the lower blot, HHH appears to be a misloaded sample. High molecular weight aggregates of F are also present in both blots. Size differences from chimera to chimera are replicated in each blot, including in the high molecular weight aggregates (see text for details). The lower blot also includes a doublet band of unknown identity (approximately 40 kDa in size) which was used as a loading control.

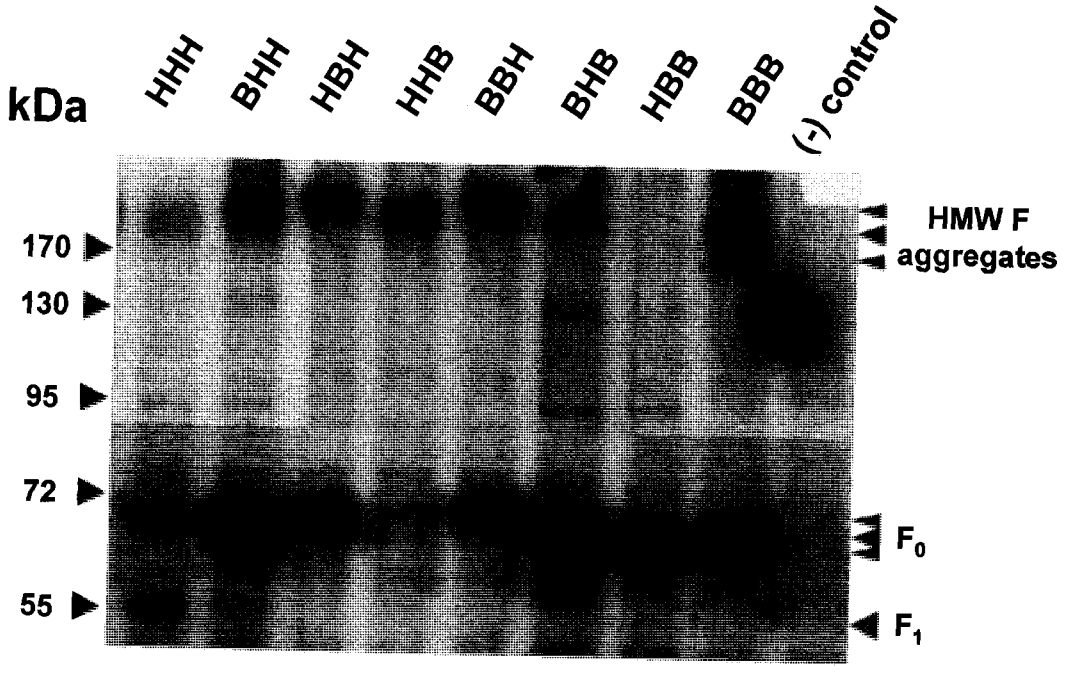
kDa
HHH
BHH
HBH
HHB
BBH
BHB
HBB
BBB
(-) control
170
130
95
72
55
HMW F aggregates
F_0
F_1

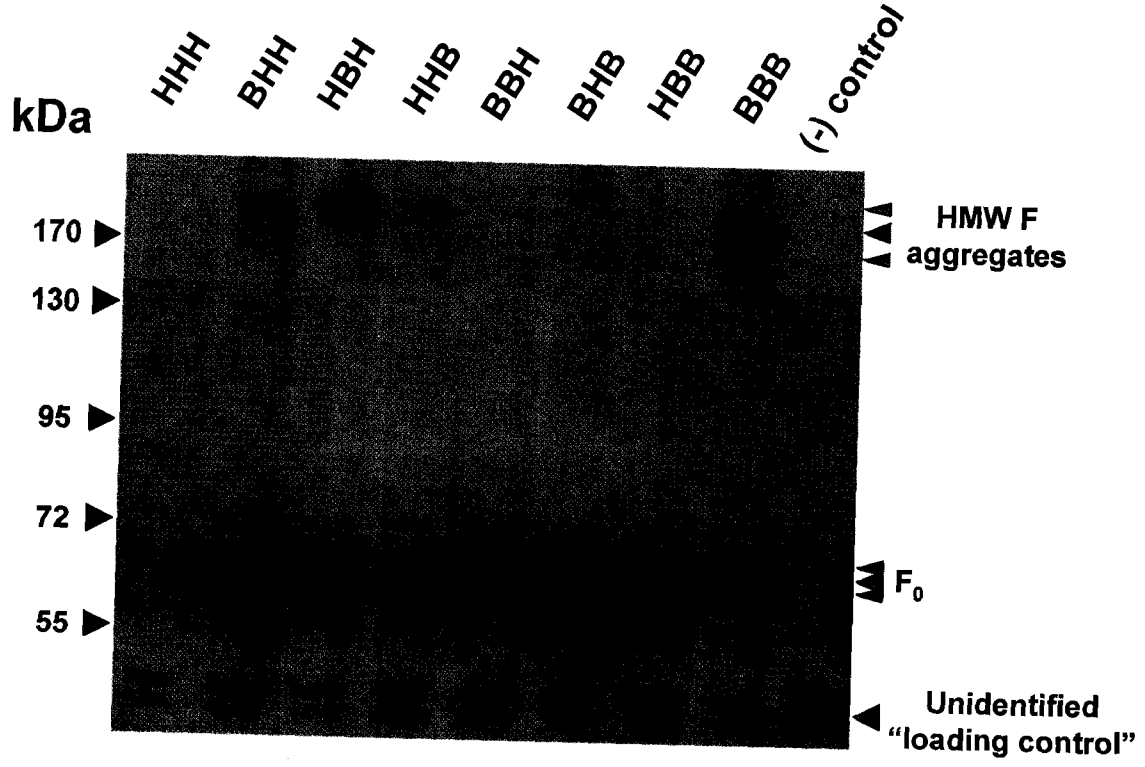
kDa
HHH
BHH
HBH
HHB
BBH
BHB
HBB
BBB
(-) control
170
130
95
72
55
HMW F aggregates
F_0
Unidentified "loading control"

Table 9. Expected and actual size differences of HPIV3/BPIV3 F protein chimeras

Chimera	N-linked glycosylation sites	Expected size relative to HHH[1]	Observed size relative to HHH[1]
HHH	3	=	=
BHH	4	>	< and = [2]
HBH	3	=	=
HHB	4	>	<
BBH	4	>	>
BHB	5	>	=
HBB	4	>	<
BBB	5	>	=

[1] "=" means equivalent in size, "<" means smaller in size, ">" means larger in size; [2]- BHH is a doublet

Characterization of heterotypic bovine/human heptad repeat interactions

While the lack of difference in fusogenicity of the chimeric F proteins was disappointing, regions I and III both contain important functional regions, including the heptad repeats. It appeared as if the three regions used for constructing the chimeric HPIV3/BPIV3 F proteins were interchangeable. However, with multiple functional domains within regions I and III, it was possible that incorporation of one domain in each chimera might compensate for the lack of functionality of another in the chimera. Since the heptad repeats of the F protein are key determinants of F protein function, further analysis of heptad repeat interactions was undertaken. An alignment of the HPIV3 and BPIV3 heptad repeats used for this study is presented in Figure 21. Sequence identity and similarity are listed in Table 10. HR2 has a lower degree of identity and similarity than HR1. Sequences based on BPIV3 HR1 and HR2 were amplified by PCR and inserted into the pGEX-4T-3 vector to yield plasmids encoding GST fusion proteins containing C-terminal BPIV3 HR sequences, similar to those containing HPIV3 HR sequences. Production, purification, and analysis of the peptides were carried out as described in Chapters 2 and 3.

Figure 21. Alignment of the heptad repeat regions of the HPIV3 and BPIV3 F proteins. Identical amino acids are shaded black, similar amino acids are shaded grey. The figure was produced using the Boxshade software to illustrate a Clustal alignment.

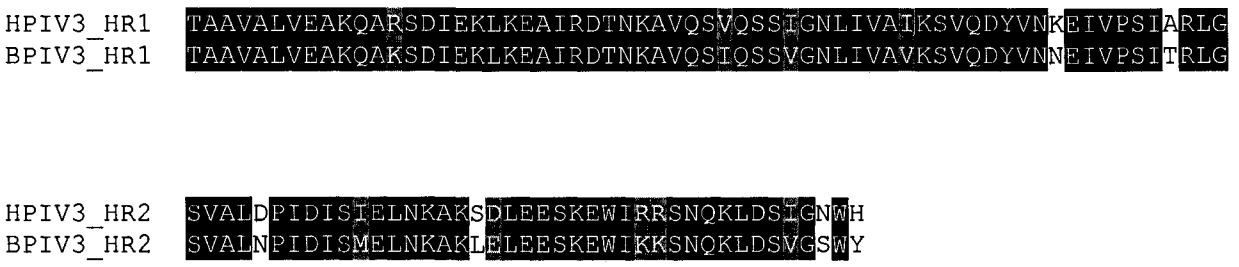
HPIV3_HR1 TAAVALVEAKQARSDIEKLKEAIRDTNKAVQSVQSSIGNLIVAIKSVQDYVNKEIVPSIARLG
BPIV3_HR1 TAAVALVEAKQAKSDIEKLKEAIRDTNKAVQSIQSSVGNLIVAVKSVQDYVNNEIVPSITRLG
HPIV3_HR2 SVALDPIDISIELNKAKSDLEESKEWIRRSNQKLDSIGNWH
BPIV3_HR2 SVALNPIDISMELNKAKLELEESKEWIKKSNQKLDSVGSWY

Table 10. Properties and sequence identity of the HPIV3 and BPIV3 F protein heptad repeat sequences

Heptad Repeat	Length (amino acids)	% identity	% similarity
HR1	63	90.4%	96.8%
HR2	41	78.0%	90.2%

Plaque inhibition

GST fusion proteins containing HR2 peptides from HPIV3 and BPIV3 F proteins were used to inhibit infection of LLC-MK2 cells by HPIV3 and BPIV3. As indicated in the results presented in Figure 22 (panel A), dose-dependent inhibition of HPIV3 infection by GST proteins containing HPIV3 or BPIV3 HR2 peptides was very similar. No statistically significant ($p>0.05$) differences in inhibition were noted. The IC_{50} values calculated for each peptide were 1.9 μM for HPIV3 HR2 and 1.2 μM for BPIV3 HR2. Similar experiments were performed using GST proteins containing the HPIV3 and BPIV3 HR2 sequences to inhibit BPIV3 infection of MDBK cells (Figure 22, panel B). Again, dose-dependent inhibition by the both GST-HR2 proteins was observed, but again no statistically significant ($p>0.05$) differences were determined. The IC_{50} values extrapolated from the data were 4.5 μM for HPIV3 HR2, and 3.9 μM for BPIV3 HR2.

Complex formation and 6-HB stability

HPIV3 and BPIV3 HR1 and HR2 sequences were tested for their ability to form homo- and heterotypic 6-HB complexes. Similar amounts of GST-HR1 and GST-HR2 proteins were mixed on ice, and then analyzed by SDS-PAGE gel electrophoresis, without heating. Examples of the results of electrophoresis on 6% and 12% polyacrylamide gels are

Figure 22. Inhibition of HPIV3 and BPIV3 infection by GST-HR2 proteins. (A) HPIV3 (100 PFU) was incubated in the presence or absence of the indicated GST-HR2 protein (representing HR2 sequences from the HPIV3 and BPIV3 F proteins) and then used to infect LLC-MK2 cells. Cells were fixed and stained, and plaques were counted 4-5 days post-infection. (B) BPIV3 (100 PFU) was incubated in the presence or absence of the indicated GST-HR2 protein (representing HR2 sequences from the HPIV3 and BPIV3 F proteins) and then used to infect MDBK cells. Cells were fixed and stained, and plaques were counted 4-5 days post-infection.

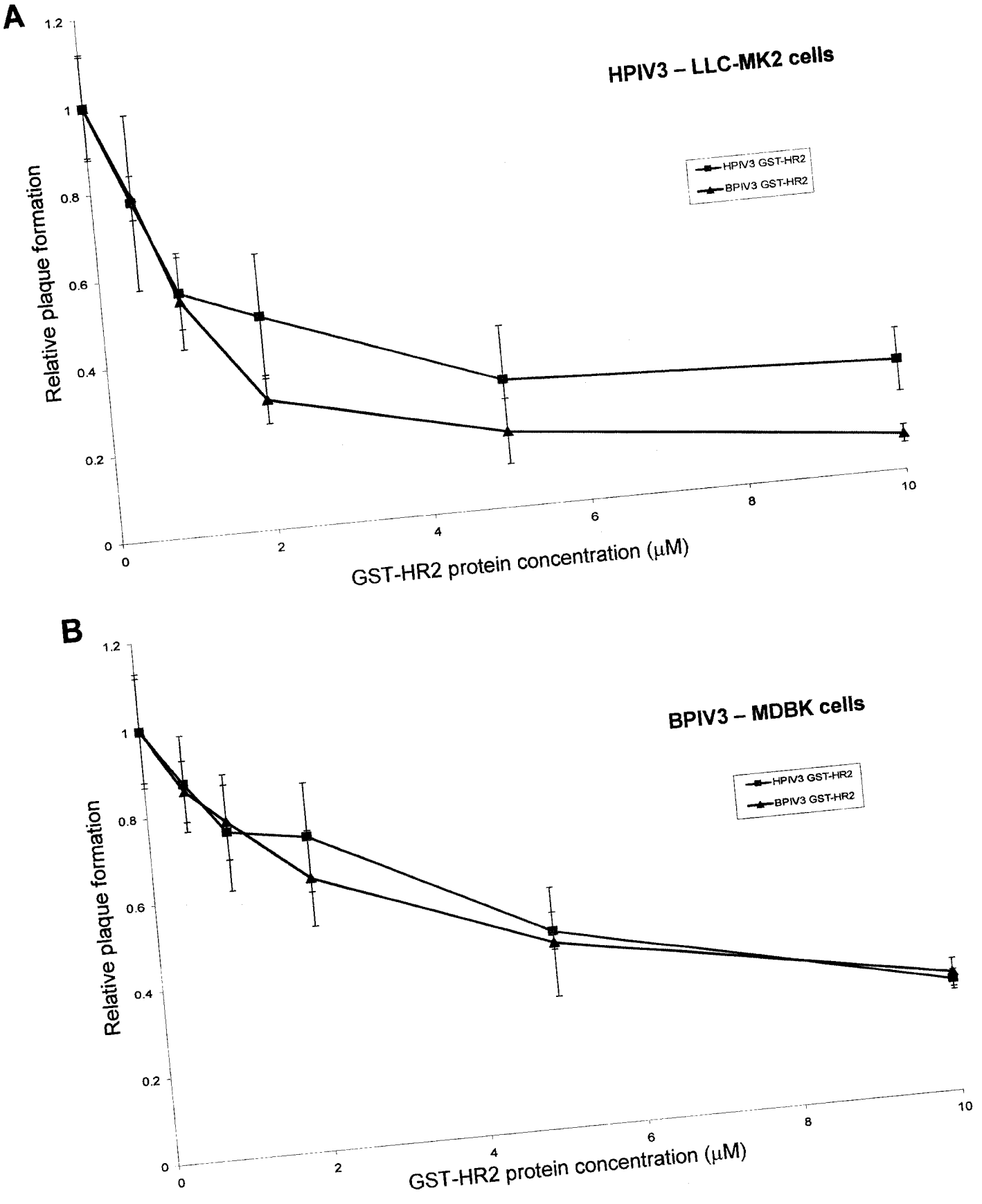
A
HPIV3 – LLC-MK2 cells
HPIV3 GST-HR2
BPIV3 GST-HR2
Relative plaque formation
GST-HR2 protein concentration (μM)
0
0.2
0.4
0.6
0.8
1
1.2
2
4
6
8
10
B
BPIV3 – MDBK cells
HPIV3 GST-HR2
BPIV3 GST-HR2
Relative plaque formation
GST-HR2 protein concentration (μM)

Figure 23. Formation of 6-helix bundles by GST-HR proteins. Lysates of *E. coli* BL21(DE3), expressing GST-HR1 or GST-HR2, containing HPIV3 or BPIV3 sequences, as indicated, were passed over glutathione affinity chromatography columns. Columns were washed, and bound proteins were eluted using reduced glutathione. The amount of protein in each eluate was quantified, and eluates were mixed, on ice, such that GST-HR1 and GST-HR2 were in approximately equal proportions. Mixtures were analyzed by SDS-PAGE at 4°C, and Coomassie staining was used to visualize protein bands. (A) SDS-PAGE on gels containing 12% polyacrylamide to show formation of high molecular weight complexes. (B) SDS-PAGE on gels containing 6% polyacrylamide to demonstrate that all complexes are of the same size. hHR1 = HPIV3 GST-HR1, hHR2 = HPIV3 GST-HR2, bHR1 = BPIV3 GST-HR1, bHR2 = BPIV3 GST-HR2.

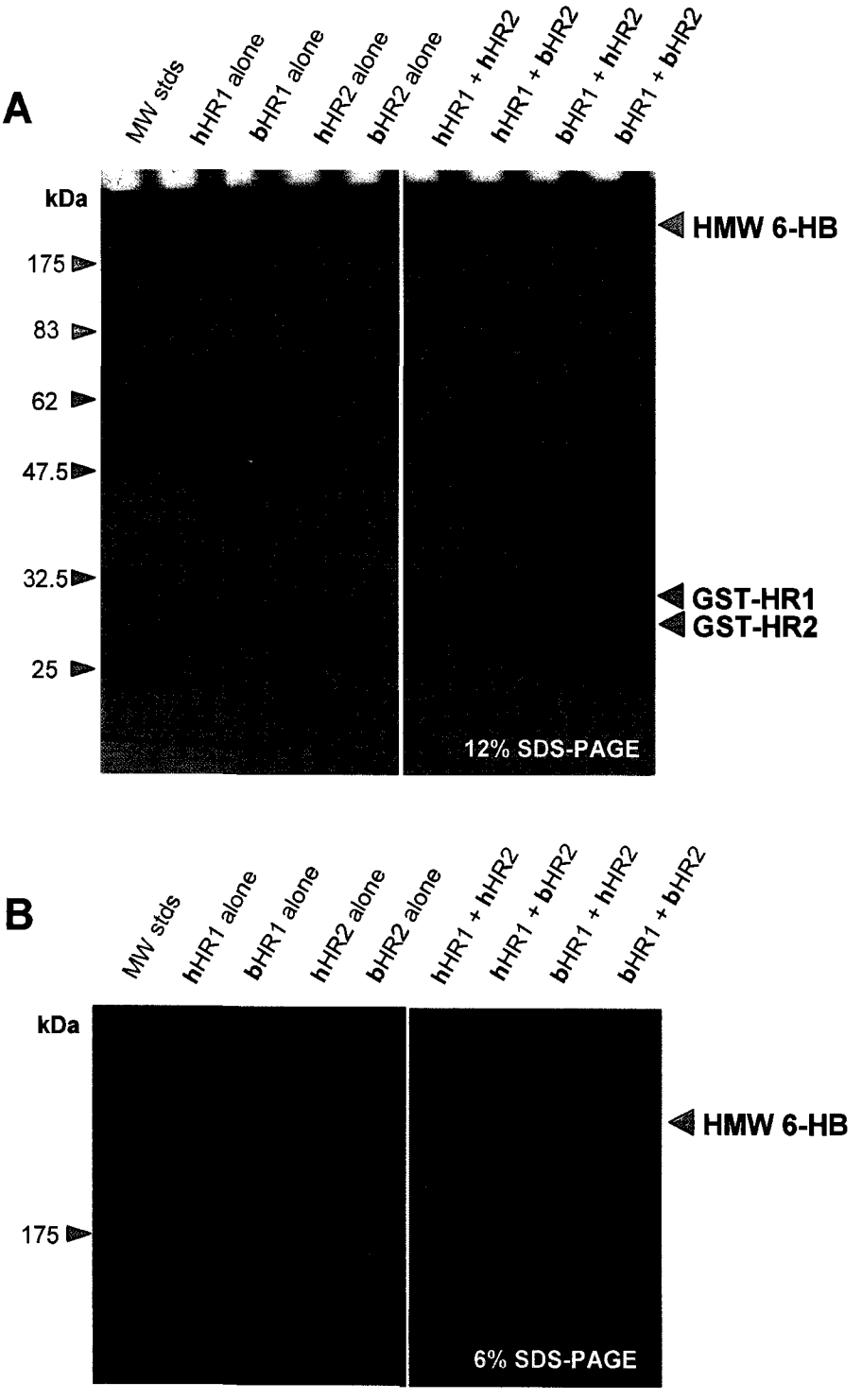
A
MW stds
hHR1 alone
bHR1 alone
hHR2 alone
bHR2 alone
hHR1 + hHR2
hHR1 + bHR2
bHR1 + hHR2
bHR1 + bHR2
kDa
175
83
62
47.5
32.5
25
HMW 6-HB
GST-HR1
GST-HR2
12% SDS-PAGE
B
MW stds
hHR1 alone
bHR1 alone
hHR2 alone
bHR2 alone
hHR1 + hHR2
hHR1 + bHR2
bHR1 + hHR2
bHR1 + bHR2
kDa
175
HMW 6-HB
6% SDS-PAGE

presented in Figure 23. Complexes with estimated molecular weights similar to a complex containing three GST-HR1 and three GST-HR2 proteins were readily detected. Evident in these experiments is that 6-HB formation, as analyzed by SDS-PAGE, is not complete, as there remain large quantities of uncomplexed GST-HR1 and GST-HR2. Melting profiles were determined by circular dichroism analysis of complexes formed using HPLC-purified HPIV3 and BPIV3 HR1 and HR2 peptides (M. Wurth and R Dutch, University of Kentucky) and are presented in Figure 24. The melting profiles for all four peptide combinations (HPIV3 HR1-HPIV3 HR2, BPIV3 HR1-HPIV3 HR2, HPIV3 HR1-BPIV3 HR2, and BPIV3 HR1-BPIV3 HR2) were very similar, and none of the complexes melted completely, even at 99°C.

Figure 24. Thermostability of homotypic and heterotypic HPIV3/BPIV3 6-HB. HPLC-purified HPIV3 and BPIV3 HR1 and HR2 peptides were mixed on ice, as indicated, to allow 6-HBs to form. Thermal stability of 6-HBs was monitored by circular dichroism while increasing the temperature from 4-99°C. The 6-HB thermal stability was monitored by circular dichroism while increasing the temperature from 4-99°C. The thermal melting profiles of HPIV3 and BPIV3 HR1 peptides are presented for comparison. 6-HB melting profiles for all combinations of HPIV3 and BPIV3 HR1 and HR2 peptides are presented. Experiment performed by Drs. M.A. Wurth and R.E. Dutch (University of Kentucky). hHR1 = HPIV3 HR1, hHR2 = HPIV3 HR2, bHR1 = BPIV3 HR1, bHR2 = BPIV3 HR2.

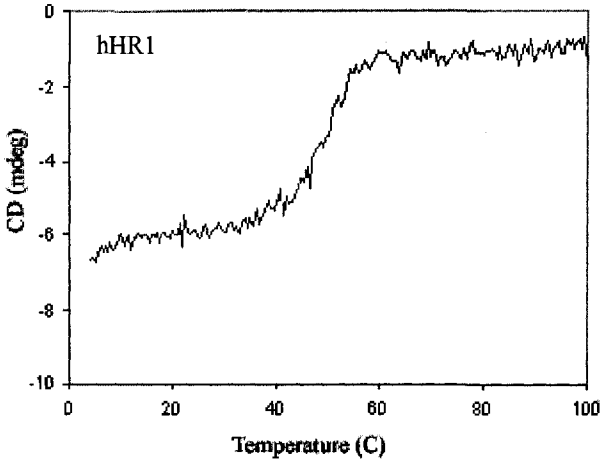
hHR1
CD (mdeg)
0
-2
-4
-6
-8
-10
0
20
40
60
80
100
Temperature (C)

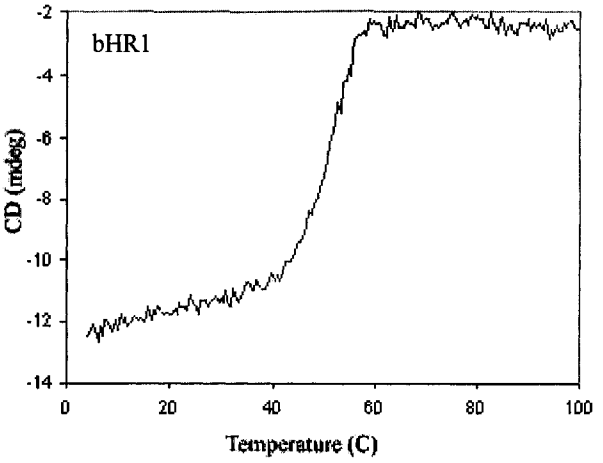
bHR1
CD (mdeg)
-2
-4
-6
-8
-10
-12
-14
0
20
40
60
80
100
Temperature (C)

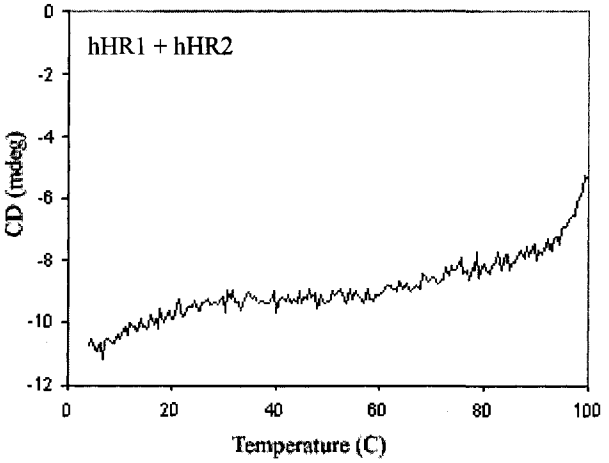
hHR1 + hHR2
CD (mdeg)
0
-2
-4
-6
-8
-10
-12
0
20
40
60
80
100
Temperature (C)

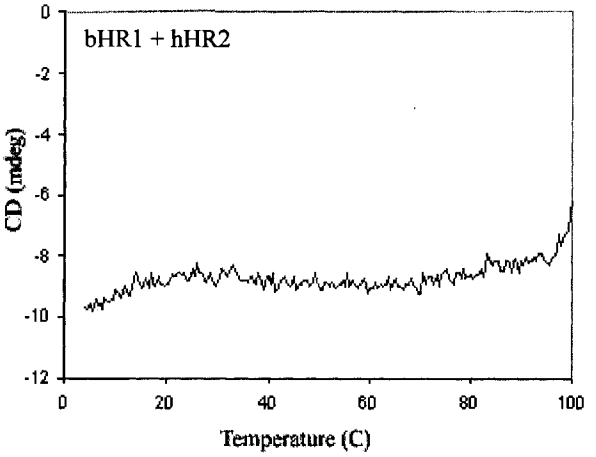
bHR1 + hHR2
CD (mdeg)
0
-2
-4
-6
-8
-10
-12
0
20
40
60
80
100
Temperature (C)

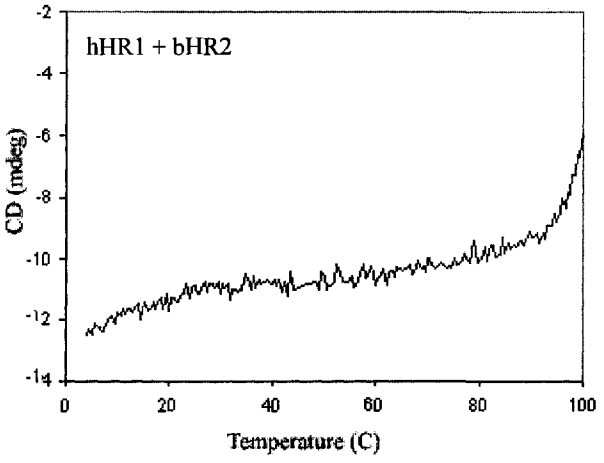
hHR1 + bHR2
CD (mdeg)
-2
-4
-6
-8
-10
-12
-14
0
20
40
60
80
100
Temperature (C)

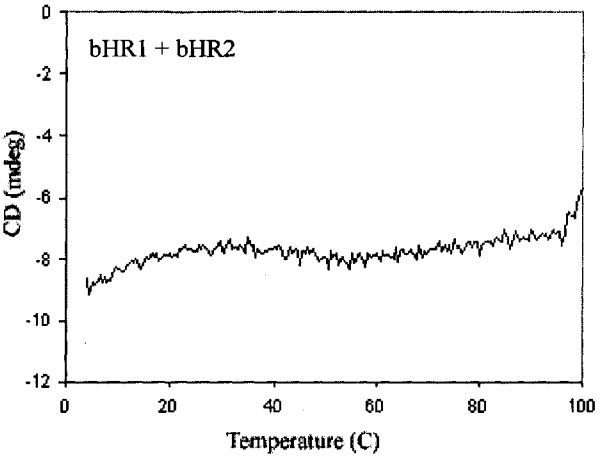
bHR1 + bHR2
CD (mdeg)
0
-2
-4
-6
-8
-10
-12
0
20
40
60
80
100
Temperature (C)

Discussion

The rationale for constructing chimeric BPIV3/HPIV3 F proteins was that the sequence differences between the BPIV3 and HPIV3 F proteins would lead to differences in the fusogenic properties of the chimeric F proteins due to differences in intermolecular interactions with the HN protein or intramolecular interactions between regions of the F protein. Alhough no significant differences in the properties of the chimeric F proteins were observed, some conclusions about regions in the F protein and their functions can still be drawn.

The signal sequence at the N-terminus of F_0 exhibits a high degree of sequence difference between the HPIV3 and BPIV3 F proteins (Figure 18**).** Because the signal sequence is cleaved cotranslationally (Lamb and Kolakofsky, 2001), it is unlikely to have any bearing on F protein function and is not considered in the following discussion.

The HR regions, known to be critical for fusion, show some sequence differences, though not many. It is important to note that there appeared to be complete functional interchangeability of the HPIV3 and BPIV3 heptad repeats – no differences in the ability of the heptad repeats to inhibit virus infection, in 6-HB formation and stability, or fusogenicity of chimeric F proteins were observed. None of the amino acid differences in HR2 are located at points of contact between HR1 and HR2, as determined by analysis of the three-dimensional structure of HPIV3 F that is available (Yin *et al.*, 2005). However, two of the HR1 differences are located at points of contact between HR1 and HR2. The difference at position 163, Ile versus Val, is highly conservative and is not likely to have any effect on HR1-HR2 interactions. A188 of HPIV3 HR1 interacts with a pocket formed by S448/V449/A450/L451 (Figure 25), residues which are perfectly conserved between HPIV3 and BPIV3 F. The change to threonine at position 188 in BPIV3 HR1 must also be tolerated, given the experimental evidence that the HR sequences are interchangeable

Figure 25. Three-dimensional model of a binding pocket for A188 in the HPIV3 F protein. A three-dimensional model of the perfectly conserved S448/V449/A450/L451 binding pocketfor A188 and T188 in HR1 of BPIV3 F HPIV3 F, respectively. Residues of interest are labelled. The figure was produced the Deepview Swiss-PDB viewer.


S448
V449
A450
L451
A188

as peptides as well as in chimeras.

The inspiration for the construction of chimeric HPIV3/BPIV3 F proteins was a previous study in which chimeric HPIV2 and SV41 F proteins were produced (Tsurudome *et al.*, 1998). Differences in the HPIV2/SV41 F proteins (70% identical, 84% similar) were significant enough that swapping of regions resulted in complete abrogation, or complete induction of fusion. Tsurudome and colleagues identified two regions as "sufficient" to impart fusogenicity to a fusion-negative F protein in concert with heterotypic HN, and two regions as "sufficient" to inhibit fusion in the homotypic HN/F pair. It was hoped that the somewhat higher level of identity between HPIV3 and BPIV3 F (80% identical, 88.7% similar) would still show differences in fusion and that short stretches of sequence involved in HN interactions, or intramolecular folding would be identified. While the end result proved that this was not the case, it is not entirely clear why. The P1 and P2 regions identified by Tsurudome *et al.* as sufficient to impair fusion, only impaired fusion when both were present. P1 is a short stretch of approximately 30 amino acids, of which 7 are different between HPIV2 and SV41 sequences (5 of which are conservative changes), and P2 is a stretch of 45 amino acids with 15 differences (7 of which are conservative). An alignment indicating the areas of interest in HPIV2 and SV41 F is found in Figure 26. P1 is entirely contained within region II of the HPIV3 and BPIV3 F proteins and there is only a single, conservative, (R236H) difference between the HPIV3 and BPIV3 sequences. In P2, which is located in a cysteine-rich head domain of region III in the HPIV3 and BPIV3 chimeras, there are ten differences between HPIV3 and BPIV3 F proteins, six of which are conservative changes. One could speculate that these differences may have had an effect, if it had been possible to demonstrate fusion promotion with the BPIV3 HN protein. Since HPIV2/SV41 HN and F do not function as heterotypic pairs, the short heterotypic regions of the HPIV2/SV41 F proteins were identified as sequences that inhibit interaction with

Figure 26. Alignment of the SV41 and HPIV2 F proteins. Key structural features of the aligned sequences are highlighted. HR1 and HR2 (purple) and the transmembrane domain (green) are indicated. The key domains of the F protein involved in HN interaction as proposed by Tsurudome *et al.* (1998), P1 (yellow), P2 (red), and M2 (blue), are indicated (see text for details). Identical amino acids are shaded black, similar amino acids are shaded grey. The figure was produced using the Boxshade software program to illustrate a Clustal alignment.

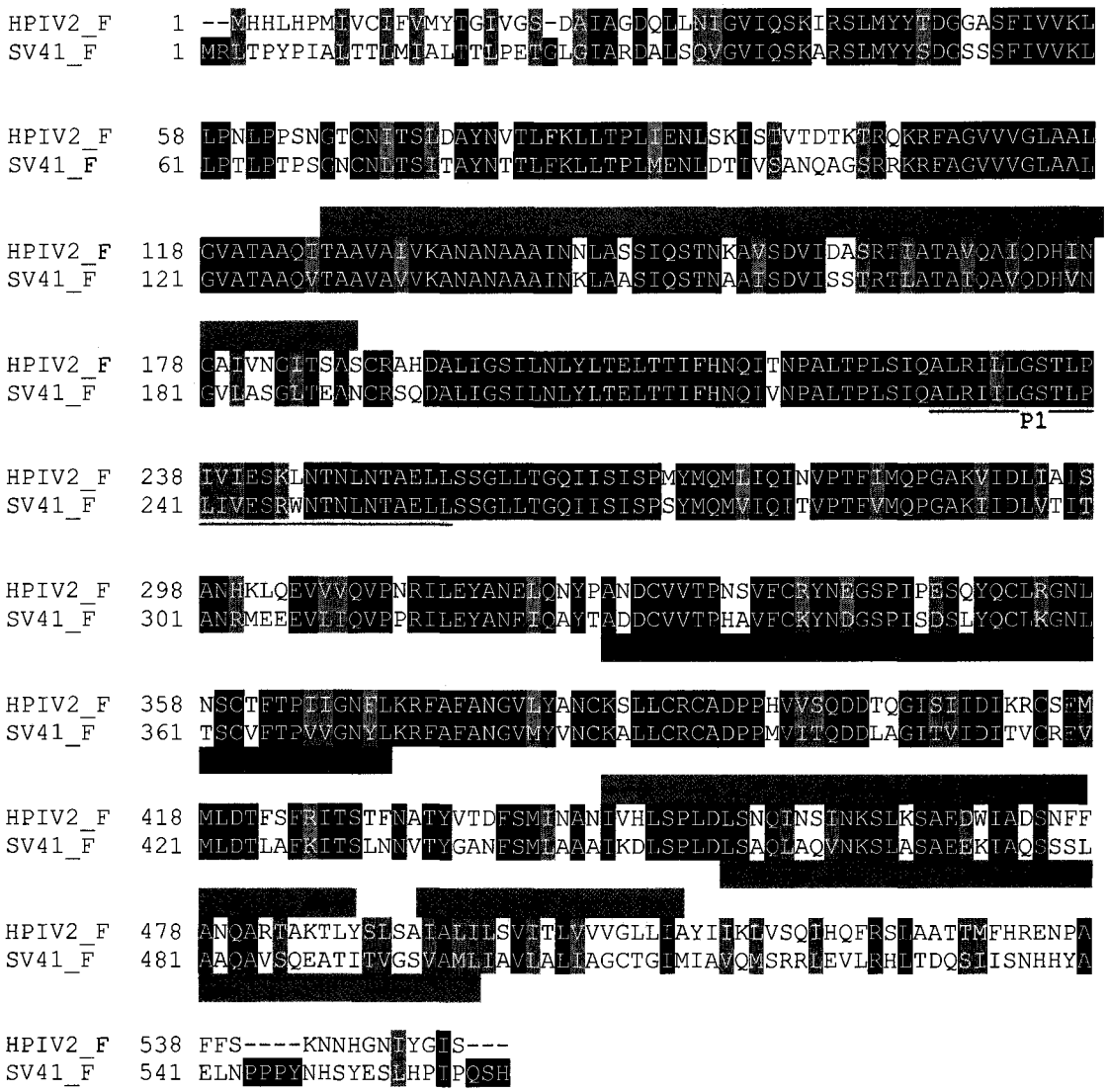
HPIV2_F 1 --MHHLHPMIVCIFVMYTGIVGS-DAIAGDQLLNIGVIQSKIRSLMYYTDGGASFIVVKL
SV41_F 1 MRITPYPIALTTLMIALTTLPETGLGIARDALSQVGVIQSKARSLMYYSDGSSSFIVVKL
HPIV2_F 58 LPNLPPSNGTCNITSLDAYNVTLFKLLTPLIENLSKISIVTDTKTRQKRFAGVVVGLAAL
SV41_F 61 LPTLPTPSGNCNLTSITAYNTTLFKLLTPLMENLDTTVSANQAGSRRKRFAGVVVGLAAL
HPIV2_F 118 GVATAAQITAAVAIVKANANAAAINNLASSIQSTNKAVSDVIDASRTIATAVQAIQDHIN
SV41_F 121 GVATAAQVTAAVAVVKANANAAAINKLAASIQSTNAAISDVISSTRTLATAIQAVQDHVN
HPIV2_F 178 CAIVNGITSASCRAHDALIGSILNLYLTELTTIFHNQITNPALTPLSIQALRILLGSTLP
SV41_F 181 GVLASGLTEANCRSQDALIGSILNLYLTELTTIFHNQIVNPALTPLSIQALRIILGSTLP
P1
HPIV2_F 238 IVIESKLNTNLNTAELLSSGLLTGQIISISPMYMQMLIQINVPTFIMQPGAKVIDLIAIS
SV41_F 241 LIVESRWNTNLNTAELLSSGLLTGQIISISPSYMQMVIQITVPTFVMQPGAKIIDLVTIT
HPIV2_F 298 ANHKLQEVVVQVPNRILEYANELQNYPANDCVVTPNSVFCRYNEGSPIPESQYQCLRGNL
SV41_F 301 ANRMEEEVLIQVPPRILEYANFIQAYTADDCVVTPHAVFCKYNDGSPISDSLYQCLKGNL
HPIV2_F 358 NSCTFTPIIGNFLKRFAFANGVLYANCKSLLCRCADPFHVVSQDDTQGISIIDIKRCSFM
SV41_F 361 TSCVFTPVVGNYLKRFAFANGVMYVNCKALLCRCADPFMVITQDDLAGITVIDITVCREV
HPIV2_F 418 MLDTFSFRITSTFNATYVTDFSMINANIVHLSPLDLSNQINSINKSLKSAFDWIADSNFF
SV41_F 421 MLDTLAFKITSLNNVTYGANFSMLAAAIKDLSPLDLSAQLAQVNKSLASAEEKIAQSSSL
HPIV2_F 478 ANQARTAKTLYSISAIALILSVITLVVVGLLIAYIIKLVSQTHQFRSIAATTMFHRENPA
SV41_F 481 AAQAVSQEATITVGSVAMLIAVLALIAGCTGIMIAVQMSRRIEVLRHLTDQSIISNHHYA
HPIV2_F 538 FFS----KNNHGNIYGIS---
SV41_F 541 ELNPPPYNHSYESLHPIPQSH

homotypic HN. In order to investigate whether the differences between HPIV3 and BPIV3 F in the P2 region of Tsurudome and colleagues could inhibit HN interaction, it would require an HN protein that promotes homotypic fusion only, or significantly limits heterotypic fusion.

Similarly, the M2 region, which contains HR2 and the membrane-proximal amino acids next to HR2, renders non-functioning chimeras fusogenic in the presence of the homotypic HN protein (Tsurudome *et al.*, 1998). This region contains some key sequence differences in the HPIV2 and SV41 proteins (Figure 26). There are 27 differences (9 conservative) in a stretch of 43 amino acids, many of which are in a- and d-residues of HR2, at points of contact between HR1 and HR2. The homologous region of HPIV3 and BPIV3 F has 13 differences (5 conservative), but none at contact points, which may explain why the HPIV3 and BPIV3 sequences are interchangeable in the chimeras and heptad repeat peptides. It is unfortunate that no follow-up to the Tsurudome *et al.* study was published, specifically examining heptad repeat interactions; it would seem as though the differences in HR1 and HR2 are well tolerated – even though HR1 of the HPIV2 and SV41 has 69.8% identity and 84% similarity, and HR2 has 38.8% identity and 50% similarity – because the fusogenicity of chimeric F proteins containing heterotypic HR sequences seemed to be unchanged from the homotypic pairs, similar to what was observed for chimeric HPIV3/BPIV3 F proteins. What the authors have identified in their study, instead, appears to be an HN-HR2 interaction that is very dependent on sequence identity. This is likely to be the same HR2-HN stalk interaction identified using peptides representing NDV HN and F protein sequences (Gravel and Morrison, 2003). It is important to note that combining the results of the studies by Gravel and Morrison and Tsurudome *et al.* confirms two roles for HR2: (1) interacting with the stalk of HN and (2) interacting with HR1, similar to what was deduced from the analysis of the I474S and I474D mutants of the HPIV3 F protein described in Chapter 3.

Other features of the parainfluenza virus glycoproteins may also provide an explanation why BPIV3 F and the HPIV3/BPIV3 F chimeras are fully functional with HPIV3 HN, while chimeric HPIV2/SV41 F proteins are not functional with heterotypic HN. The 12 amino acids of the F protein in the extracellular domain adjacent to the transmembrane domain are critical to fusogenicity: insertions in this region have generally been shown to produce non-fusogenic F proteins, while substitutions and deletions have been shown to have significant deleterious effects on fusion (Tong *et al.*, 2001). One contradictory study indicated that deletion in this region had little effect on fusion mediated by the PIV5 F protein, though substitutions in this region impaired fusion (Zhou *et al.*, 1997). These 12 amino acids are all different, with four conservative changes, in HPIV2 and SV41 F proteins; the corresponding region in HPIV3 and BPIV3 has only 3 differences, one of which is conservative, and none of which is consecutive. It is tantalizing to speculate that this short stretch of amino acids is a key HN-interacting region, given the evidence that HPIV3 and BPIV3 F protein sequences are interchangeable but the HPIV2 and SV41 sequences are not.

Size differences between the chimeric F_0 proteins (Figure 20) are not easily explained by sequence differences noted when the coding sequences of each chimera was determined. The difference in length of the HPIV3 and BPIV3 F proteins is one residue, with the additional residue found in region III of the BPIV3 F protein. This cannot explain the apparent mass differences observed following SDS-PAGE. Glycosylation differences between the proteins may provide an explanation, as region I and region III of the BPIV3 F protein each contain an additional site for N-linked glycosylation, however, the mobilities of the chimeras are not consistent with the predicted number of glycosylation sites (Table 9), though there may be differences in usage at a single site in different chimeras. Differences are unlikely to be due to folding of the proteins, for two reasons. Firstly, all protein samples were heated to 99°C for 5 minutes, theoretically denaturing secondary structures. Secondly,

the high molecular weight bands observed for all F proteins, which, presumably, are undissociated trimers of F, mirror the size differences for the corresponding monomers. Cleavage differences could be an issue; the only readily observed F_1 protein is that of the HHH chimera. Quantitative cleavage of the F protein is not necessary for cell-cell fusion to occur (see Chapter 3). Even though F_1 is not detected, or is barely detected, in these experiments, cell-cell fusion was observed. The size differences, while intriguing, do not appear to have any bearing on the fusogenicity of the chimeric F proteins.

The data presented in this chapter indicate that despite the significant sequence differences between the cytoplasmic tail (CT) of the HPIV3 and BPIV3 F proteins (40% identity and 52% similarity), these sequences appear to be interchangeable. The CT has been shown to be involved in fusion activation of PIV5 and SER virus (Waning *et al.*, 2004; Seth *et al.*, 2004), and regulation of the fusion activity of multiple F proteins, specifically during fusion pore enlargement (Seth *et al.*, 2003; Tong *et al.*, 2002; Dutch and Lamb, 2001; Bagai and Lamb, 1996), similar to CT mutants of the influenza HA (Kozerski *et al.*, 2000; Ohuchi *et al.*, 1998; Melikyan *et al.*, 1997). However, fusion impairment is not observed for all paramyovirus F proteins with CT mutations; deletion and/or mutagenesis of measles virus and RSV F protein CTs have no effect on fusogenicity (Branigan *et al.*, 2006; Moll *et al.*, 2002). Consistent with the experimental observations described in this chapter is the fact that the BPIV3 glycoproteins can be substituted into a HPIV3 background with no effect on *in vitro* replication of the chimeric virus in LLC-MK2 (monkey kidney) cells (Schmidt *et al.*, 2000). Taken together, these data indicate that the fusion promotion/regulation and assembly functions of the F protein that are localized to the CT of the F protein, do not differ significantly between BPIV3 and HPIV3.

The results presented in this chapter indicate that sequence differences in the three regions of the F proteins of HPIV3 and BPIV3 exchanged during the construction of the chimeric F proteins, are not sufficient to alter the functions associated with each region.

Chapter 6 – Development of HPIV3 resistant to heptad repeat 2-based inhibition of infection

Introduction

The conserved and critical nature of the class I fusion mechanism makes it a tempting target for inhibition of viral infection. Peptides based on HR2 sequences have been shown to be highly effective inhibitors of viral fusion for paramyxoviruses (Porotto *et al.*, 2006b; Bossart *et al.*, 2005; Wang *et al.*, 2005; Bossart *et al.*, 2005; Wang *et al.*, 2003; Yu *et al.*, 2002; San Roman *et al.*, 2002; Young *et al.*, 1999; Dutch *et al.*, 1999; Joshi *et al.*, 1998; Young *et al.*, 1997; Wild and Buckland, 1997; Yao and Compans, 1996; Lambert *et al.*, 1996), coronaviruses (Yuan *et al.*, 2004; Bosch *et al.*, 2004; Bosch *et al.*, 2003) and retroviruses, particularly HIV (Wild *et al.*, 1994; Wild *et al.*, 1994; Wild *et al.*, 1993; Wild *et al.*, 1992). Inhibition of HIV-1 infection with nanomolar concentrations of a conserved 36-residue gp41 HR2-based peptide alternately known as DP-178, T-20, or Enfuvirtide (Enf) was first shown *in vitro* (Chen *et al.*, 1995; Wild *et al.*, 1994; Wild *et al.*, 1993). Enf and similar peptides were rapidly developed as clinical anti-retroviral agents (Greenberg and Cammack, 2004). HR2-based peptides are believed to inhibit fusion through a stable interaction with exposed HR1 *in situ*, during refolding of fusion proteins, thereby preventing the assembly of the HR1/HR2 6-HB (Eckert and Kim, 2001). However, HR2 peptides derived from the NDV F protein have also been shown to bind to specific sequences in the HN protein, specifically the membrane-proximal stalk region (Gravel and Morrison, 2003), although there is no evidence that this interaction plays a role in fusion inhibition.

Viruses with single-stranded RNA genomes exhibit a unique, but key replication feature: RNA-dependent RNA polymerases with high error rates. Error rates can be as high as 10^{-4} mutations per nucleotide replicated (i.e. one mutation per 10,000 bases) for positive- and negative-sense RNA viruses such as the picornaviruses and the

paramyxoviruses (Drake and Holland, 1999; Drake, 1993), and 10^{-5} for retroviruses such as HIV (Drake and Holland, 1999; Holland and Domingo, 1998; Drake *et al.*, 1998; Drake, 1993). To contrast these values, mutation rates of commonly studied organisms are 10^{-10} for *Drosophila melanogaster, Mus musclus, Caenorhabditis elegans,* and *Escherichia coli*, and 10^{-11} for *Homo sapiens* (Drake, 1999; Drake *et al.*, 1998). It is unsurprising, then, that application of heavy selection pressure on viruses with RNA genomes by antiviral drugs, such as Enf, in combination with the low fidelity and rapid replication rates of the viruses, can rapidly produce drug resistance. Repeated *in vitro* passage of HIV-1 in the presence of increasing concentrations (starting at the 95% inhibitory concentration) of Enf rapidly produced isolates of the virus resistant to the peptide at 10-fold higher concentrations (Nameki *et al.*, 2005; Armand-Ugon *et al.*, 2003; Rimsky *et al.*, 1998). Similarly, reports from early clinical trials using Enf showed rapid appearance (14 days after starting the drug regimen) of resistant isolates of the virus (Xu *et al.*, 2005; Wei *et al.*, 2002). Interestingly, several of the clinical isolates contained the same adaptive mutations as the *in vitro*-selected virus, a three-residue stretch at position 36-38 (GIV) in HR1 of gp41 (Wei *et al.*, 2002; Rimsky *et al.*, 1998); multiple mutations appeared to have an additive effect on resistance. Further analysis of the GIV region by site-directed mutagenesis and analysis of clinically-derived mutants highlighted a ten-residue stretch of gp41 between amino acids 36 and 45 to be critical for development of resistance (Lu *et al.*, 2006; Menzo *et al.*, 2004; Johnson *et al.*, 2003; Labrosse *et al.*, 2003; Wei *et al.*, 2002). It is key to note that for all adaptive mutations that were associated with Enf-resistance, corresponding mutations in HR2 that enabled the formation of a modified, but stable, 6-HB, were also observed (Xu *et al.*, 2005; Nameki *et al.*, 2005). Another gp41 HR2-based 36-residue peptide, which includes a 10 amino acid overlap with Enf, and inhibits HIV infection, also produced *in vitro* resistance resulting from mutations in HR1, in residues distinct from the GIV motif (Lohrengel *et al.*, 2005; Derdeyn *et al.*, 2001). Adaptive mutations producing resistance

localized to HR1, for both peptides, clearly indicate a key role for *in situ* interaction between HR1 and HR2 peptides.

Conservation of the mechanism of 6-HB formation between class I virus fusion proteins suggested that HPIV3 would develop resistance to inhibition by HR2 peptides, similar to what was observed for HIV. The specific goal of the work described in this chapter was to use HR2 peptides to select HPIV3 resistant to HR2 inhibition, and to determine the specific mutations responsible for the resistance. It was hypothesized that adaptive mutations producing resistance to HR2 peptide would be found in HR1 of the HPIV3 F protein, given that F protein refolding during membrane fusion is mechanistically similar to refolding of the HIV gp41 protein.

Results

Selection of HPIV3 resistant to inhibition by GST-HR2

As reported in chapter 3, HPIV3 infection of LLC-MK2 cells was inhibited by incubation of virus with a peptide derived from the HR2 sequence of the HPIV3 F protein. A recombinant GST fusion protein containing C-terminal HR2 peptide (GST-HR2) was also able to inhibit infection in a dose-dependent manner, though at an IC_{50} approximately two orders of magnitude greater than that of the peptide itself. HPLC purification of HR2 peptides is time-consuming and prone to significant losses of peptide. Therefore, due to the ease of production and the inhibitory properties of GST-HR2, it was decided to use affinity chromatography-purified GST-HR2 protein rather than HR2 peptide to select for a HPIV3 resistant to fusion inhibition by the HR2 sequences. Simultaneously, virus was selected using affinity-purified GST alone as a control.

In previous studies a resistant HIV-1 was selected in increasing concentrations of HR2 peptide, beginning with concentrations that inhibited 95-98% of virus infection (Rimsky *et al.*, 1998), which corresponds to approximately 100-200 times the IC_{50} value (Wild *et al.*, 1994), or where the initial concentration of peptide was 2-4 times the IC_{50} value (Armand-Ugon *et al.*, 2003). The initial concentration chosen for HPIV3 selection was 20 μM GST-HR2, which, by extrapolation of the inhibition curve (Figure 27) represents a concentration that inhibits HPIV3 infection by >95%, and is 20 times the IC_{50}. In each subsequent passage of HPIV3, the concentration of GST-HR2 was increased by 10 μM. For each passage, virus was incubated for 10 minutes on ice with GST or GST-HR2, then confluent LLC-MK2 cells in 6-well dishes were infected with the virus/GST or GST-HR2 mixture, diluted approximately 1:3 with culture medium. Infected cultures were incubated until cytopathic effects (CPE) were observed. For each passage, virus-containing supernatants were harvested, and the HPIV3 titre in the presence or absence of GST-HR2 was

Figure 27. Dose-dependent inhibition of HPIV3 infection by GST and GST-HR2 proteins. HPIV3 (50-100 PFU) was incubated in the presence or absence of various concentrations of the GST or GST-HR2 protein and then used to infect LLC-MK2 cells. Plaques were scored 5 days post-infection. Data is the average of triplicate experiments, using duplicate wells each experiment, ± the standard deviation.

determined. Virus was subjected to six consecutive passages in the presence of increasing concentration of GST-HR2, as detailed in Table 11.

Table 11. Passage history and nomenclature of GST-heptad repeat 2-selected HPIV3 clones

Passage #	Peptide concentration	Nomenclature	
		GST selected	GST-HR2 selected
1	20 μM	20GST-1	20C-1
2	30 μM	30GST-2	30C-2
3	40 μM	40GST-3	40C-3
4	50 μM	50GST-4	50C-4
5	60 μM	60GST-5	60C-5
6	70 μM	70GST-6	70C-6

Titration of population resistance to GST-HR2

To detect population resistance to GST-HR2, each passage was assayed using triplicate plaque reduction assays, in LLC-MK2 cells in the presence of 10 μM GST-HR2. The threshold value of 10 times the IC_{50} for resistance screening was the same as used in the original HIV resistance study (Rimsky *et al.*, 1998). Population resistance to peptide is presented in Figure 28. Interestingly, population resistance to peptide appeared to peak at passage 4 (50 μM peptide) when compared to GST-selected control virus. Statistically significant ($p<0.05$) differences in sensitivity to GST-HR2 was observed between GST-HR2- and GST-selected at passage 3 (40 μM peptide), passage 4 (50 μM) and passage 5 (60 μM, $p<0.005$). The peak of GST-HR2-selected resistance noted at passage 4 is also statistically significant ($p<0.05$) compared to the level of resistance in passages 3, 5, and 6.

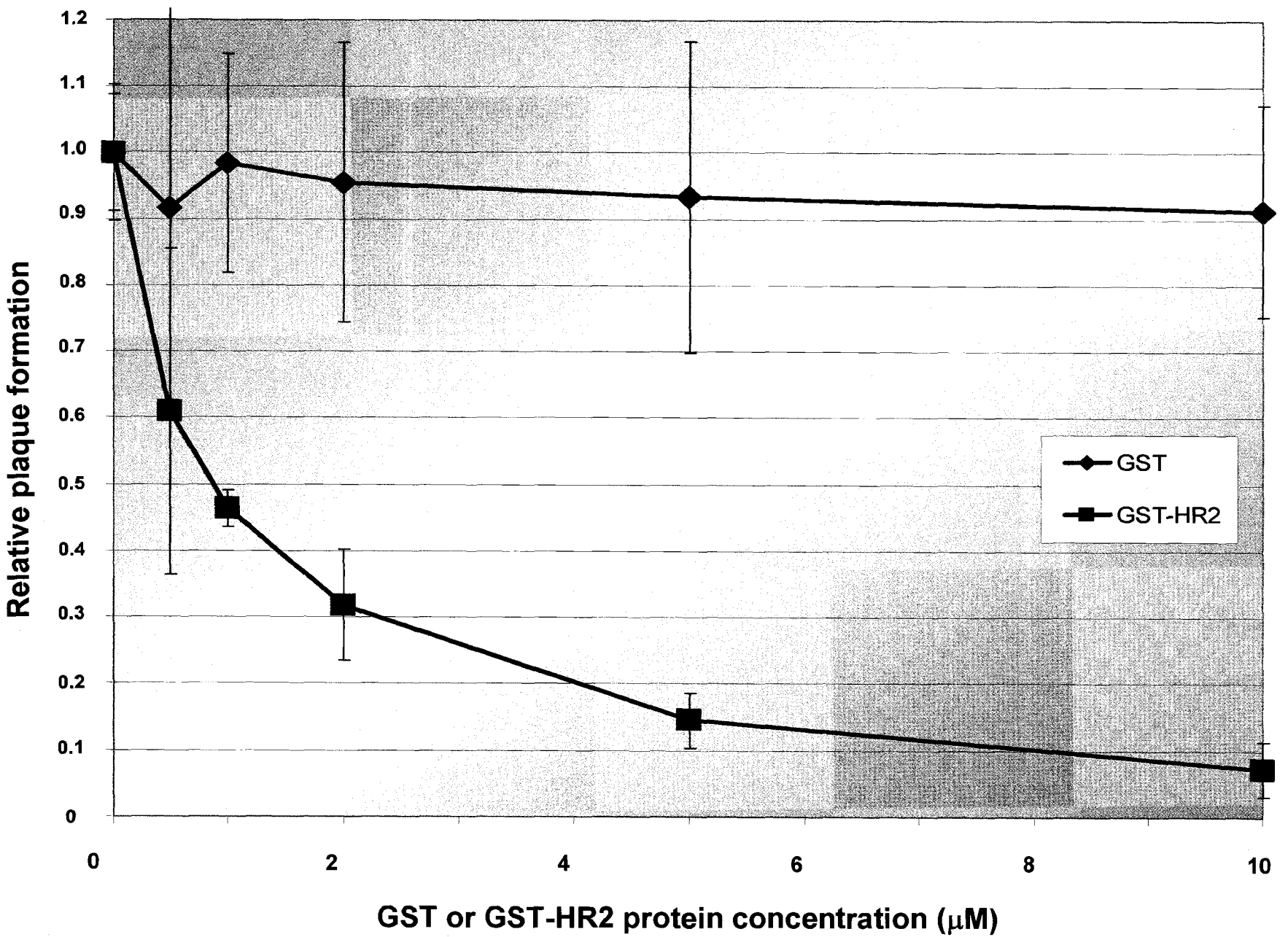
Relative plaque formation
1.2
1.1
1.0
0.9
0.8
0.7
0.6
0.5
0.4
0.3
0.2
0.1
0
0
2
4
6
8
10
GST or GST-HR2 protein concentration (μM)
GST
GST-HR2

Figure 28. Analysis of GST-HR2-selected HPIV3 populations for resistance to inhibition by GST-HR2. HPIV3 was subjected to six passages in the presence of increasing concentrations of GST-HR2 fusion protein, or GST alone. Virus was harvested from infected cell supernatants at each passage and, after pre-incubation in the presence or absence of 10 μM GST-HR2, was titrated on LLC-MK2 cells. 10 μM GST-HR2 represents a concentration approximately 10 times the IC_{50}. Cells were fixed and plaques scored five days post-infection. For each passage, values are presented as the average number of plaques in the presence of GST-HR2, compared to plaque numbers in the absence of GST-HR2. GST-selected control populations are indicated by the red bars, GST-HR2-selected populations are indicated by the blue bars. Statistically significant differences between the GST-selected and the GST-HR2-selected populations are indicated by asterisks ($p<0.05$) or crosses ($p<0.005$). Data is the mean of triplicate wells per sample, ± the standard deviation.

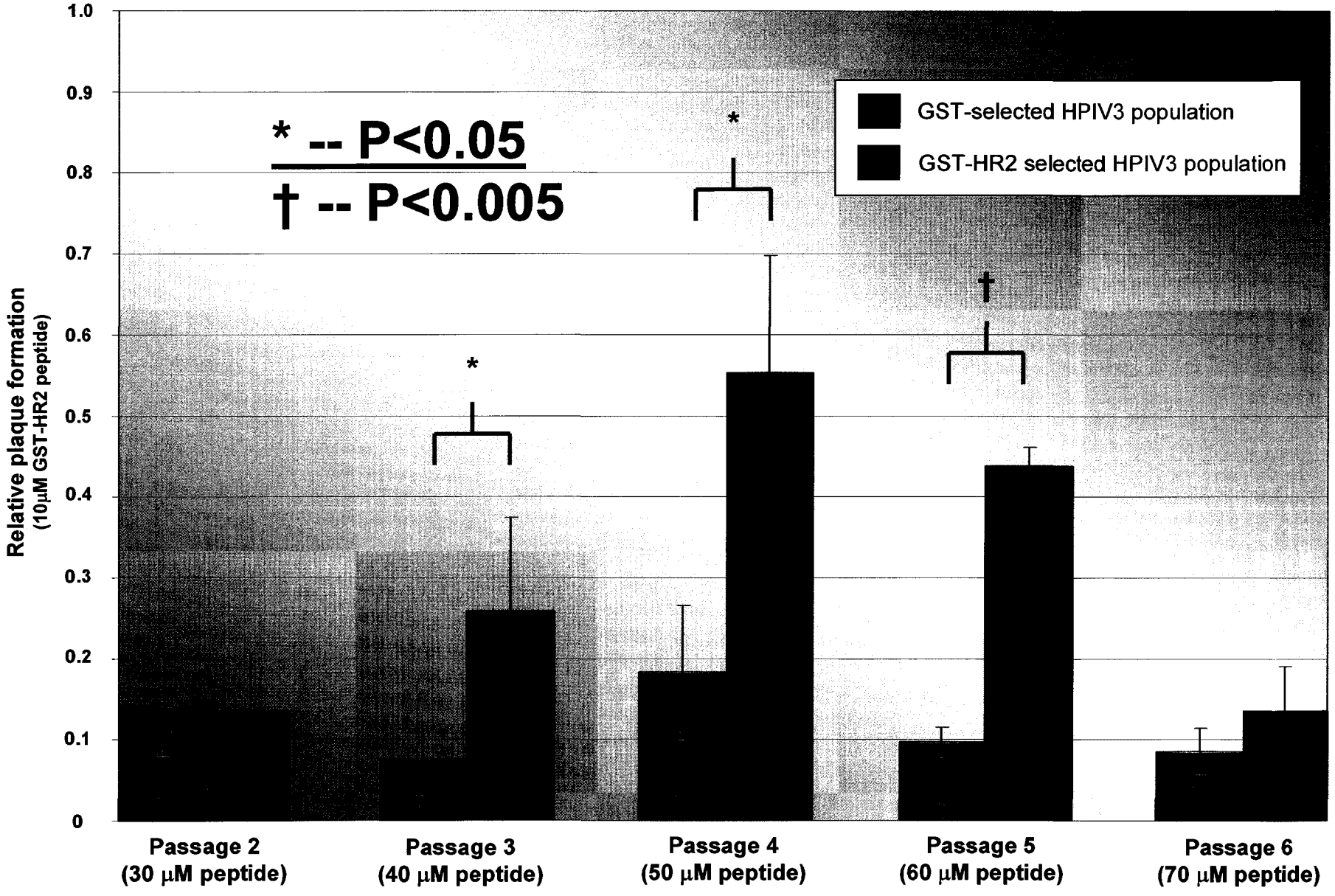
1.0
0.9
0.8
0.7
0.6
0.5
0.4
0.3
0.2
0.1
0
Relative plaque formation
(10μM GST-HR2 peptide)
* -- P<0.05
† -- P<0.005
GST-selected HPIV3 population
GST-HR2 selected HPIV3 population
*
*
†
Passage 2
(30 μM peptide)
Passage 3
(40 μM peptide)
Passage 4
(50 μM peptide)
Passage 5
(60 μM peptide)
Passage 6
(70 μM peptide)

Characterization of plaque-purified GST-HR2-resistant clones

Given the peak of population resistance to GST-HR2 at passage 4, and the subsequent decline in resistance at passage 6, individual virus clones from these two passages were selected for further characterization. Five to seven plaque-purified clones from passage 4 and passage 6 for both GST- and GST-HR2-passaged virus were propagated and characterized. One plaque-purified clone from GST-HR2-selected passage 6 (clone 70C-6.70.1) was grown in the presence of 70 μM peptide; the remainder were grown in the absence of peptide. Resistance of each virus clone was determined by plaque reduction in the presence of 10 μM GST-HR2. Samples were plated in triplicated. A spectrum of resistance was noted (Figure 29). Resistance ranged from 50% (70C-6.70.1) to >90% (70C-6.0.2). Virus clones represented by the coloured bars in Figure 29 were randomly chosen for further analysis. Somewhat fortuitously, the two clones chosen for the GST-HR2-selected passage 6 population were the highest and lowest resistance of the entire set of clones. Statistically significant differences ($p<0.01$) in resistance between the GST-selected and GST-HR2-selected clones were observed for each specific passage.

To ensure that differences in observed resistance among the various clones were not due to growth defects in any of the viruses, a multi-step growth curve was carried out for six clones, one from each of the GST passages, and two from each of the GST-HR2 passages. Monolayers of LLC-MK2 cells were infected in triplicate at a MOI of 0.01, and aliquots were collected at 0 h, 12 h, 24 h, 48 h, 72 h, and 96 h post-infection. Virus was titrated in duplicate by plaque assay on LLC-MK2 cells. A statistically significant ($p<0.05$) lag in virus production was noted at 12 hours (see Figure 30) for the passage 6 virus clone selected in GST (clone 70GST-6.0.1) and for passage 6 virus clones selected in GST-HR2 (clones 70C-6.0.2 and 70C-6.70.1). This lag was not significant beyond 24 hours ($p>0.05$), and growth of all clones was similar to that of parental Wash/57 virus at 48 hours after

Figure 29. Analysis of GST-HR2-selected clones of HPIV3 for resistance to GST-HR2. Following titration of HPIV3 in supernatants from passage 4 and passage 6 on LLC-MK2 cells, plaque-purified clones were harvested and assayed for to GST-HR2 protein. LLC-MK2 cells were infected with 50-100 PFU of plaque-purified clones, after pre-incubation in the presence or absence of 10 μM GST-HR2. Cells were fixed and plaques were scored five days post-infection. Values for each virus clone are presented as average plaque numbers in the presence of GST-HR2, relative to plaque numbers in the absence of GST-HR2, and are the average of triplicate wells per sample, ± the standard deviation. See text for a detailed explanation of the nomenclature. Clones chosen for further analysis are highlighted (red for the GST-selected clones and blue for the GST-HR2-selected clones). Statistically significant differences were observed between the GST-selected and the GST-HR2-selected clones from passage 4 and passage 6 ($p<0.01$).

Figure 30. Multiple-step growth curve of GST- and GST-HR2-selected HPIV3. LLC-MK2 cells were infected with individual plaque-purified clones of HPIV3, or with the parental Wash/57 strain of HPIV3, at a MOI of 0.01. Infected cells were incubated at 37°C for 96 hours, and supernatants were removed and replaced at 0, 12, 24, 48, 72, and 96 hours post-infection. Supernatants were titrated by plaque assay on LLC-MK2 cells. The growth curve of Wash/57 is bolded for emphasis.

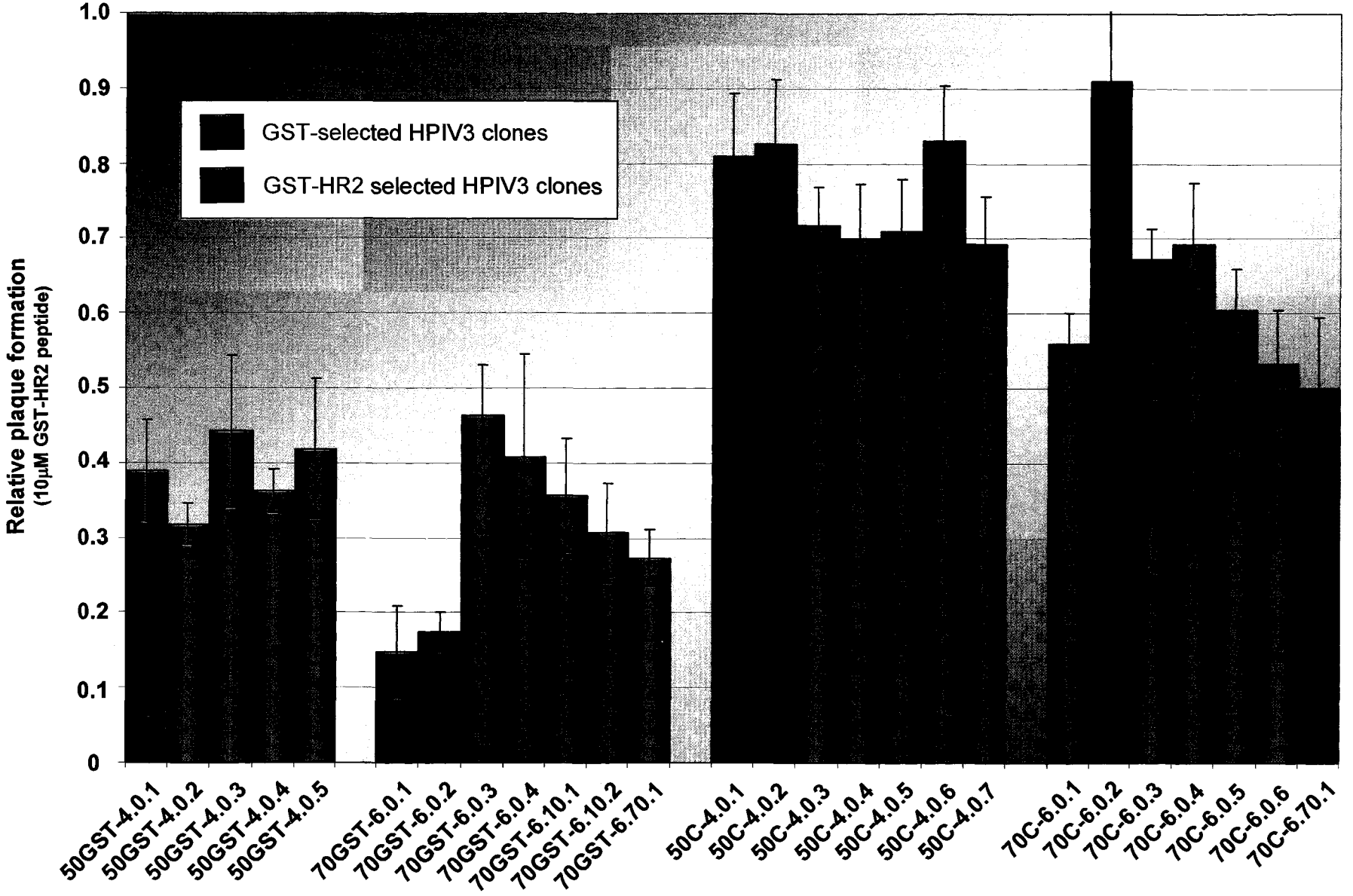
GST-selected HPIV3 clones
GST-HR2 selected HPIV3 clones
Relative plaque formation
(10μM GST-HR2 peptide)
1.0
0.9
0.8
0.7
0.6
0.5
0.4
0.3
0.2
0.1
0
50GST-4.0.1
50GST-4.0.2
50GST-4.0.3
50GST-4.0.4
50GST-4.0.5
70GST-6.0.1
70GST-6.0.2
70GST-6.0.3
70GST-6.0.4
70GST-6.10.1
70GST-6.10.2
70GST-6.70.1
50C-4.0.1
50C-4.0.2
50C-4.0.3
50C-4.0.4
50C-4.0.5
50C-4.0.6
50C-4.0.7
70C-6.0.1
70C-6.0.2
70C-6.0.3
70C-6.0.4
70C-6.0.5
70C-6.0.6
70C-6.70.1

infection. These results indicate that there are no major defects in the growth properties of the virus clones compared to controls, suggesting that resistant virus clones are of equal "fitness" compared to wild-type parental Wash/57 clones in the absence of selective pressure.

Analysis of F gene sequences in GST-HR2-resistant clones

The selected virus clones were analyzed for sequence differences following RT-PCR amplification of F gene sequences. LLC-MK2 cells were infected with each clone at a MOI of 0.01 in the absence of peptide, and incubated at 37°C for 48 hours, the time when virus production was at its peak (Figure 30). At 48 hours, supernatant was discarded, cells were lysed and RNA was isolated using the Trizol reagent. cDNA was produced by reverse transcriptase using a combination of oligo-dT and F gene-specific reverse primers. Two overlapping PCR products, each approximately 1 kb in length were produced, using primers based on 5' and 3' F gene end sequences, paired with internal reverse (AB146rev) and forward primers (AB141), respectively. The overlap was approximately 400 bp. Each fragment was amplified and sequenced at least twice. All sequences were compared to F gene sequences of the parental Wash/57 strain, for which RT-PCR products were amplified using identical conditions. An alignment of all sequences, including parental Wash/57 sequences, is presented in Figure 31.

Unfortunately, no mutations in F gene sequences that might correlate with resistance to GST-HR2 were observed. All mutations, with the exception of P537T in 50C-4.0.2, were also found in the F gene of virus selected by GST alone, (e.g. Q198K in 70GST-6.0.1 and in 50C-4.0.2, 70C-6.0.2 and 70C-6.70.1; V328I in 70GST-6.0.1 and 70C-6.0.2), or in the F gene of parental virus Wash/57 (e.g. D398G in all sequences except Wash/57 and 70C-6.70.1).

Figure 31. Alignment of F protein sequences determined for clones of GST- and GST-HR2-selected HPIV3. RNA was extracted from LLC-MK2 cells 48 hours after infection (MOI=0.01) with individual clones of HPIV3 or with Wash/57 and used as templates for RT-PCR. RT-PCR products were sequenced, and the nucleotide sequences were assembled and translated for alignment. Identical amino acids are shaded black, similar amino acids are shaded grey. The alignment was produced using the Boxshade software program to illustrate a Clustal alignment.

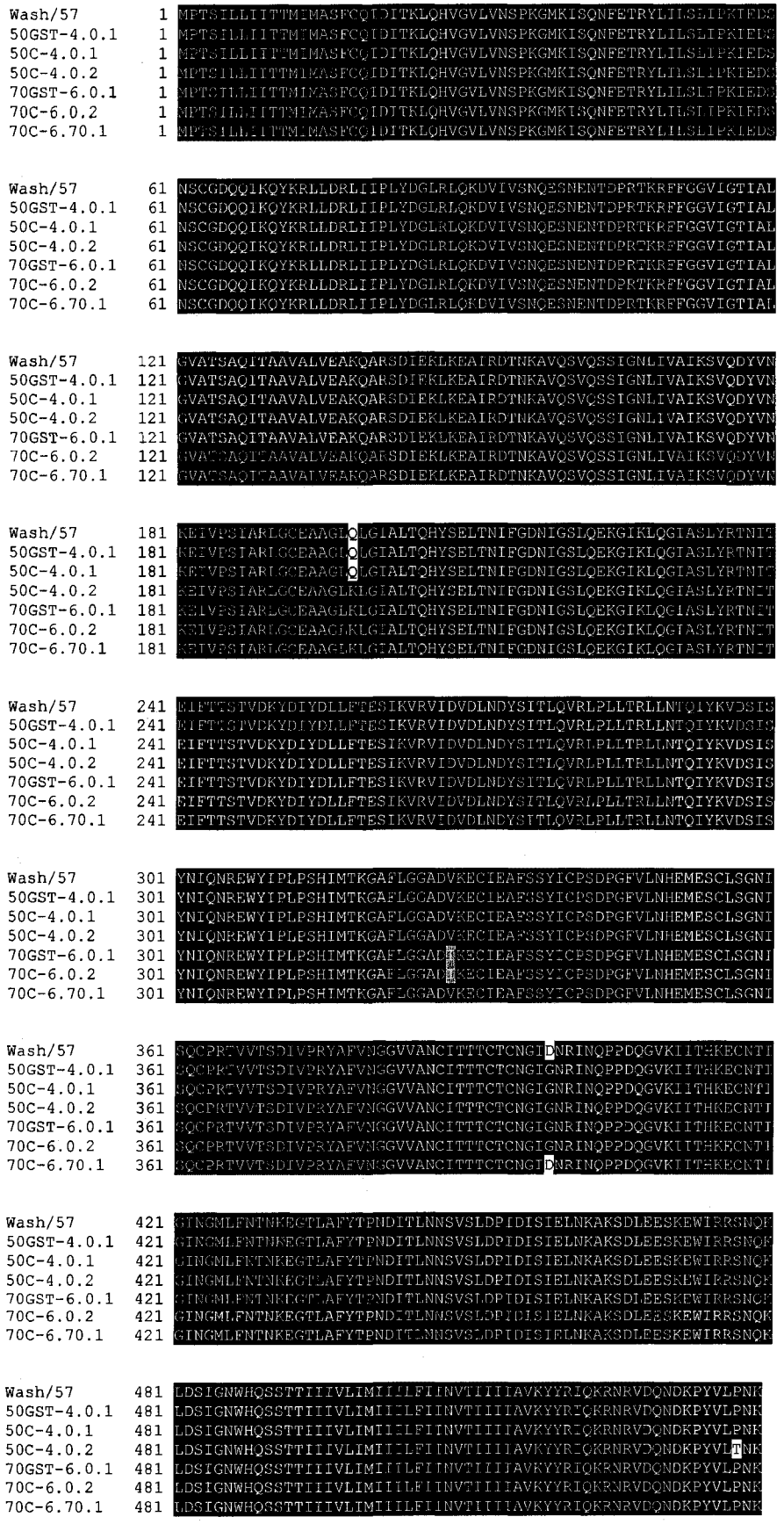

Discussion

Application of strong selective pressure on RNA viruses, such as antiviral therapy, has long been identified as being problematic because of the high rate of nucleotide errors introduced by RNA-dependent RNA polymerase, which leads to rapid development of resistance to antivirals. Therefore, it was not surprising that HPIV3, with an RNA polymerase error rate of approximately one change per replicated genome (Drake and Holland, 1999; Drake, 1993), rapidly developed resistance to GST-HR2 peptide. It has been proposed that the mechanism of inhibition of class I fusion virus infection by HR2 peptides occurs as a result of exogenous HR2 peptide binding to the HR1 sequence of the fusion protein *in situ*, thereby preventing formation of the 6-HB (Eckert and Kim, 2001). This model holds true for all class I fusion proteins, including HIV gp41 and paramyxovirus F proteins. Enf was developed specifically as a fusion inhibitor for HIV-1, and is based on a 36-residue stretch of HR2 of gp41. A comparison of Enf and the HPIV3 HR2 peptide sequence used in this project is shown in Figure 32. The two sequences are similar in length (36 residues for Enf versus 41 for HPIV3 HR2) and similar in character; they are both 4-3 heptad repeats. Given these similar properties, and because the mechanism of fusion by class I fusion proteins is assumed to be conserved, it seemed reasonable to expect that development of resistance to HR2 peptide would arise in a similar manner as resistance of HIV-1 to Enf. Mutations providing resistance to Enf in both clinical and *in vitro*-derived variants cluster in a 10-amino acid stretch in HR1 of gp41 between position 36 and 45 (sequence GIVQQQNNLL), and particularly in the GIV tripeptide (Lu *et al.*, 2006; Miller and Hazuda, 2004; Menzo *et al.*, 2004; Greenberg and Cammack, 2004; Derdeyn *et al.*, 2000). Although there is significant sequence variation between HR1 of HIV gp41 and HPIV3 F, alignment of the HR1 sequences using the 4-3 heptad repeat a-residues (Figure 32) indicates that the analogous HR1 residues in HPIV3 are QARSDIEKLK. Similarly, mutations in gp41

Figure 32. Alignment of HR1 and HR2 sequences of HPIV3 F and HIV gp41. The sequence of the HIV-1 HR2-based fusion inhibitor Enfuvirtide (T-20; Enf) is indicated by the yellow highlighting. Identical amino acids are shaded black, similar amino acids are shaded grey. The figure was produced using the Boxshade software program to illustrate a Clustal alignment.

HR1 alignment

```
HIV1_gp41_HR1     1 LTVQARQLLSGIVQQQNNLLRAIEAQQHLLQLTVWGIKQLQARILAVERYLKDQQLLGIWGCSGKLICTT
HPIV3_F_HR1       1 TAAVALVEAKQARSDIEKLKEAIRDTNKAVQSVQSSIGNLIVAIKSVQDYVN-KEIVPSIARLG---C--
```

HR2 alignment

```
                            Enfuvirtide (T20)
                  ---------------------------------- ---
HIV1_gp41_HR2     1 YTSLIHSLIEESQNQQEKNEQELLELDKWASLWN-WFN-ITNWL
HPIV3_F_HR2       1 --SVALDPIDISIELM-KAKSDLEESKEWIRRSNQKLDSIGNWH
```

associated with resistance to T649, a 36-residue HR2 peptide which partially overlaps with Enf, resulted in mutations approximately 17 amino acids downstream (at positions H53-L54) of the mutations associated with resistance to Enf (Derdeyn *et al.*, 2001). These residues correspond to K148-A149 in the HPIV3 HR1 sequence.

No mutations that could be associated with resistance of HPIV3 to inhibition by HR2 peptide were identified in HR1 sequences or anywhere else in the F protein-coding sequences. There are several possible explanations. The first possibility is that propagation of resistant virus clones in the absence of HR2 peptide following plaque purification, immediately prior to isolation of RNA for RT-PCR amplification and sequencing resulted in the loss of the resistance genotype/phenotype. However, one clone (70C-6.70.1) was propagated in the presence of high concentrations of the peptide but no adaptive mutations were identified in the F gene sequence of this clone (Figure 31).

It is also possible that mutations conferring resistance to HR2 peptide may be present in sequences other than F protein sequences. The most likely candidate is the HN protein. Some lines of evidence support this possibility. Firstly, a functional and physical interaction between paramyxovirus HN and F exists (Bossart *et al.*, 2002; Deng *et al.*, 1999; Tsurudome *et al.*, 1998; Yao *et al.*, 1997; Stone-Hulslander and Morrison, 1997; Bagai and Lamb, 1995; Deng *et al.*, 1995; Heminway *et al.*, 1994; Bousse *et al.*, 1994; Malvoisin and Wild, 1993; Horvath *et al.*, 1992; Tanabayashi *et al.*, 1992; Hu *et al.*, 1992; Wild *et al.*, 1991; Ebata *et al.*, 1991), and more specifically, evidence for an interaction between the HR2 peptide and the stalk region of HN has been reported (Gravel and Morrison, 2003). Secondly, a close correlation exists between HIV-1 specificity for CCR5 or CXCR4, determined by the gp120 protein in HIV, and sensitivity to HR2 peptide inhibition. The IC50 for HR2 peptide inhibition of CCR5-specific viruses is 0.8 logs greater than for CXCR4-specific viruses (Derdeyn *et al.*, 2001; Derdeyn *et al.*, 2000). This suggests that gp120 sequences may affect sensitivity of HIV-1 to HR2-based inhibitors. While there is very little

similarity between HPIV3 HN and HIV gp120 in sequence, they are both receptor binding proteins, so it would be worthwhile to analyze HN sequences in the HR2 resistant isolates of HPIV3.

GST-HR2 fusion proteins were used to select HPIV3 resistant to inhibition by HR2 peptide. While HPLC-purified HPIV3 HR2 peptide was approximately 100-fold more effective at inhibition, it required significantly more effort, resources, and time to purify, in addition to being subject to significant peptide loss during the recovery process. GST-HR2 consistently reduced HPIV3 yields at concentrations that were relatively easy to achieve. Given that the GST protein alone had no effect on virus infection, and that the GST-HR2 fusion protein was used at concentrations that inhibited virus yield by >95%, it is unlikely that the use of this protein as a selective reagent, rather than HPLC-purified peptide, was problematic.

Some notable observations which merit discussion include the statistically significant peak of population resistance to peptide observed at passage 4 (Figure 28), and the apparent reduction in population resistance by passage 6. The reason for this is unclear. However, no large differences in resistance between HR2 peptide-selected clones picked at passage 4 or passage 6 were observed upon plaque purification. Also, the GST and the GST-HR2 passage 6 clones selected for further analysis, showed a lag in growth (figure 30). Perhaps the slower initial growth of the passage 6 viruses is reflected in the reduced resistance of the population as a whole, though it in unclear why there is a difference between the population resistance at different passages. An important point which cannot be ignored is that it took between five (Armand-Ugon *et al.*, 2003; Rimsky *et al.*, 1998) and seventeen (Armand-Ugon *et al.*, 2003) passages to produce HIV-1 resistant to Enf (depending on the strain); for HPIV3, resistance appeared by the third passage, and statistically significant resistance by the fourth passage; perhaps the higher mutation rate

for HPIV3 as compared to HIV (Drake and Holland, 1999; Drake, 1999) is important in this regard.

The plaque-purified virus clones from passages 4 and 6 that were chosen for further analysis exhibited some interesting properties. Although the clones were picked randomly prior to resistance analysis, the choice of 70C-6.0.2 and 70C-6.70.1 was somewhat fortuitous, as they happen to be the clones from the HR2-selected population (Figure 29) that have the highest and lowest levels of resistance. In fact, the resistance of clone 70C-6.70.1, is not significantly more resistant than 70GST-6.0.3 ($p>0.05$) which was only exposed to GST. Meanwhile, 70C-6.0.2 is the virus that exhibits the highest resistance to peptide inhibition, with >90% yield in the presence of a concentration of peptide that is ten times the IC_{50}. There is clearly a great deal of variability in the resistance characteristics of individual clones, with more variability seen in clones from passage 6 than from passage 4. This may account for the observed difference in population resistance, or the unusual growth lag. This growth lag lasted for a maximum of 48 hours, at which point growth reached the wild-type level. This is in contrast to Enf-resistant HIV, where for all clinic- and laboratory-derived viruses, fitness was inversely correlated to resistance, and this fitness defect lasted for the life of the virus (Lu *et al.*, 2004).

The main conclusion that can be drawn from the work described in this chapter is that HPIV3 developed resistance to HR2 sequences, even though no mutations that could account for this resistance were detected in the F gene. Resistant clones should be propagated in the presence of HR2 sequences and the HN gene, as well as the F gene, should be screened for resistance-associated mutations.

Conclusion

The results presented in this dissertation have relevance for several different stages of HPIV3 fusion. Polar substitutions at I474 in HR2 of the F protein produce F proteins that are uncleaved and non-fusogenic, and form 6-HB that are destabilized. The lack of cleavage predicts a role for HR2 in stabilization of a pre-cleavage structure of the F protein. These same mutations, however, do not affect the ability of the F protein to interact with HN, as observed by isolation of native HN-F complexes using hexahistidine tagging of HN and Ni-affinity chromatography. Isolation of HN-F complexes containing F proteins that are deficient in cleavage, fusion, and 6-HB formation suggests that HR2 plays roles in stabilization of (1) a pre-cleavage F structure, (2) the 6-HB, and (3) the HN-F complex. The functional interaction of HN and F in transfected cells begins before exit from the ER, as downregulation of HN expression occurs even when ER exit of HN and F is abrogated by BFA. Chimeras constructed using parts of the BPIV3 and HPIV3 F proteins were not different in their ability to fuse cells in concert with the HPIV3 HN protein. Stability of the homo- and heterotypic 6-HBs were similar, as was the ability of GST-HR2 proteins to inhibit HPIV3 and BPIV3 infection. HPIV3, selected using increasing concentrations of inhibitory GST-HR2 protein, developed statistically significant resistance to GST-HR2 by the third passage, with a population resistance peak at passage 4. HPIV3 clones from passage 4 and 6 demonstrated statistically significant resistance to inhibition by GST-HR2 at a concentration ten times the IC_{50}. Unexpectedly, no adaptive mutations were identified in the F proteins of the plaque-purified clones.

A detailed, speculative model for the roles of the HN and F proteins of paramyxoviruses from synthesis to fusion can be produced, based on data from published reports and experimental evidence described in this thesis. A cartoon representation of the proposed model is presented in Figure 33, with the characteristic refolding of the F protein detailed as another cartoon in Figure 34.

Figure 33. A model for paramyxovirus membrane fusion. HN and F are translated **(1)** at the surface of the rough ER, where expression of HPIV3 F protein downregulates expression of the HN protein, in transfected cells. HN and F, in their immature forms, self-associate into trimers (F) or tetramers (HN – illustrated as a dimer for simplicity), and interact with one another inside the lumen of the ER **(2)**. The HN-F interaction may occur through interactions between the stalk region of the HN protein, and HR2 region of the F protein (illustrated by the lightly-shaded, coloured cylinders on the F protein). The HN/F complex **(3)** exits the ER (4), and is transported through the *cis*-Golgi **(5)** and the medial Golgi **(6)** to the *trans*-Golgi, where the exposed cleavage loop of F_0 is cleaved by furin (orange half-circles) **(7)**. The HN/F complex is then transported to the cell surface **(8).** In this model, cell-cell and virion-cell fusion is assumed to be identical. Upon surface presentation, HN binds to sialic acid **(9)**, which induces a conformational change in the HN protein, including a tightening of the dimer interface **(10)**. Conformational changes in HN lead to conformational changes in $F_{1,2}$ **(11)**, possibly transmitted to $F_{1,2}$ though HN stalk-HR2 interactions. HR1 (darkly shaded, coloured cylinders) is unfolded from a pre-fusion, partially buried conformation, to a rigid stalk-like trimer **(12)**, the fusion peptide (squiggly lines) is exposed, and buries itself in the target membrane. The characteristic class I fusion protein refolding event **(13)**, in which HR1 and HR2 pull together to form the 6-HB, pulls virion (or host cell) and target cell membranes in close enough proximity for fusion to occur, with the F protein ending up in its stable, 6-HB, form **(14)**.

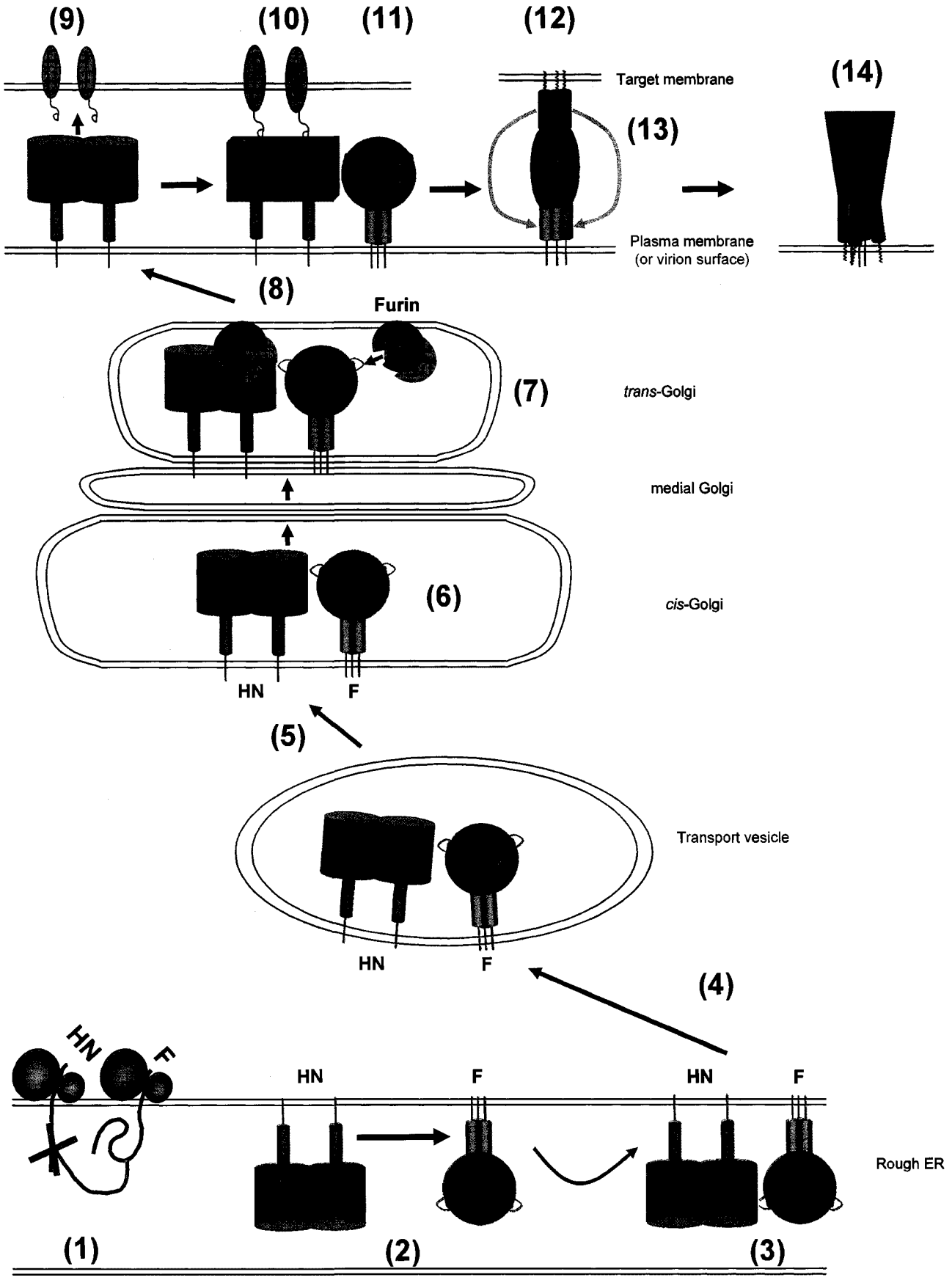
(9)
(10)
(11)
(12)
Target membrane
(14)
(13)
Plasma membrane
(or virion surface)
(8)
Furin
(7)
trans-Golgi
medial Golgi
(6)
cis-Golgi
HN
F
(5)
Transport vesicle
HN
F
(4)
HN
F
HN
F
HN
F
Rough ER
(1)
(2)
(3)

Figure 34. Schematic representation of the refolding intermediates of the paramyxovirus F protein. The various refolding intermediates of the F protein, as detailed in the text, are presented as both monomers (top) and trimers (bottom). Trimerization of the F_0 protein occurs in the ER. The pre-cleavage form of the F_0 protein contains surface-exposed loops (black arrows), which include the furin recognition sequence. In both the pre-cleavage, and post-cleavage/pre-fusion forms of F, HR2 is a rigid stalk at the base of the protein (light-coloured cylinders, blue arrows), which stabilizes the pre-cleavage form of F. Also, HR1 is unfolded into a series of helix/loop/helix structures in the head of F (dark-coloured cylinders). Upon receptor binding by HN, the F protein adopts a high-energy pre-hairpin conformation, exposing HR1, in a rigid trimer form, at the "top" of the molecule. This releases and exposes the fusion peptide (squiggly lines) for interaction with target membranes. F refolds again, with the HR1 and HR2 pulling together to form the 6-HB, resulting in membrane merger, and F assumes its final, stable, post-fusion conformation.

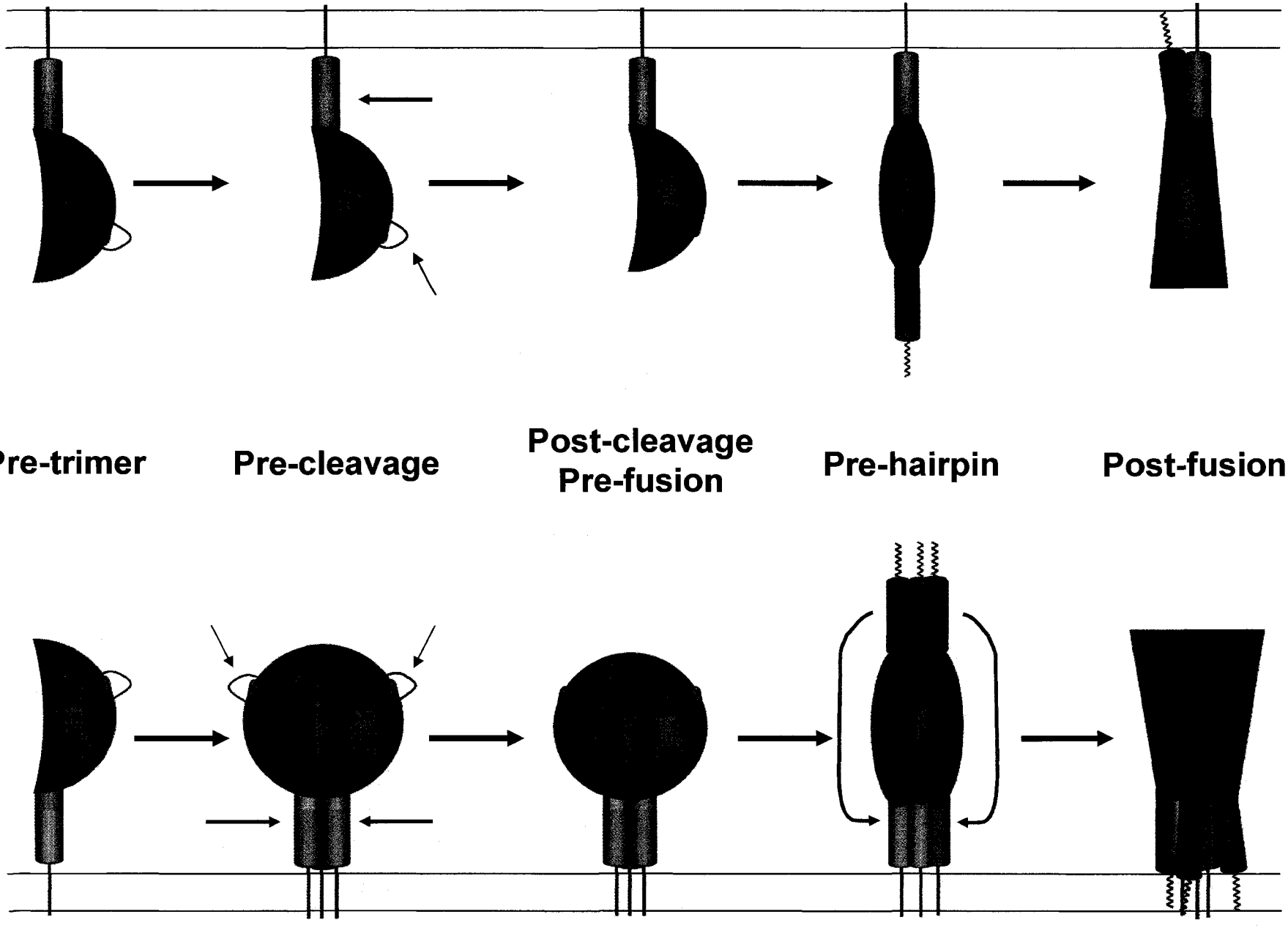
Pre-trimer
Pre-cleavage
Post-cleavage
Pre-fusion
Pre-hairpin
Post-fusion

In the lumen of the ER, glycosylation and oligomerization of both HN and F occur (Lamb and Kolakofsky, 2001; Ng *et al.*, 1989). Downregulation of HN expression when F is coexpressed must occur either cotranslationally or soon after translation (Bousse *et al.*, 1997). Reduced levels of HN in the presence of brefeldin A indicate that the downregulation must occur prior to HN transport out of the ER. Notably, downregulation of HN appears to occur only in transfected cells; expression of HN in infected cells is mainly regulated at the level of transcription (Bousse *et al.*, 1997). There is a preponderance of evidence to suggest that HN and F form some sort of complex while still in the ER, as both functional and physical interactions were shown using ER-retention mutants (Plemper *et al.*, 2001; Tong and Compans, 1999; Tanaka *et al.*, 1996). The conformations adopted by HN and F in this early complex, or required for formation of the complex, are unknown, although it would seem likely that HN is in a pre-receptor-binding conformation – a prediction somewhat borne out by the lack of coimmunoprecipition (Deng *et al.*, 1999) or His_6-trapping of HN-F complexes when lysates of cells separately expressing HN and F are mixed, where the conformation of HN can be assumed to have been altered by receptor binding.

The regions of HN and F responsible for their interaction do not provide any clues as to where or when the interaction occurs. However, the regions involved appear to include approximately 30 stalk residues in HN, and HR2 of F (Gravel and Morrison, 2003). It is possible that the twelve carboxy-terminal residues of the extracellular domain of F, ten of which are included in NDV HN stalk peptide, may be key to the HN-F interaction, as supported by the results with chimeric HPIV2/SV41 F proteins (Tsurudome *et al.*, 1998), and the tolerance of HPIV3/BPIV3 F chimeras for heterotypic HN in fusion promotion. In the intracellular HN-F complex, F is assumed to be in its pre-cleavage form, in which HR2 is exposed and can interact with HN. This may be supported by the observation that peptides based on HR1 sequences of the class I MLV Env protein, interact with HR2 and block maturation (Ou and Silver, 2005), but cannot interact with HR2 sequences in an inhibitory,

pre-6-HB intermediate, if analogies between paramyxovirus F proteins and MLV Env can be drawn.

The HN-F complex is then transported to the Golgi apparatus. The key event that occurs in the Golgi apparatus is cleavage of paramyxovirus F_0 protein by the *trans*-Golgi resident protease, furin (Ortmann *et al.*, 1994). The cleavage of F_0 is dependent on the sequence at the cleavage site (reviewed in Lamb and Kolakofsky, 2001), and, as has been suggested from results presented in this dissertation, by a conformation that is destabilized by mutations in HR2. Cleavage of F_0 is HN-independent since F_0 is cleaved when expressed in the absence of HN, and no increase in F_0 cleavage in the presence of HN was observed, nor has been mentioned in the published literature. In a similar vein, cleavage, or lack thereof, does not appear to affect the ability of F to interact with HN, since both $F_{1,2}$ and F_0 (Deng *et al.*, 1999, this study) and the I474S and I474D cleavage-negative F mutants form complexes with HN.

Following F_0 cleavage, HN and F are transported to the cell surface, likely as a complex. HN and F of NDV have been shown to cluster into lipid rafts on the cell surface (Laliberte *et al.*, 2007; Laliberte *et al.*, 2006; Dolganiuc *et al.*, 2003). Raft clustering plays a key role in the release of virions, but may or may not play a role in fusion, as assembly of functional HN-F complexes in NDV virions was shown to be raft-independent (Laliberte *et al.*, 2007). However, reduced infectivity of canine distemper virus was shown when cholesterol was depleted from the viral envelope (Imhoff *et al.*, 2007). An important point to note is while fusion activities of viral cell-surface glycoproteins and virion-associated glycoproteins have long been assumed to be identical, a recent study indicated that there may be some differences, including differences in the membrane areas in contact, densities of HN and F proteins in the membrane, and cytoskeletal effects on fusion rates (Connolly and Lamb, 2006).

HN binds to sialic acid, presumably through receptor binding site "1", identified in the three-dimensional structures for NDV, PIV5, and HPIV3 HN proteins (Yuan *et al.*, 2005; Lawrence *et al.*, 2004; Connaris *et al.*, 2002; Crennell *et al.*, 2000). Binding is then followed by a tightening of the HN dimer interface (within the active tetramer) which may result in an overall conformational change in HN, as shown for NDV HN (Crennell *et al.*, 2000), or not, as for HPIV3 HN (Lawrence *et al.*, 2004). This change is then transmitted to F, presumably through an interaction between the stalk of HN and HR2 of F. Mutations in the stalk region of HN that have no effect on receptor binding activity abolish fusion by abrogating HN-F interactions (Melanson and Iorio, 2006; Melanson and Iorio, 2004; Porotto *et al.*, 2003). Alternatively, HN binding to sialic acid could weaken HN-F interactions, releasing the F protein and initiating its conformational changes.

In a second model for paramyxovirus F protein-mediated membrane fusion, uncomplexed HN recruits F into the HN-F complex at the cell surface, following receptor binding, to initiate the fusion process. This model is not consistent with most ER retention studies, in which both intracellular association of HPIV2 and HPIV3 HN and F were demonstrated (Tong and Compans, 1999; Tanaka *et al.*, 1996), nor with the isolation of intracellular measles virus H-F complexes (Plemper *et al.*, 2001). Similarly, a mutant NDV HN protein that was deficient in receptor-binding and fusion promotion, was expressed on the cell surface, and was shown to physically interact with F (Li *et al.*, 2004), indicating that receptor binding is not required for HN and F to interact.

Once receptor binding has occurred in functional HN-F complexes, the characteristic conformational changes in F proceed. A recent review by Russell and Luque (2006) describes a model for these conformational changes. First is the transition from the proposed pre-fusion form presented by Yin and colleagues (2006) to a conformation that exposes the fusion peptide. At this stage, HR1, which in the pre-fusion structure is only partially helical and is partially buried in the head region of F_1, rapidly refolds to form a rigid

triple-stranded coiled- coil at the top of the F_1 protein. The hydrophobic fusion peptide, which is exposed at the "tip" of the F_1 protein, can now bury itself in the target membrane. The trigger for this conformational shift is likely to come from changes in the HR2 structure; a switch from an HN-interacting, "trigger-signal- receptor" conformation, to a fusion-inducing, 6-HB-forming conformation (Russell *et al.*, 2001).

It is likely at this stage, where the amphipathic α-helices of HR1 and HR2 are exposed in an unstable conformation, that exogenously added HR1 or HR2 peptides can interact with the cognate sequence *in situ* and inhibit refolding of F and the fusion process. HR1 appears to be unavailable for HR2 binding in the pre-fusion form of the F trimer (Yin *et al.*, 2006), but in this new conformation, is exposed as an α-helix, adjacent to the fusion peptide at the tip of the protein. Inhibition of fusion and virus infection by HR2 peptides was observed to be more efficient than by HR1 peptides. There are a few reasons why this may occur. Firstly, 6-HB structures for all class I fusion proteins consist of a central core made up of HR1, with HR2 peptides surrounding the outside (Xu *et al.*, 2004b; Bosch *et al.*, 2003; Malashkevich *et al.*, 2001; Matthews *et al.*, 2000; Zhao *et al.*, 2000; Lu *et al.*, 1999; Baker *et al.*, 1999; Dutch *et al.*, 1999; Malashkevich *et al.*, 1998; Chan *et al.*, 1997); HR1 in an intermediate, exposed, conformation would be easily accessible to HR2 peptide inhibition, while HR1 would need to "get in" to the HR2 "trimer" in the intermediate form of F, although Russell and Luque (2006) have proposed an opening up of the HR2 "trimer" very late in fusion, and refolding to produce the 6-HB. Secondly, HR1 is exposed and distal to the plasma (or viral) membrane. It is unclear if HR2 peptide can bind prior to fusion peptide insertion in the target membrane, though advanced studies by Russell and colleagues have shown that addition of HR2 peptide can "freeze" fusion as late as the lipid-transferring stage, just prior to membrane merger (Russell *et al.*, 2001). The GST moiety of GST-HR2 may sterically hinder the interaction of HR2 with HR1, which would explain the 100-fold difference in the calculated IC_{50} values determined for HPIV3 HR2 peptide and GST-HR2.

Steric hindrance by GST may also explain why the HR1 peptide of HPIV3 weakly inhibits fusion and GST-HR1 does not inhibit at all. The accessibility of HR2 sequences to HR1 peptide is probably hindered by (1) the proximity of HR2 to the cell/virion membrane and/or (2) the bulk and conformation of the F protein. The inability of exogenous HR1 to access HR2 would be exacerbated by the presence of GST sequences, and provides an explanation why GST-HR1 does not inhibit membrane fusion or HPIV3 infection.

The high level of conservation of the TNxAV motif of HR1 among members of the *Paramyxoviridae* suggests that a well-designed small-molecule inhibitor that binds to this pocket in F, would likely block the refolding of F into the post-fusion conformation, as efficiently, or potentially more efficiently, than HR2 peptides, for which synthesis is complicated and expensive.

Following the insertion of the fusion peptide into the target membrane, HR1-HR2 interactions result in the formation of the 6-HB, and refolding of F into the post-fusion form described by Yin and colleagues (2005). It has been proposed that refolding relies on a molecular "switch" located at the extreme N-terminus of HR2, which is also involved in the activation of F following receptor binding (Russell *et al.*, 2003). Curiously, in the post-fusion trimer structure of HPIV3 F, the 6-HB that is formed is an intermonomer interaction, rather than an intramonomer interaction (i.e. refolding forms 6-HB between HR1 of monomer 1 and HR2 of monomer 2, HR1 of monomer 2 and HR2 of monomer 3, and HR1 of monomer 3 and HR2 of monomer 1). The post-fusion, 6-HB-containing trimer is highly stable, and is presumably what is detected as a high molecular weight band in western immunoblots of octyl glucoside-lysed cells expressing the F protein. Perhaps heating induces the formation of the 6-HB, as suggested in work by Connolly and colleagues, in which structural analysis of soluble, anchor-free PIV5 F proteins in various intermediate conformations was determined by electron microscopy of samples, with heat being used as a refolding trigger (Connolly *et al.*, 2006). Also, in the structures published for HPIV3 (Yin *et al.*, 2005) and

NDV F proteins (Chen *et al.*, 2001), both proteins are uncleaved, yet are found in their stable post-fusion 6-HB conformation; conditions under which crystals are formed from soluble HPIV3 and NDV F proteins may be sufficient to trigger uncleaved F_0 proteins to refold into a stable post-fusion form.

The refolding of F allows the target and host membranes to be pulled together closely enough such that formation of a fusion pore can start. The observation that F proteins with I474A and I474E mutations had wild-type fusion activity despite the fact that these mutations affected 6-HB stability, indicates that the HR1-HR2 interaction can be weakened without affecting fusogenicity. Russell and Lamb (2003) showed previously that some N-terminal "switch" mutants with destabilized 6-HB were in fact hyperfusogenic in the full-length F protein. While formation of a stable 6-HB is critical for fusion, these results indicate that fusogenicity is not strictly dependent on 6-HB stability.

While speculative, this model for the function of HN and F in the fusion process, which is supported by several different lines of evidence, including data presented in this dissertation, identifies several critical stages in the fusion process and associated conformations of the F protein that are tempting targets for inhibitors that will interfere with paramyxovirus entry.

Reference list

Alexander,D.J. (2000). Newcastle disease and other avian paramyxoviruses. Rev. Sci. Tech. **19**, 443-462.

Ali,A. and Nayak,D.P. (2000). Assembly of Sendai virus: M protein interacts with F and HN proteins and with the cytoplasmic tail and transmembrane domain of F protein. Virology **276**, 289-303.

Amonsen,M., Smith,D.F., Cummings,R.D., and Air,G.M. (2007). Human Parainfluenza Viruses hPIV1 and hPIV3 Bind Oligosaccharides with {alpha}2-3-Linked Sialic Acids That Are Distinct from Those Bound by H5 Avian Influenza Virus Hemagglutinin. J. Virol. **81**, 8341-8345.

Armand-Ugon,M., Gutierrez,A., Clotet,B., and Este,J.A. (2003). HIV-1 resistance to the gp41-dependent fusion inhibitor C-34. Antiviral Res. **59**, 137-142.

Ausubel,F.M., Brent,R., Kingston,R.E., Moore,D.D., Seidman,J.G., Smith,J.A., and Struhl,K. (1999). Short Protocols in Molecular Biology. (New York, NY: Wiley John and Sons, Inc.).

Bagai,S. and Lamb,R.A. (1995). Quantitative measurement of paramyxovirus fusion: differences in requirements of glycoproteins between simian virus 5 and human parainfluenza virus 3 or Newcastle disease virus. J. Virol. **69**, 6712-6719.

Bagai,S. and Lamb,R.A. (1996). Truncation of the COOH-terminal region of the paramyxovirus SV5 fusion protein leads to hemifusion but not complete fusion. J. Cell Biol. **135**, 73-84.

Bailly,J.E., McAuliffe,J.M., Skiadopoulos,M.H., Collins,P.L., and Murphy,B.R. (2000). Sequence determination and molecular analysis of two strains of bovine parainfluenza virus type 3 that are attenuated for primates. Virus Genes **20**, 173-182.

Baker,K.A., Dutch,R.E., Lamb,R.A., and Jardetzky,T.S. (1999). Structural basis for paramyxovirus-mediated membrane fusion. Mol. Cell **3**, 309-319.

Barrett,T. (1999). Morbillivirus infections, with special emphasis on morbilliviruses of carnivores. Vet. Microbiol. **69**, 3-13.

Belshe,R.B., Newman,F.K., Anderson,E.L., Wright,P.F., Karron,R.A., Tollefson,S., Henderson,F.W., Meissner,H.C., Madhi,S., Roberton,D., Marshall,H., Loh,R., Sly,P., Murphy,B., Tatem,J.M., Randolph,V., Hackell,J., Gruber,W., and Tsai,T.F. (2004). Evaluation of combined live, attenuated respiratory syncytial virus and parainfluenza 3 virus vaccines in infants and young children. J. Infect. Dis. **190**, 2096-2103.

Belshe,R.B., Newman,F.K., Tsai,T.F., Karron,R.A., Reisinger,K., Roberton,D., Marshall,H., Schwartz,R., King,J., Henderson,F.W., Rodriguez,W., Severs,J.M., Wright,P.F., Keyserling,H., Weinberg,G.A., Bromberg,K., Loh,R., Sly,P., McIntyre,P., Ziegler,J.B., Hackell,J., Deatly,A., Georgiu,A., Paschalis,M., Wu,S.L., Tatem,J.M., Murphy,B., and Anderson,E. (2004). Phase 2 evaluation of parainfluenza type 3 cold passage mutant 45 live attenuated vaccine in healthy children 6-18 months old. J. Infect. Dis. **189**, 462-470.

Blacklow,S.C., Lu,M., and Kim,P.S. (1995). A trimeric subdomain of the simian immunodeficiency virus envelope glycoprotein. Biochemistry **34**, 14955-14962.

Bolt,G. and Pedersen,I.R. (1998). The role of subtilisin-like proprotein convertases for cleavage of the measles virus fusion glycoprotein in different cell types. Virology **252**, 387-398.

Bolt,G., Pedersen,L.O., and Birkeslund,H.H. (2000). Cleavage of the respiratory syncytial virus fusion protein is required for its surface expression: role of furin. Virus Res. **68**, 25-33.

Bosch,B.J., Martina,B.E., Van Der,Z.R., Lepault,J., Haijema,B.J., Versluis,C., Heck,A.J., De,G.R., Osterhaus,A.D., and Rottier,P.J. (2004). Severe acute respiratory syndrome coronavirus (SARS-CoV) infection inhibition using spike protein heptad repeat-derived peptides. Proc. Natl. Acad. Sci. U. S. A **101**, 8455-8460.

Bosch,B.J., Van Der,Z.R., de Haan,C.A., and Rottier,P.J. (2003). The coronavirus spike protein is a class I virus fusion protein: structural and functional characterization of the fusion core complex. J. Virol. **77**, 8801-8811.

Bossart,K.N. and Broder,C.C. (2004). Viral glycoprotein-mediated cell fusion assays using vaccinia virus vectors. Methods Mol. Biol. **269**, 309-332.

Bossart,K.N., Mungall,B.A., Crameri,G., Wang,L.F., Eaton,B.T., and Broder,C.C. (2005). Inhibition of Henipavirus fusion and infection by heptad-derived peptides of the Nipah virus fusion glycoprotein. Virol. J. **2**, 57.

Bossart,K.N., Wang,L.F., Flora,M.N., Chua,K.B., Lam,S.K., Eaton,B.T., and Broder,C.C. (2002). Membrane fusion tropism and heterotypic functional activities of the Nipah virus and Hendra virus envelope glycoproteins. J. Virol. **76**, 11186-11198.

Bousse,T. and Takimoto,T. (2006). Mutation at residue 523 creates a second receptor binding site on human parainfluenza virus type 1 hemagglutinin-neuraminidase protein. J. Virol. **80**, 9009-9016.

Bousse,T., Takimoto,T., Gorman,W.L., Takahashi,T., and Portner,A. (1994). Regions on the hemagglutinin-neuraminidase proteins of human parainfluenza virus type-1 and Sendai virus important for membrane fusion. Virology **204**, 506-514.

Bousse,T., Takimoto,T., Murti,K.G., and Portner,A. (1997). Elevated expression of the human parainfluenza virus type 1 F gene downregulates HN expression. Virology **232**, 44-52.

Bousse,T., Takimoto,T., and Portner,A. (1995). A single amino acid changes enhances the fusion promotion activity of human parainfluenza virus type 1 hemagglutinin-neuraminidase glycoprotein. Virology **209**, 654-657.

Branigan,P.J., Day,N.D., Liu,C., Gutshall,L.L., Melero,J.A., Sarisky,R.T., and Del Vecchio,A.M. (2006). The cytoplasmic domain of the F protein of Human respiratory syncytial virus is not required for cell fusion. J. Gen. Virol. **87**, 395-398.

Broer,R., Boson,B., Spaan,W., Cosset,F.L., and Corver,J. (2006). Important role for the transmembrane domain of severe acute respiratory syndrome coronavirus spike protein during entry. J. Virol. **80**, 1302-1310.

Brown,E.G., Dimock,K., and Wright,K.E. (1996). The Urabe AM9 mumps vaccine is a mixture of viruses differing at amino acid 335 of the hemagglutinin-neuraminidase gene with one form associated with disease. J. Infect. Dis. **174**, 619-622.

Browne,H., Bruun,B., Whiteley,A., and Minson,T. (2003). Analysis of the role of the membrane-spanning and cytoplasmic tail domains of herpes simplex virus type 1 glycoprotein D in membrane fusion. J. Gen. Virol. **84**, 1085-1089.

Buckland,R., Malvoisin,E., Beauverger,P., and Wild,F. (1992). A leucine zipper structure present in the measles virus fusion protein is not required for its tetramerization but is essential for fusion. J. Gen. Virol. **73 (Pt 7)**, 1703-1707.

Burkhard,P., Stetefeld,J., and Strelkov,S.V. (2001). Coiled coils: a highly versatile protein folding motif. Trends Cell Biol. **11**, 82-88.

Cairns,T.M., Milne,R.S., Ponce-de-Leon,M., Tobin,D.K., Cohen,G.H., and Eisenberg,R.J. (2003). Structure-function analysis of herpes simplex virus type 1 gD and gH-gL: clues from gDgH chimeras. J. Virol. **77**, 6731-6742.

Cathomen,T., Naim,H.Y., and Cattaneo,R. (1998). Measles viruses with altered envelope protein cytoplasmic tails gain cell fusion competence. J. Virol. **72**, 1224-1234.

Cattaneo,R., Regmann,G., Baczko,K., ter Meulen,V., and Billeter,M. A. (1987). Altered ratios of measles virus transcripts in diseased human brains. Virology **160**, 523–526.

Chan,D.C., Fass,D., Berger,J.M., and Kim,P.S. (1997). Core structure of gp41 from the HIV envelope glycoprotein. Cell **89**, 263-273.

Chanock,R.M., ,M.B.R., and Collins,P.L. (2001). Parainfluenza viruses. In **Fields Virology**, D.M.Knipe, P.M.Howley, D.E.Griffin, R.A.Lamb, M.A.Martin, B.Roizman, and S.E.Strauss, eds. (Philadelphia: Lippincott Williams & Wilkins), pp. 1341-1379.

Chatziandreou,N., Stock,N., Young,D., Andrejeva,J., Hagmaier,K., McGeoch,D.J., and Randall,R.E. (2004). Relationships and host range of human, canine, simian and porcine isolates of simian virus 5 (parainfluenza virus 5). J. Gen. Virol. **85**, 3007-3016.

Chen,C.H., Matthews,T.J., McDanal,C.B., Bolognesi,D.P., and Greenberg,M.L. (1995). A molecular clasp in the human immunodeficiency virus (HIV) type 1 TM protein determines the anti-HIV activity of gp41 derivatives: implication for viral fusion. J. Virol. **69**, 3771-3777.

Chen,L., Gorman,J.J., Kimm-Breschkin,J., Lawrence,L.J., Tulloch,P.A., Smith,B.J., Colman,P.M., and Lawrence,M.C. (2001). The structure of the fusion glycoprotein of Newcastle disease virus suggests a novel paradigm for the molecular mechanism of membrane fusion. Structure. (Camb.) **9**, 255-266.

Chernomordik,L.V. and Kozlov,M.M. (2003). Protein-lipid interplay in fusion and fission of biological membranes. Annu. Rev. Biochem. **72**, 175-207.

Connaris,H., Takimoto,T., Russell,R., Crennell,S., Moustafa,I., Portner,A., and Taylor,G. (2002). Probing the sialic acid binding site of the hemagglutinin-neuraminidase of Newcastle disease virus: identification of key amino acids involved in cell binding, catalysis, and fusion. J. Virol. **76**, 1816-1824.

Connolly,S.A. and Lamb,R.A. (2006). Paramyxovirus fusion: real-time measurement of parainfluenza virus 5 virus-cell fusion. Virology **355**, 203-212.

Connolly,S.A., Leser,G.P., Yin,H.S., Jardetzky,T.S., and Lamb,R.A. (2006). Refolding of a paramyxovirus F protein from prefusion to postfusion conformations observed by liposome binding and electron microscopy. Proc. Natl. Acad. Sci. U. S. A **103**, 17903-17908.

Corey,E.A. and Iorio,R.M. (2007). Mutations in the stalk of the measles virus hemagglutinin protein decrease fusion, but do not interfere with the virus-specific interaction with the homologous fusion protein. J. Virol.

Corey,E.A., Mirza,A.M., Levandowsky,E., and Iorio,R.M. (2003). Fusion deficiency induced by mutations at the dimer interface in the Newcastle disease virus hemagglutinin-neuraminidase is due to a temperature-dependent defect in receptor binding. J. Virol. **77**, 6913-6922.

Cosby,S.L., Duprex,W.P., Hamill,L.A., Ludlow,M., and McQuaid,S. (2002). Approaches in the understanding of morbillivirus neurovirulence. J. Neurovirol. **8 Suppl 2**, 85-90.

Cote, M. J. **The human parainfluenza virus 3 fusion protein: cloning, mapping, sequence analysis and expression**. 1989. University of Ottawa. Ph.D. thesis. 144 pp.

Crennell,S., Takimoto,T., Portner,A., and Taylor,G. (2000). Crystal structure of the multifunctional paramyxovirus hemagglutinin-neuraminidase. Nat. Struct. Biol. **7**, 1068-1074.

del Real,G., Jimenez-Baranda,S., Mira,E., Lacalle,R.A., Lucas,P., Gomez-Mouton,C., Alegret,M., Pena,J.M., Rodriguez-Zapata,M., varez-Mon,M., Martinez,A., and Manes,S. (2004). Statins inhibit HIV-1 infection by down-regulating Rho activity. J. Exp. Med. **200**, 541-547.

Deng,R., Mirza,A.M., Mahon,P.J., and Iorio,R.M. (1997). Functional chimeric HN glycoproteins derived from Newcastle disease virus and human parainfluenza virus-3. Arch. Virol. Suppl **13**, 115-130.

Deng,R., Wang,Z., Glickman,R.L., and Iorio,R.M. (1994). Glycosylation within an antigenic site on the HN glycoprotein of Newcastle disease virus interferes with its role in the promotion of membrane fusion. Virology **204**, 17-26.

Deng,R., Wang,Z., Mahon,P.J., Marinello,M., Mirza,A., and Iorio,R.M. (1999). Mutations in the Newcastle disease virus hemagglutinin-neuraminidase protein that interfere with its ability to interact with the homologous F protein in the promotion of fusion. Virology **253**, 43-54.

Deng,R., Wang,Z., Mirza,A.M., and Iorio,R.M. (1995). Localization of a domain on the paramyxovirus attachment protein required for the promotion of cellular fusion by its homologous fusion protein spike. Virology **209**, 457-469.

Derdeyn,C.A., Decker,J.M., Sfakianos,J.N., Wu,X., O'Brien,W.A., Ratner,L., Kappes,J.C., Shaw,G.M., and Hunter,E. (2000). Sensitivity of human immunodeficiency virus type 1 to the fusion inhibitor T-20 is modulated by coreceptor specificity defined by the V3 loop of gp120. J. Virol. **74**, 8358-8367.

Derdeyn,C.A., Decker,J.M., Sfakianos,J.N., Zhang,Z., O'Brien,W.A., Ratner,L., Shaw,G.M., and Hunter,E. (2001). Sensitivity of human immunodeficiency virus type 1 to fusion inhibitors targeted to the gp41 first heptad repeat involves distinct regions of gp41 and is consistently modulated by gp120 interactions with the coreceptor. J. Virol. **75**, 8605-8614.

Dinter,A. and Berger,E.G. (1998). Golgi-disturbing agents. Histochem. Cell Biol. **109**, 571-590.

Dolganiuc,V., McGinnes,L., Luna,E.J., and Morrison,T.G. (2003). Role of the cytoplasmic domain of the Newcastle disease virus fusion protein in association with lipid rafts. J. Virol. **77**, 12968-12979.

Drake,J.W. (1993). Rates of spontaneous mutation among RNA viruses. Proc. Natl. Acad. Sci. U. S. A **90**, 4171-4175.

Drake,J.W. (1999). The distribution of rates of spontaneous mutation over viruses, prokaryotes, and eukaryotes. Ann. N. Y. Acad. Sci. **870**, 100-107.

Drake,J.W., Charlesworth,B., Charlesworth,D., and Crow,J.F. (1998). Rates of spontaneous mutation. Genetics **148**, 1667-1686.

Drake,J.W. and Holland,J.J. (1999). Mutation rates among RNA viruses. Proc. Natl. Acad. Sci. U. S. A **96**, 13910-13913.

Dutch,R.E. and Lamb,R.A. (2001). Deletion of the cytoplasmic tail of the fusion protein of the paramyxovirus simian virus 5 affects fusion pore enlargement. J. Virol. **75**, 5363-5369.

Dutch,R.E., Leser,G.P., and Lamb,R.A. (1999). Paramyxovirus fusion protein: characterization of the core trimer, a rod-shaped complex with helices in anti-parallel orientation. Virology **254**, 147-159.

Earp,L.J., Delos,S.E., Park,H.E., and White,J.M. (2005). The many mechanisms of viral membrane fusion proteins. Curr. Top. Microbiol. Immunol. **285**, 25-66.

Eaton,B.T., Broder,C.C., Middleton,D., and Wang,L.F. (2006). Hendra and Nipah viruses: different and dangerous. Nat. Rev. Microbiol. **4**, 23-35.

Ebata, S. N. **Requirements for syncytium formation mediated by the fusion glycoprotein of human parainfluenza virus type 3**. 1996. University of Ottawa.
Ph.D. Thesis. 180 pp.

Ebata,S.N., Cote,M.J., Kang,C.Y., and Dimock,K. (1991). The fusion and hemagglutinin-neuraminidase glycoproteins of human parainfluenza virus 3 are both required for fusion. Virology **183**, 437-441.

Eckert,D.M. and Kim,P.S. (2001). Mechanisms of viral membrane fusion and its inhibition. Annu. Rev. Biochem. **70**, 777-810.

Epand,R.F., Macosko,J.C., Russell,C.J., Shin,Y.K., and Epand,R.M. (1999). The ectodomain of HA2 of influenza virus promotes rapid pH dependent membrane fusion. J. Mol. Biol. **286**, 489-503.

Faisca,P. and Desmecht,D. (2007). Sendai virus, the mouse parainfluenza type 1: a longstanding pathogen that remains up-to-date. Res. Vet. Sci. **82**, 115-125.

Fass,D. (2003). Conformational changes in enveloped virus surface proteins during cell entry. Adv. Protein Chem. **64**, 325-362.

Ferreira,L., Munoz-Barroso,I., Marcos,F., Shnyrov,V.L., and Villar,E. (2004). Sialidase, receptor-binding and fusion-promotion activities of Newcastle disease virus haemagglutinin-neuraminidase glycoprotein: a mutational and kinetic study. J. Gen. Virol. **85**, 1981-1988.

Fouillot-Coriou,N. and Roux,L. (2000). Structure-function analysis of the Sendai virus F and HN cytoplasmic domain: different role for the two proteins in the production of virus particle. Virology **270**, 464-475.

Fuerst,T.R., Niles,E.G., Studier,F.W., and Moss,B. (1986). Eukaryotic transient-expression system based on recombinant vaccinia virus that synthesizes bacteriophage T7 RNA polymerase. Proc. Natl. Acad. Sci. U. S. A **83**, 8122-8126.

Gardner,A.E. and Dutch,R.E. (2007). A conserved region in the f2 subunit of paramyxovirus fusion proteins is involved in fusion regulation. J. Virol. **81**, 8303-8314.

Gardner,A.E., Martin,K.L., and Dutch,R.E. (2007). A Conserved Region between the Heptad Repeats of Paramyxovirus Fusion Proteins Is Critical for Proper F Protein Folding. Biochemistry **46**, 5094-5105.

Ghosh,J.K. and Shai,Y. (1999). Direct evidence that the N-terminal heptad repeat of Sendai virus fusion protein participates in membrane fusion. J. Mol. Biol. **292**, 531-546.

Gill,S.C. and von Hippel,P.H. (1989). Calculation of protein extinction coefficients from amino acid sequence data. Anal. Biochem. **182**, 319-326.

Gower,T.L., Pastey,M.K., Peeples,M.E., Collins,P.L., McCurdy,L.H., Hart,T.K., Guth,A., Johnson,T.R., and Graham,B.S. (2005). RhoA signaling is required for respiratory syncytial virus-induced syncytium formation and filamentous virion morphology. J. Virol. **79**, 5326-5336.

Gower,T.L., Peeples,M.E., Collins,P.L., and Graham,B.S. (2001). RhoA is activated during respiratory syncytial virus infection. Virology **283**, 188-196.

Gravel,K.A. and Morrison,T.G. (2003). Interacting domains of the HN and F proteins of newcastle disease virus. J. Virol. **77**, 11040-11049.

Greenberg,M.L. and Cammack,N. (2004). Resistance to enfuvirtide, the first HIV fusion inhibitor. J. Antimicrob. Chemother. **54**, 333-340.

Gupta,R.K., Best,J., and MacMahon,E. (2005). Mumps and the UK epidemic 2005. BMJ **330**, 1132-1135.

Haanes,E.J., Guimond,P., and Wardley,R. (1997). The bovine parainfluenza virus type-3 (BPIV-3) hemagglutinin/neuraminidase glycoprotein expressed in baculovirus protects calves against experimental BPIV-3 challenge. Vaccine **15**, 730-738.

Hall,C.B. (2001). Respiratory syncytial virus and parainfluenza virus. N. Engl. J. Med. **344**, 1917-1928.

Harrison,S.C. (2005). Mechanism of membrane fusion by viral envelope proteins. Adv. Virus Res. **64**, 231-261.

Heminway,B.R., Yu,Y., and Galinski,M.S. (1994). Paramyxovirus mediated cell fusion requires co-expression of both the fusion and hemagglutinin-neuraminidase glycoproteins. Virus Res. **31**, 1-16.

Henrickson,K.J. (2003). Parainfluenza viruses. Clin. Microbiol. Rev. **16**, 242-264.

Holland,J. and Domingo,E. (1998). Origin and evolution of viruses. Virus Genes **16**, 13-21.

Horvath,C.M., Paterson,R.G., Shaughnessy,M.A., Wood,R., and Lamb,R.A. (1992). Biological activity of paramyxovirus fusion proteins: factors influencing formation of syncytia. J. Virol. **66**, 4564-4569.

Hu,X.L., Ray,R., and Compans,R.W. (1992). Functional interactions between the fusion protein and hemagglutinin-neuraminidase of human parainfluenza viruses. J. Virol. **66**, 1528-1534.

Imhoff,H., von,M., V, Herrler,G., and Haas,L. (2007). Canine distemper virus infection requires cholesterol in the viral envelope. J. Virol. **81**, 4158-4165.

Johnson,V.A., Brun-Vezinet,F., Clotet,B., Conway,B., D'Aquila,R.T., Demeter,L.M., Kuritzkes,D.R., Pillay,D., Schapiro,J.M., Telenti,A., and Richman,D.D. (2003). Drug resistance mutations in HIV-1. Top. HIV. Med. **11**, 215-221.

Joshi,S.B., Dutch,R.E., and Lamb,R.A. (1998). A core trimer of the paramyxovirus fusion protein: parallels to influenza virus hemagglutinin and HIV-1 gp41. Virology **248**, 20-34.

Kido,H., Murakami,M., Oba,K., Chen,Y., and Towatari,T. (1999). Cellular proteinases trigger the infectivity of the influenza A and Sendai viruses. Mol. Cells **9**, 235-244.

Kim,F.J., Seiliez,I., Denesvre,C., Lavillette,D., Cosset,F.L., and Sitbon,M. (2000). Definition of an amino-terminal domain of the human T-cell leukemia virus type 1 envelope surface unit that extends the fusogenic range of an ecotropic murine leukemia virus. J. Biol. Chem. **275**, 23417-23420.

Klausner,R.D., Donaldson,J.G., and Lippincott-Schwartz,J. (1992). Brefeldin A: insights into the control of membrane traffic and organelle structure. J. Cell Biol. **116**, 1071-1080.

Kozerski,C., Ponimaskin,E., Schroth-Diez,B., Schmidt,M.F., and Herrmann,A. (2000). Modification of the cytoplasmic domain of influenza virus hemagglutinin affects enlargement of the fusion pore. J. Virol. **74**, 7529-7537.

Labrosse,B., Labernardiere,J.L., Dam,E., Trouplin,V., Skrabal,K., Clavel,F., and Mammano,F. (2003). Baseline susceptibility of primary human immunodeficiency virus type 1 to entry inhibitors. J. Virol. **77**, 1610-1613.

Laemmli,U.K. (1970). Cleavage of structural proteins during the assembly of the head of bacteriophage T4. Nature **227**, 680-685.

Laliberte,J.P., McGinnes,L.W., and Morrison,T.G. (2007). Incorporation of Functional HN-F Glycoprotein-Containing Complexes into Newcastle Disease Virus Is Dependent on Cholesterol and Membrane Lipid Raft Integrity. J. Virol. **81**, 10636-10648.

Laliberte,J.P., McGinnes,L.W., Peeples,M.E., and Morrison,T.G. (2006). Integrity of membrane lipid rafts is necessary for the ordered assembly and release of infectious Newcastle disease virus particles. J. Virol. **80**, 10652-10662.

Lamb,R.A. and Kolakofsky,D. (2001). Paramyxoviridae: The Viruses and Their Replication. In **Fields Virology**, D.M.Knipe, P.M.Howley, D.E.Griffin, R.A.Lamb, M.A.Martin, B.Roizman, and S.E.Strauss, eds. (Philadelphia: Lippincott Williams & Wilkins), pp. 1305-1339.

Lamb,R.A., Paterson,R.G., and Jardetzky,T.S. (2006). Paramyxovirus membrane fusion: lessons from the F and HN atomic structures. Virology **344**, 30-37.

Lambert,D.M., Barney,S., Lambert,A.L., Guthrie,K., Medinas,R., Davis,D.E., Bucy,T., Erickson,J., Merutka,G., and Petteway,S.R., Jr. (1996). Peptides from conserved regions of paramyxovirus fusion (F) proteins are potent inhibitors of viral fusion. Proc. Natl. Acad. Sci. U. S. A **93**, 2186-2191.

Larsen,L.E. (2000). Bovine respiratory syncytial virus (BRSV): a review. Acta Vet. Scand. **41**, 1-24.

Lawrence,M.C., Borg,N.A., Streltsov,V.A., Pilling,P.A., Epa,V.C., Varghese,J.N., Kimm-Breschkin,J.L., and Colman,P.M. (2004). Structure of the haemagglutinin-neuraminidase from human parainfluenza virus type III. J. Mol. Biol. **335**, 1343-1357.

Lee,M.S., Walker,R.E., and Mendelman,P.M. (2005). Medical burden of respiratory syncytial virus and parainfluenza virus type 3 infection among US children. Implications for design of vaccine trials. Hum. Vaccin. **1**, 6-11.

Li,J., Quinlan,E., Mirza,A., and Iorio,R.M. (2004). Mutated form of the Newcastle disease virus hemagglutinin-neuraminidase interacts with the homologous fusion protein despite deficiencies in both receptor recognition and fusion promotion. J. Virol. **78**, 5299-5310.

Li,Z., Sergel,T., Razvi,E., and Morrison,T. (1998). Effect of cleavage mutants on syncytium formation directed by the wild- type fusion protein of Newcastle disease virus. J. Virol. **72**, 3789-3795.

Liu,Y., Zhu,J., Feng,M.G., Tien,P., and Gao,G.F. (2004). Six-helix bundle assembly and analysis of the central core of mumps virus fusion protein. Arch. Biochem. Biophys. **421**, 143-148.

Lohrengel,S., Hermann,F., Hagmann,I., Oberwinkler,H., Scrivano,L., Hoffmann,C., von,L.D., and Dittmar,M.T. (2005). Determinants of human immunodeficiency virus type 1 resistance to membrane-anchored gp41-derived peptides. J. Virol. **79**, 10237-10246.

Loughlin,G.M. and Moscona,A. (2006). The cell biology of acute childhood respiratory disease: therapeutic implications. Pediatr. Clin. North Am. **53**, 929-92x.

Lu,J., Deeks,S.G., Hoh,R., Beatty,G., Kuritzkes,B.A., Martin,J.N., and Kuritzkes,D.R. (2006). Rapid emergence of enfuvirtide resistance in HIV-1-infected patients: results of a clonal analysis. J. Acquir. Immune. Defic. Syndr. **43**, 60-64.

Lu,J., Sista,P., Giguel,F., Greenberg,M., and Kuritzkes,D.R. (2004). Relative replicative fitness of human immunodeficiency virus type 1 mutants resistant to enfuvirtide (T-20). J. Virol. **78**, 4628-4637.

Lu,M., Blacklow,S.C., and Kim,P.S. (1995). A trimeric structural domain of the HIV-1 transmembrane glycoprotein. Nat. Struct. Biol. **2**, 1075-1082.

Lu,M., Ji,H., and Shen,S. (1999). Subdomain folding and biological activity of the core structure from human immunodeficiency virus type 1 gp41: implications for viral membrane fusion. J. Virol. **73**, 4433-4438.

Luque,L.E. and Russell,C.J. (2007). Spring-Loaded Heptad Repeat Residues Regulate the Expression and Activation of the Paramyxovirus Fusion (F) Protein. J. Virol.

Malashkevich,V.N., Chan,D.C., Chutkowski,C.T., and Kim,P.S. (1998). Crystal structure of the simian immunodeficiency virus (SIV) gp41 core: conserved helical interactions underlie the broad inhibitory activity of gp41 peptides. Proc. Natl. Acad. Sci. U. S. A **95**, 9134-9139.

Malashkevich,V.N., Singh,M., and Kim,P.S. (2001). The trimer-of-hairpins motif in membrane fusion: Visna virus. Proc. Natl. Acad. Sci. U. S. A **98**, 8502-8506.

Malvoisin,E. and Wild,T.F. (1993). Measles virus glycoproteins: studies on the structure and interaction of the haemagglutinin and fusion proteins. J. Gen. Virol. **74 (Pt 11)**, 2365-2372.

Matthews,J.M., Young,T.F., Tucker,S.P., and Mackay,J.P. (2000). The core of the respiratory syncytial virus fusion protein is a trimeric coiled coil. J. Virol. **74**, 5911-5920.

McGinnes,L.W. and Morrison,T.G. (1994). The role of the individual cysteine residues in the formation of the mature, antigenic HN protein of Newcastle disease virus. Virology **200**, 470-483.

Melanson,V.R. and Iorio,R.M. (2004). Amino acid substitutions in the F-specific domain in the stalk of the newcastle disease virus HN protein modulate fusion and interfere with its interaction with the F protein. J. Virol. **78**, 13053-13061.

Melanson,V.R. and Iorio,R.M. (2006). Addition of N-glycans in the stalk of the Newcastle disease virus HN protein blocks its interaction with the F protein and prevents fusion. J. Virol. **80**, 623-633.

Melikyan,G.B., Jin,H., Lamb,R.A., and Cohen,F.S. (1997). The role of the cytoplasmic tail region of influenza virus hemagglutinin in formation and growth of fusion pores. Virology **235**, 118-128.

Melikyan,G.B., Lin,S., Roth,M.G., and Cohen,F.S. (1999). Amino acid sequence requirements of the transmembrane and cytoplasmic domains of influenza virus hemagglutinin for viable membrane fusion. Mol. Biol. Cell **10**, 1821-1836.

Menzo,S., Castagna,A., Monachetti,A., Hasson,H., Danise,A., Carini,E., Bagnarelli,P., Lazzarin,A., and Clementi,M. (2004). Genotype and phenotype patterns of human immunodeficiency virus type 1 resistance to enfuvirtide during long-term treatment. Antimicrob. Agents Chemother. **48**, 3253-3259.

Miller,M.D. and Hazuda,D.J. (2004). HIV resistance to the fusion inhibitor enfuvirtide: mechanisms and clinical implications. Drug Resist. Updat. **7**, 89-95.

Moll,M., Klenk,H.D., and Maisner,A. (2002). Importance of the cytoplasmic tails of the measles virus glycoproteins for fusogenic activity and the generation of recombinant measles viruses. J. Virol. **76**, 7174-7186.

Morrison,T.G. (2003). Structure and function of a paramyxovirus fusion protein. Biochim. Biophys. Acta **1614**, 73-84.

Moulard,M. and Decroly,E. (2000). Maturation of HIV envelope glycoprotein precursors by cellular endoproteases. Biochim. Biophys. Acta **1469**, 121-132.

Mukerjee,P. and Chan,C.C. (2002). Effects of High Salt Concentrations on the Micellization of Octyl Glucoside: Salting-Out of Monomers and Electrolyte Effects on the Micelle-Water Interfacial Tension. Langmuir **18**, 5375-5381.

Nakamura,H., Takeda,A., and Matano,T. (2001). Postbinding fusion function contributed by a chimeric murine leukemia virus envelope protein. Arch. Virol. **146**, 953-961.

Nakayama,K. (1997). Furin: a mammalian subtilisin/Kex2p-like endoprotease involved in processing of a wide variety of precursor proteins. Biochem. J. **327 (Pt 3)**, 625-635.

Nameki,D., Kodama,E., Ikeuchi,M., Mabuchi,N., Otaka,A., Tamamura,H., Ohno,M., Fujii,N., and Matsuoka,M. (2005). Mutations conferring resistance to human immunodeficiency virus type 1 fusion inhibitors are restricted by gp41 and Rev-responsive element functions. J. Virol. **79**, 764-770.

Ng,D.T., Randall,R.E., and Lamb,R.A. (1989). Intracellular maturation and transport of the SV5 type II glycoprotein hemagglutinin-neuraminidase: specific and transient association with GRP78-BiP in the endoplasmic reticulum and extensive internalization from the cell surface. J. Cell Biol. **109**, 3273-3289.

Ng,D.T., Watowich,S.S., and Lamb,R.A. (1992). Analysis in vivo of GRP78-BiP/substrate interactions and their role in induction of the GRP78-BiP gene. Mol. Biol. Cell **3**, 143-155.

Nicholls,J.M., Chan,M.C., Chan,W.Y., Wong,H.K., Cheung,C.Y., Kwong,D.L., Wong,M.P., Chui,W.H., Poon,L.L., Tsao,S.W., Guan,Y., and Peiris,J.S. (2007). Tropism of avian influenza A (H5N1) in the upper and lower respiratory tract. Nat. Med. **13**, 147-149.

Nussbaum,O., Broder,C.C., and Berger,E.A. (1994). Fusogenic mechanisms of enveloped-virus glycoproteins analyzed by a novel recombinant vaccinia virus-based assay quantitating cell fusion-dependent reporter gene activation. J. Virol. **68**, 5411-5422.

Ohuchi,M., Fischer,C., Ohuchi,R., Herwig,A., and Klenk,H.D. (1998). Elongation of the cytoplasmic tail interferes with the fusion activity of influenza virus hemagglutinin. J. Virol. **72**, 3554-3559.

Ortmann,D., Ohuchi,M., Angliker,H., Shaw,E., Garten,W., and Klenk,H.D. (1994). Proteolytic cleavage of wild type and mutants of the F protein of human parainfluenza virus type 3 by two subtilisin-like endoproteases, furin and Kex2. J. Virol. **68**, 2772-2776.

Ou,W. and Silver,J. (2005). Inhibition of murine leukemia virus envelope protein (env) processing by intracellular expression of the env N-terminal heptad repeat region. J. Virol. **79**, 4782-4792.

Panda,A., Huang,Z., Elankumaran,S., Rockemann,D.D., and Samal,S.K. (2004). Role of fusion protein cleavage site in the virulence of Newcastle disease virus. Microb. Pathog. **36**, 1-10.

Parks,G.D. and Lamb,R.A. (1993). Role of NH2-terminal positively charged residues in establishing membrane protein topology. J. Biol. Chem. **268**, 19101-19109.

Patel,A.H., Wood,J., Penin,F., Dubuisson,J., and McKeating,J.A. (2000). Construction and characterization of chimeric hepatitis C virus E2 glycoproteins: analysis of regions critical for glycoprotein aggregation and CD81 binding. J. Gen. Virol. **81**, 2873-2883.

Patel,J., Patel,A.H., and McLauchlan,J. (2001). The transmembrane domain of the hepatitis C virus E2 glycoprotein is required for correct folding of the E1 glycoprotein and native complex formation. Virology **279**, 58-68.

Paterson,R.G., Johnson,M.L., and Lamb,R.A. (1997). Paramyxovirus fusion (F) protein and hemagglutinin-neuraminidase (HN) protein interactions: intracellular retention of F and HN does not affect transport of the homotypic HN or F protein. Virology **237**, 1-9.

Paterson,R.G. and Lamb,R.A. (1987). Ability of the hydrophobic fusion-related external domain of a paramyxovirus F protein to act as a membrane anchor. Cell **48**, 441-452.

Peisajovich,S.G., Epand,R.F., Pritsker,M., Shai,Y., and Epand,R.M. (2000). The polar region consecutive to the HIV fusion peptide participates in membrane fusion. Biochemistry **39**, 1826-1833.

Plemper,R.K. and Compans,R.W. (2003). Mutations in the putative HR-C region of the measles virus F2 glycoprotein modulate syncytium formation. J. Virol. **77**, 4181-4190.

Plemper,R.K., Doyle,J., Sun,A., Prussia,A., Cheng,L.T., Rota,P.A., Liotta,D.C., Snyder,J.P., and Compans,R.W. (2005). Design of a small-molecule entry inhibitor with activity against primary measles virus strains. Antimicrob. Agents Chemother. **49**, 3755-3761.

Plemper,R.K., Erlandson,K.J., Lakdawala,A.S., Sun,A., Prussia,A., Boonsombat,J., ki-Sener,E., Yalcin,I., Yildiz,I., Temiz-Arpaci,O., Tekiner,B., Liotta,D.C., Snyder,J.P., and Compans,R.W. (2004). A target site for template-based design of measles virus entry inhibitors. Proc. Natl. Acad. Sci. U. S. A **101**, 5628-5633.

Plemper,R.K., Hammond,A.L., and Cattaneo,R. (2001). Measles virus envelope glycoproteins hetero-oligomerize in the endoplasmic reticulum. J. Biol. Chem. **276**, 44239-44246.

Plemper,R.K., Lakdawala,A.S., Gernert,K.M., Snyder,J.P., and Compans,R.W. (2003). Structural features of paramyxovirus F protein required for fusion initiation. Biochemistry **42**, 6645-6655.

Pontow,S.E., Heyden,N.V., Wei,S., and Ratner,L. (2004). Actin cytoskeletal reorganizations and coreceptor-mediated activation of rac during human immunodeficiency virus-induced cell fusion. J. Virol. **78**, 7138-7147.

Porotto,M., Doctor,L., Carta,P., Fornabaio,M., Greengard,O., Kellogg,G.E., and Moscona,A. (2006a). Inhibition of hendra virus fusion. J. Virol. **80**, 9837-9849.

Porotto,M., Fornabaio,M., Greengard,O., Murrell,M.T., Kellogg,G.E., and Moscona,A. (2006b). Paramyxovirus receptor-binding molecules: engagement of one site on the hemagglutinin-neuraminidase protein modulates activity at the second site. J. Virol. **80**, 1204-1213.

Porotto,M., Fornabaio,M., Kellogg,G.E., and Moscona,A. (2007). A second receptor binding site on the human parainfluenza 3 hemagglutinin-neuraminidase contributes to activation of the fusion mechanism. J. Virol.

Porotto,M., Murrell,M., Greengard,O., Doctor,L., and Moscona,A. (2005). Influence of the human parainfluenza virus 3 attachment protein's neuraminidase activity on its capacity to activate the fusion protein. J. Virol. **79**, 2383-2392.

Porotto,M., Murrell,M., Greengard,O., and Moscona,A. (2003). Triggering of human parainfluenza virus 3 fusion protein (F) by the hemagglutinin-neuraminidase (HN) protein: an HN mutation diminishes the rate of F activation and fusion. J. Virol. **77**, 3647-3654.

Principi,N., Bosis,S., and Esposito,S. (2006). Human metapneumovirus in paediatric patients. Clin. Microbiol. Infect. **12**, 301-308.

Rassa,J.C., and Parks,G.D. (1998). Molecular basis for naturally occurring elevated readthrough transcription across the M-F gene junction of the paramyxovirus SV5. Virology **247**, 274-286.

Reitter,J.N., Sergel,T., and Morrison,T.G. (1995). Mutational analysis of the leucine zipper motif in the Newcastle disease virus fusion protein. J. Virol. **69**, 5995-6004.

Ridley,A.J. (2006). Rho GTPases and actin dynamics in membrane protrusions and vesicle trafficking. Trends Cell Biol. **16**, 522-529.

Rima,B.K. and Duprex,W.P. (2006). Morbilliviruses and human disease. J. Pathol. **208**, 199-214.

Rimsky,L.T., Shugars,D.C., and Matthews,T.J. (1998). Determinants of human immunodeficiency virus type 1 resistance to gp41-derived inhibitory peptides. J. Virol. **72**, 986-993.

Rockwell,N.C. and Thorner,J.W. (2004). The kindest cuts of all: crystal structures of Kex2 and furin reveal secrets of precursor processing. Trends Biochem. Sci. **29**, 80-87.

Roux,L. (1990). Selective and transient association of Sendai virus HN glycoprotein with BiP. Virology **175**, 161-166.

Russell,C.J., Jardetzky,T.S., and Lamb,R.A. (2001). Membrane fusion machines of paramyxoviruses: capture of intermediates of fusion. EMBO J. **20**, 4024-4034.

Russell,C.J., Kantor,K.L., Jardetzky,T.S., and Lamb,R.A. (2003). A dual-functional paramyxovirus F protein regulatory switch segment: activation and membrane fusion. J. Cell Biol. **163**, 363-374.

Russell,C.J. and Luque,L.E. (2006). The structural basis of paramyxovirus invasion. Trends Microbiol. **14**, 243-246.

Russell,R., Paterson,R.G., and Lamb,R.A. (1994). Studies with cross-linking reagents on the oligomeric form of the paramyxovirus fusion protein. Virology **199**, 160-168.

Ryan,C., Zaitsev,V., Tindal,D.J., Dyason,J.C., Thomson,R.J., Alymova,I., Portner,A., von,I.M., and Taylor,G. (2006). Structural analysis of a designed inhibitor complexed with the hemagglutinin-neuraminidase of Newcastle disease virus. Glycoconj. J. **23**, 135-141.

San Roman,K., Villar,E., and Munoz-Barroso,I. (2002). Mode of action of two inhibitory peptides from heptad repeat domains of the fusion protein of Newcastle disease virus. Int. J. Biochem. Cell Biol. **34**, 1207-1220.

Sanderson,C.M., Avalos,R., Kundu,A., and Nayak,D.P. (1995). Interaction of Sendai viral F, HN, and M proteins with host cytoskeletal and lipid components in Sendai virus-infected BHK cells. Virology **209**, 701-707.

Scamuffa,N., Calvo,F., Chretien,M., Seidah,N.G., and Khatib,A.M. (2006). Proprotein convertases: lessons from knockouts. FASEB J. **20**, 1954-1963.

Schmidt,A.C., McAuliffe,J.M., Huang,A., Surman,S.R., Bailly,J.E., Elkins,W.R., Collins,P.L., Murphy,B.R., and Skiadopoulos,M.H. (2000). Bovine parainfluenza virus type 3 (BPIV3) fusion and hemagglutinin-neuraminidase glycoproteins make an important contribution to the restricted replication of BPIV3 in primates. J. Virol. **74**, 8922-8929.

Schmitt,A.P., He,B., and Lamb,R.A. (1999). Involvement of the cytoplasmic domain of the hemagglutinin- neuraminidase protein in assembly of the paramyxovirus simian virus 5. J. Virol. **73**, 8703-8712.

Schmitt,A.P., Leser,G.P., Waning,D.L., and Lamb,R.A. (2002). Requirements for budding of paramyxovirus simian virus 5 virus-like particles. J. Virol. **76**, 3952-3964.

Schnell,M.J., Buonocore,L., Boritz,E., Ghosh,H.P., Chernish,R., and Rose,J.K. (1998). Requirement for a non-specific glycoprotein cytoplasmic domain sequence to drive efficient budding of vesicular stomatitis virus. EMBO J. **17**, 1289-1296.

Schowalter,R.M., Wurth,M.A., Aguilar,H.C., Lee,B., Moncman,C.L., McCann,R.O., and Dutch,R.E. (2006). Rho GTPase activity modulates paramyxovirus fusion protein-mediated cell-cell fusion. Virology **350**, 323-334.

Schroth-Diez,B., Ponimaskin,E., Reverey,H., Schmidt,M.F., and Herrmann,A. (1998). Fusion activity of transmembrane and cytoplasmic domain chimeras of the influenza virus glycoprotein hemagglutinin. J. Virol. **72**, 133-141.

Sciaky,N., Presley,J., Smith,C., Zaal,K.J., Cole,N., Moreira,J.E., Terasaki,M., Siggia,E., and Lippincott-Schwartz,J. (1997). Golgi tubule traffic and the effects of brefeldin A visualized in living cells. J. Cell Biol. **139**, 1137-1155.

Sergel,T., McGinnes,L.W., Peeples,M.E., and Morrison,T.G. (1993). The attachment function of the Newcastle disease virus hemagglutinin- neuraminidase protein can be separated from fusion promotion by mutation. Virology **193**, 717-726.

Sergel,T.A., McGinnes,L.W., and Morrison,T.G. (2000). A single amino acid change in the Newcastle disease virus fusion protein alters the requirement for HN protein in fusion. J. Virol. **74**, 5101-5107.

Sergel,T.A., McGinnes,L.W., and Morrison,T.G. (2001). Mutations in the fusion peptide and adjacent heptad repeat inhibit folding or activity of the Newcastle disease virus fusion protein. J. Virol. **75**, 7934-7943.

Sergel-Germano,T., McQuain,C., and Morrison,T. (1994). Mutations in the fusion peptide and heptad repeat regions of the Newcastle disease virus fusion protein block fusion. J. Virol. **68**, 7654-7658.

Seth,S., Goodman,A.L., and Compans,R.W. (2004). Mutations in multiple domains activate paramyxovirus F protein-induced fusion. J. Virol. **78**, 8513-8523.

Seth,S. and Shaila,M.S. (2001). The fusion protein of Peste des petits ruminants virus mediates biological fusion in the absence of hemagglutinin-neuraminidase protein. Virology **289**, 86-94.

Seth,S., Vincent,A., and Compans,R.W. (2003). Mutations in the cytoplasmic domain of a paramyxovirus fusion glycoprotein rescue syncytium formation and eliminate the hemagglutinin-neuraminidase protein requirement for membrane fusion. J. Virol. **77**, 167-178.

Singh,M., Berger,B., and Kim,P.S. (1999). LearnCoil-VMF: computational evidence for coiled-coil-like motifs in many viral membrane-fusion proteins. J. Mol. Biol. **290**, 1031-1041.

Skehel,J.J. and Wiley,D.C. (2002). Influenza haemagglutinin. Vaccine **20 Suppl 2**, S51-S54.

Sparrelid,E., Ljungman,P., Ekelof-Andstrom,E., Aschan,J., Ringden,O., Winiarski,J., Wahlin,B., and Andersson,J. (1997). Ribavirin therapy in bone marrow transplant recipients with viral respiratory tract infections. Bone Marrow Transplant. **19**, 905-908.

Spriggs,M.K. and Collins,P.L. (1986). Human parainfluenza virus type 3: Messenger RNAs, polypeptide coding assignment, intergenic sequences, and genetic map. J. Virol. **59**, 646–654.

Spriggs,M.K. and Collins,P.L. (1990). Intracellular processing and transport of NH2-terminally truncated forms of a hemagglutinin-neuraminidase type II glycoprotein. J. Cell Biol. **111**, 31-44.

Stieneke-Grober,A., Vey,M., Angliker,H., Shaw,E., Thomas,G., Roberts,C., Klenk,H.D., and Garten,W. (1992). Influenza virus hemagglutinin with multibasic cleavage site is activated by furin, a subtilisin-like endoprotease. EMBO J. **11**, 2407-2414.

Stone-Hulslander,J. and Morrison,T.G. (1997). Detection of an interaction between the HN and F proteins in Newcastle disease virus-infected cells. J. Virol. **71**, 6287-6295.

Sun,A., Prussia,A., Zhan,W., Murray,E.E., Doyle,J., Cheng,L.T., Yoon,J.J., Radchenko,E.V., Palyulin,V.A., Compans,R.W., Liotta,D.C., Plemper,R.K., and Snyder,J.P. (2006). Nonpeptide inhibitors of measles virus entry. J. Med. Chem. **49**, 5080-5092.

Suzuki,T., Portner,A., Scroggs,R.A., Uchikawa,M., Koyama,N., Matsuo,K., Suzuki,Y., and Takimoto,T. (2001). Receptor specificities of human respiroviruses. J. Virol. **75**, 4604-4613.

Tailor,C.S. and Kabat,D. (1997). Variable regions A and B in the envelope glycoproteins of feline leukemia virus subgroup B and amphotropic murine leukemia virus interact with discrete receptor domains. J. Virol. **71**, 9383-9391.

Tailor,C.S., Nouri,A., and Kabat,D. (2000). A comprehensive approach to mapping the interacting surfaces of murine amphotropic and feline subgroup B leukemia viruses with their cell surface receptors. J. Virol. **74**, 237-244.

Takimoto,T., Bousse,T., Coronel,E.C., Scroggs,R.A., and Portner,A. (1998). Cytoplasmic domain of Sendai virus HN protein contains a specific sequence required for its incorporation into virions. J. Virol. **72**, 9747-9754.

Takimoto,T., Murti,K.G., Bousse,T., Scroggs,R.A., and Portner,A. (2001). Role of matrix and fusion proteins in budding of Sendai virus. J. Virol. **75**, 11384-11391.

Takimoto,T. and Portner,A. (2004). Molecular mechanism of paramyxovirus budding. Virus Res. **106**, 133-145.

Tan,K., Liu,J., Wang,J., Shen,S., and Lu,M. (1997). Atomic structure of a thermostable subdomain of HIV-1 gp41. Proc. Natl. Acad. Sci. U. S. A **94**, 12303-12308.

Tanabayashi,K. and Compans,R.W. (1996). Functional interaction of paramyxovirus glycoproteins: identification of a domain in Sendai virus HN which promotes cell fusion. J. Virol. **70**, 6112-6118.

Tanabayashi,K., Takeuchi,K., Okazaki,K., Hishiyama,M., and Yamada,A. (1992). Expression of mumps virus glycoproteins in mammalian cells from cloned cDNAs: both F and HN proteins are required for cell fusion. Virology **187**, 801-804.

Tanaka,Y. and Galinski,M.S. (1995). Human parainfluenza virus type 3: analysis of the cytoplasmic tail and transmembrane anchor of the hemagglutinin-neuraminidase protein in promoting cell fusion. Virus Res. **36**, 131-149.

Tanaka,Y., Heminway,B.R., and Galinski,M.S. (1996). Down-regulation of paramyxovirus hemagglutinin-neuraminidase glycoprotein surface expression by a mutant fusion protein containing a retention signal for the endoplasmic reticulum. J. Virol. **70**, 5005-5015.

Tanaka,Y., Kato,J., Kohara,M., and Galinski,M.S. (2006). Antiviral effects of glycosylation and glucose trimming inhibitors on human parainfluenza virus type 3. Antiviral Res. **72**, 1-9.

Thomas,D., Newcomb,W.W., Brown,J.C., Wall,J.S., Hainfeld,J.F., Trus,B.L., and Steven,A.C. (1985). Mass and molecular composition of vesicular stomatitis virus: a scanning transmission electron microscopy analysis. J. Virol. **54**, 598-607.

Tong,S. and Compans,R.W. (1999). Alternative mechanisms of interaction between homotypic and heterotypic parainfluenza virus HN and F proteins. J. Gen. Virol. **80 (Pt 1)**, 107-115.

Tong,S., Li,M., Vincent,A., Compans,R.W., Fritsch,E., Beier,R., Klenk,C., Ohuchi,M., and Klenk,H.D. (2002). Regulation of fusion activity by the cytoplasmic domain of a paramyxovirus F protein. Virology **301**, 322-333.

Tong,S., Yi,F., Martin,A., Yao,Q., Li,M., and Compans,R.W. (2001). Three membrane-proximal amino acids in the human parainfluenza type 2 (HPIV 2) F protein are critical for fusogenic activity. Virology **280**, 52-61.

Tripet,B., Howard,M.W., Jobling,M., Holmes,R.K., Holmes,K.V., and Hodges,R.S. (2004). Structural characterization of the SARS-coronavirus spike S fusion protein core. J. Biol. Chem. **279**, 20836-20849.

Tsurudome,M., Ito,M., Nishio,M., Kawano,M., Okamoto,K., Kusagawa,S., Komada,H., and Ito,Y. (1998). Identification of regions on the fusion protein of human parainfluenza virus type 2 which are required for haemagglutinin-neuraminidase proteins to promote cell fusion. J. Gen. Virol. **79 (Pt 2)**, 279-289.

Tsurudome,M., Kawano,M., Yuasa,T., Tabata,N., Nishio,M., Komada,H., and Ito,Y. (1995). Identification of regions on the hemagglutinin-neuraminidase protein of human parainfluenza virus type 2 important for promoting cell fusion. Virology **213**, 190-203.

van Wyke-Coelingh,K. and Tierney,E.L. (1989). Antigenic and functional organization of human parainfluenza virus type 3 fusion glycoprotein. J. Virol. **63**, 375-382.

Vilchez,R.A., Dauber,J., McCurry,K., Iacono,A., and Kusne,S. (2003). Parainfluenza virus infection in adult lung transplant recipients: an emergent clinical syndrome with implications on allograft function. Am. J. Transplant. **3**, 116-120.

Villar,E. and Barroso,I.M. (2006). Role of sialic acid-containing molecules in paramyxovirus entry into the host cell: a minireview. Glycoconj. J. **23**, 5-17.

Volchkov,V.E., Feldmann,H., Volchkova,V.A., and Klenk,H.D. (1998). Processing of the Ebola virus glycoprotein by the proprotein convertase furin. Proc. Natl. Acad. Sci. U. S. A **95**, 5762-5767.

Wang,E., Sun,X., Qian,Y., Zhao,L., Tien,P., and Gao,G.F. (2003). Both heptad repeats of human respiratory syncytial virus fusion protein are potent inhibitors of viral fusion. Biochem. Biophys. Res. Commun. **302**, 469-475.

Wang,X.J., Bai,Y.D., Zhang,G.Z., Zhao,J.X., Wang,M., and Gao,G.F. (2005). Structure and function study of paramyxovirus fusion protein heptad repeat peptides. Arch. Biochem. Biophys. **436**, 316-322.

Waning,D.L., Russell,C.J., Jardetzky,T.S., and Lamb,R.A. (2004). Activation of a paramyxovirus fusion protein is modulated by inside-out signaling from the cytoplasmic tail. Proc. Natl. Acad. Sci. U. S. A **101**, 9217-9222.

Waning,D.L., Schmitt,A.P., Leser,G.P., and Lamb,R.A. (2002). Roles for the cytoplasmic tails of the fusion and hemagglutinin-neuraminidase proteins in budding of the paramyxovirus simian virus 5. J. Virol. **76**, 9284-9297.

Wasylewski,Z. and Kozik,A. (1979). Protein--non-ionic detergent interaction. Interaction of bovine serum albumin with alkyl glucosides studied by equilibrium dialysis and infrared spectroscopy. Eur. J. Biochem. **95**, 121-126.

Wei,X., Decker,J.M., Liu,H., Zhang,Z., Arani,R.B., Kilby,J.M., Saag,M.S., Wu,X., Shaw,G.M., and Kappes,J.C. (2002). Emergence of resistant human immunodeficiency virus type 1 in patients receiving fusion inhibitor (T-20) monotherapy. Antimicrob. Agents Chemother. **46**, 1896-1905.

Weinberg,G.A. (2006). Parainfluenza viruses: an underappreciated cause of pediatric respiratory morbidity. Pediatr. Infect. Dis. J. **25**, 447-448.

Weissenhorn,W., Dessen,A., Calder,L.J., Harrison,S.C., Skehel,J.J., and Wiley,D.C. (1999). Structural basis for membrane fusion by enveloped viruses. Mol. Membr. Biol. **16**, 3-9.

Weissenhorn,W., Dessen,A., Harrison,S.C., Skehel,J.J., and Wiley,D.C. (1997). Atomic structure of the ectodomain from HIV-1 gp41. Nature **387**, 426-430.

West,D.S., Sheehan,M.S., Segeleon,P.K., and Dutch,R.E. (2005). Role of the simian virus 5 fusion protein N-terminal coiled-coil domain in folding and promotion of membrane fusion. J. Virol. **79**, 1543-1551.

Wild,C., Dubay,J.W., Greenwell,T., Baird,T., Jr., Oas,T.G., McDanal,C., Hunter,E., and Matthews,T. (1994). Propensity for a leucine zipper-like domain of human immunodeficiency virus type 1 gp41 to form oligomers correlates with a role in virus-induced fusion rather than assembly of the glycoprotein complex. Proc. Natl. Acad. Sci. U. S. A **91**, 12676-12680.

Wild,C., Greenwell,T., and Matthews,T. (1993). A synthetic peptide from HIV-1 gp41 is a potent inhibitor of virus-mediated cell-cell fusion. AIDS Res. Hum. Retroviruses **9**, 1051-1053.

Wild,C., Greenwell,T., Shugars,D., Rimsky-Clarke,L., and Matthews,T. (1995). The inhibitory activity of an HIV type 1 peptide correlates with its ability to interact with a leucine zipper structure. AIDS Res. Hum. Retroviruses **11**, 323-325.

Wild,C., Oas,T., McDanal,C., Bolognesi,D., and Matthews,T. (1992). A synthetic peptide inhibitor of human immunodeficiency virus replication: correlation between solution structure and viral inhibition. Proc. Natl. Acad. Sci. U. S. A **89**, 10537-10541.

Wild,C.T., Shugars,D.C., Greenwell,T.K., McDanal,C.B., and Matthews,T.J. (1994). Peptides corresponding to a predictive alpha-helical domain of human immunodeficiency virus type 1 gp41 are potent inhibitors of virus infection. Proc. Natl. Acad. Sci. U. S. A **91**, 9770-9774.

Wild,T.F. and Buckland,R. (1997). Inhibition of measles virus infection and fusion with peptides corresponding to the leucine zipper region of the fusion protein. J. Gen. Virol. **78 (Pt 1)**, 107-111.

Wild,T.F., Malvoisin,E., and Buckland,R. (1991). Measles virus: both the haemagglutinin and fusion glycoproteins are required for fusion. J. Gen. Virol. **72 (Pt 2)**, 439-442.

Xu,L., Pozniak,A., Wildfire,A., Stanfield-Oakley,S.A., Mosier,S.M., Ratcliffe,D., Workman,J., Joall,A., Myers,R., Smit,E., Cane,P.A., Greenberg,M.L., and Pillay,D. (2005). Emergence and evolution of enfuvirtide resistance following long-term therapy involves heptad repeat 2 mutations within gp41. Antimicrob. Agents Chemother. **49**, 1113-1119.

Xu,Y., Zhu,J., Liu,Y., Lou,Z., Yuan,F., Liu,Y., Cole,D.K., Ni,L., Su,N., Qin,L., Li,X., Bai,Z., Bell,J.I., Pang,H., Tien,P., Gao,G.F., and Rao,Z. (2004a). Characterization of the heptad repeat regions, HR1 and HR2, and design of a fusion core structure model of the spike protein from severe acute respiratory syndrome (SARS) coronavirus. Biochemistry **43**, 14064-14071.

Xu,Y., Gao,S., Cole,D.K., Zhu,J., Su,N., Wang,H., Gao,G.F., and Rao,Z. (2004a). Basis for fusion inhibition by peptides: analysis of the heptad repeat regions of the fusion proteins from Nipah and Hendra viruses, newly emergent zoonotic paramyxoviruses. Biochem. Biophys. Res. Commun. **315**, 664-670.

Yao,Q. and Compans,R.W. (1996). Peptides corresponding to the heptad repeat sequence of human parainfluenza virus fusion protein are potent inhibitors of virus infection. Virology **223**, 103-112.

Yao,Q., Hu,X., and Compans,R.W. (1997). Association of the parainfluenza virus fusion and hemagglutinin-neuraminidase glycoproteins on cell surfaces. J. Virol. **71**, 650-656.

Yin,H.S., Paterson,R.G., Wen,X., Lamb,R.A., and Jardetzky,T.S. (2005). Structure of the uncleaved ectodomain of the paramyxovirus (hPIV3) fusion protein. Proc. Natl. Acad. Sci. U. S. A **102**, 9288-9293.

Yin,H.S., Wen,X., Paterson,R.G., Lamb,R.A., and Jardetzky,T.S. (2006). Structure of the parainfluenza virus 5 F protein in its metastable, prefusion conformation. Nature **439**, 38-44.

Young,J.K., Hicks,R.P., Wright,G.E., and Morrison,T.G. (1997). Analysis of a peptide inhibitor of paramyxovirus (NDV) fusion using biological assays, NMR, and molecular modeling. Virology **238**, 291-304.

Young,J.K., Li,D., Abramowitz,M.C., and Morrison,T.G. (1999). Interaction of peptides with sequences from the Newcastle disease virus fusion protein heptad repeat regions. J. Virol. **73**, 5945-5956.

Yu,M., Wang,E., Liu,Y., Cao,D., Jin,N., Zhang,C.W., Bartlam,M., Rao,Z., Tien,P., and Gao,G.F. (2002). Six-helix bundle assembly and characterization of heptad repeat regions from the F protein of Newcastle disease virus. J. Gen. Virol. **83**, 623-629.

Yuan,K., Yi,L., Chen,J., Qu,X., Qing,T., Rao,X., Jiang,P., Hu,J., Xiong,Z., Nie,Y., Shi,X., Wang,W., Ling,C., Yin,X., Fan,K., Lai,L., Ding,M., and Deng,H. (2004a). Suppression of SARS-CoV entry by peptides corresponding to heptad regions on spike glycoprotein. Biochem. Biophys. Res. Commun. **319**, 746-752.

Yuan,P., Thompson,T.B., Wurzburg,B.A., Paterson,R.G., Lamb,R.A., and Jardetzky,T.S. (2005). Structural studies of the parainfluenza virus 5 hemagglutinin-neuraminidase tetramer in complex with its receptor, sialyllactose. Structure. **13**, 803-815.

Zaitsev,V., von,I.M., Groves,D., Kiefel,M., Takimoto,T., Portner,A., and Taylor,G. (2004). Second sialic acid binding site in Newcastle disease virus hemagglutinin-neuraminidase: implications for fusion. J. Virol. **78**, 3733-3741.

Zhao,X., Singh,M., Malashkevich,V.N., and Kim,P.S. (2000). Structural characterization of the human respiratory syncytial virus fusion protein core. Proc. Natl. Acad. Sci. U. S. A **97**, 14172-14177.

Zhou,J., Dutch,R.E., and Lamb,R.A. (1997). Proper spacing between heptad repeat B and the transmembrane domain boundary of the paramyxovirus SV5 F protein is critical for biological activity. Virology **239**, 327-339.

Zhu,J., Jiang,X., Liu,Y., Tien,P., and Gao,G.F. (2005). Design and characterization of viral polypeptide inhibitors targeting Newcastle disease virus fusion. J. Mol. Biol. **354**, 601-613.

Zhu,J., Xiao,G., Xu,Y., Yuan,F., Zheng,C., Liu,Y., Yan,H., Cole,D.K., Bell,J.I., Rao,Z., Tien,P., and Gao,G.F. (2004). Following the rule: formation of the 6-helix bundle of the fusion core from severe acute respiratory syndrome coronavirus spike protein and identification of potent peptide inhibitors. Biochem. Biophys. Res. Commun. **319**, 283-288.

Zhu,J., Zhang,C.W., Qi,Y., Tien,P., and Gao,G.F. (2002). The fusion protein core of measles virus forms stable coiled-coil trimer. Biochem. Biophys. Res. Commun. **299**, 897-902.

Zhu,J.Q., Zhang,C.W., Rao,Z., Tien,P., and Gao,G.F. (2003). Biochemical and biophysical analysis of heptad repeat regions from the fusion protein of Menangle virus, a newly emergent paramyxovirus. Arch. Virol. **148**, 1301-1316.

Zhu,P., Liu,J., Bess,J., Jr., Chertova,E., Lifson,J.D., Grise,H., Ofek,G.A., Taylor,K.A., and Roux,K.H. (2006). Distribution and three-dimensional structure of AIDS virus envelope spikes. Nature **441**, 847-852.

Zimmer,G., Budz,L., and Herrler,G. (2001). Proteolytic activation of respiratory syncytial virus fusion protein. Cleavage at two furin consensus sequences. J. Biol. Chem. **276**, 31642-31650.